FLUORESCENCE INDUCTION IN *CHLORELLA PYRENOIDOSA* AND *ANACYSTIS NIDULANS* AND ITS RELATION TO PHOTOPHOSPHORYLATION

BY

GEORGE PAPAGEORGIOU
Dipl., Aristotelian University of Thessaloniki, Greece, 1958

THESIS

Submitted in partial fulfillment of the requirements
for the degree of Doctor of Philosophy in Biophysics
in the Graduate College of the
University of Illinois, 1968

Urbana, Illinois

UNIVERSITY OF ILLINOIS

THE GRADUATE COLLEGE

DECEMBER, 1967

I HEREBY RECOMMEND THAT THE THESIS PREPARED UNDER MY SUPERVISION BY GEORGE PAPAGEORGIOU

ENTITLED FLUORESCENCE INDUCTION IN CHLORELLA PYRENOIDOSA AND ANACYSTIS NIDULANS AND ITS RELATION TO PHOTOPHOSPHORYLATION

BE ACCEPTED IN PARTIAL FULFILLMENT OF THE REQUIREMENTS FOR THE DEGREE OF DOCTOR OF PHILOSOPHY

Govindjee
In Charge of Thesis

C. Ladd Prosser
Head of Department

Recommendation concurred in†

B C Abbott
Jerry Hoffman
Floyd Dunn
J Rabinowitch

Committee on Final Examination†

† Required for doctor's degree but not for master's

D517

ACKNOWLEDGMENTS

I wish to express my sincere appreciation to Professor Govindjee for his guidance, encouragement and support during this investigation. I am also greatly indebted to Dr. Rajni Govindjee for the polarographic measurements of the rate of oxygen evolution and to Mrs Linda Miller for growing the algae cultures used in these experiments. I owe thanks to my colleagues in the photosynthesis laboratory for the numerous and eye-eopening debates on research problems and to Dr. G. S. Singhal for reading the manuscript. Thanks are also due to Mr. Jobie Spencer for the maintenance of the instrumentsused, to Mrs. Marion Bedell for typing and to Mr. Stanley Jones for the india-ink drawing of the figures appearing in this thesis.

I wish to express my appreciation to Professors Eugene Rabinowitch and Christiaan Sybesma for their encouragement and suggestions in the course of this investigation. I thank also Dr. P. G. Heytler for a gift of FCCP — an uncoupler of phosphorylation — used in the present work.

My special thanks are due to my wife Sophie. Without her constant support, this thesis would not have been possible.

This work was supported by two research grants (NSF GB4040 and USPHS GM 13913).

TABLE OF CONTENTS

I. INTRODUCTION

The fundamental concepts of photosynthesis will be reviewed briefly, for the easier understanding of this investigation. Photosynthesis is the endergonic process of plants in which light energy is utilized for the reduction of CO_2 to carbohydrates and the oxidation of H_2O to O_2. The whole process occurs in two successive steps, a light requiring production of assimilatory power in the form of reduced nicotinamide adenine dinucleotide phosphate (NADPH) and adenosine triphosphate (ATP), and a dark chemosynthetic reduction of CO_2. These steps are represented by the following equations:

(1) $4H_2O + 2NADP^+ \xrightarrow[(ADP+P_iATP)]{nh} 2H_2O + O_2 + 2NADPH + 2H^+$

(2) $2NADPH + 2H^+ + CO_2 + 3ATP \longrightarrow (CHOH) + H_2O + 2NADP^+ + 3ADP + 3P_i$

where P_i refers to inorganic phosphate and (CHOH) to carbohydrate. In what follows, we shall deal only with the first process, by which the light energy is converted and stored as chemical free energy.

A. THE PHOTOSYNTHETIC PROCESS

1. Two Light Reactions.

It is now generally accepted that light is utilized in two consecutive quantum steps, known as the two light reactions of photosynthesis.[1,2] The first, arbitrarily called light reaction II, leads to the oxidation of H_2O to O_2 and to the reduction of a cytochrome. The second, or light reaction I[3], reoxidizes the cytochrome and reduces $NADP^+$. A fraction of the absorbed light energy is conserved as ATP (fig. 1).

The classical experiments of Emerson and Arnold[4] established that a set of 2400 chlorophyll a (Chl a) molecules cooperate in evolving one O_2

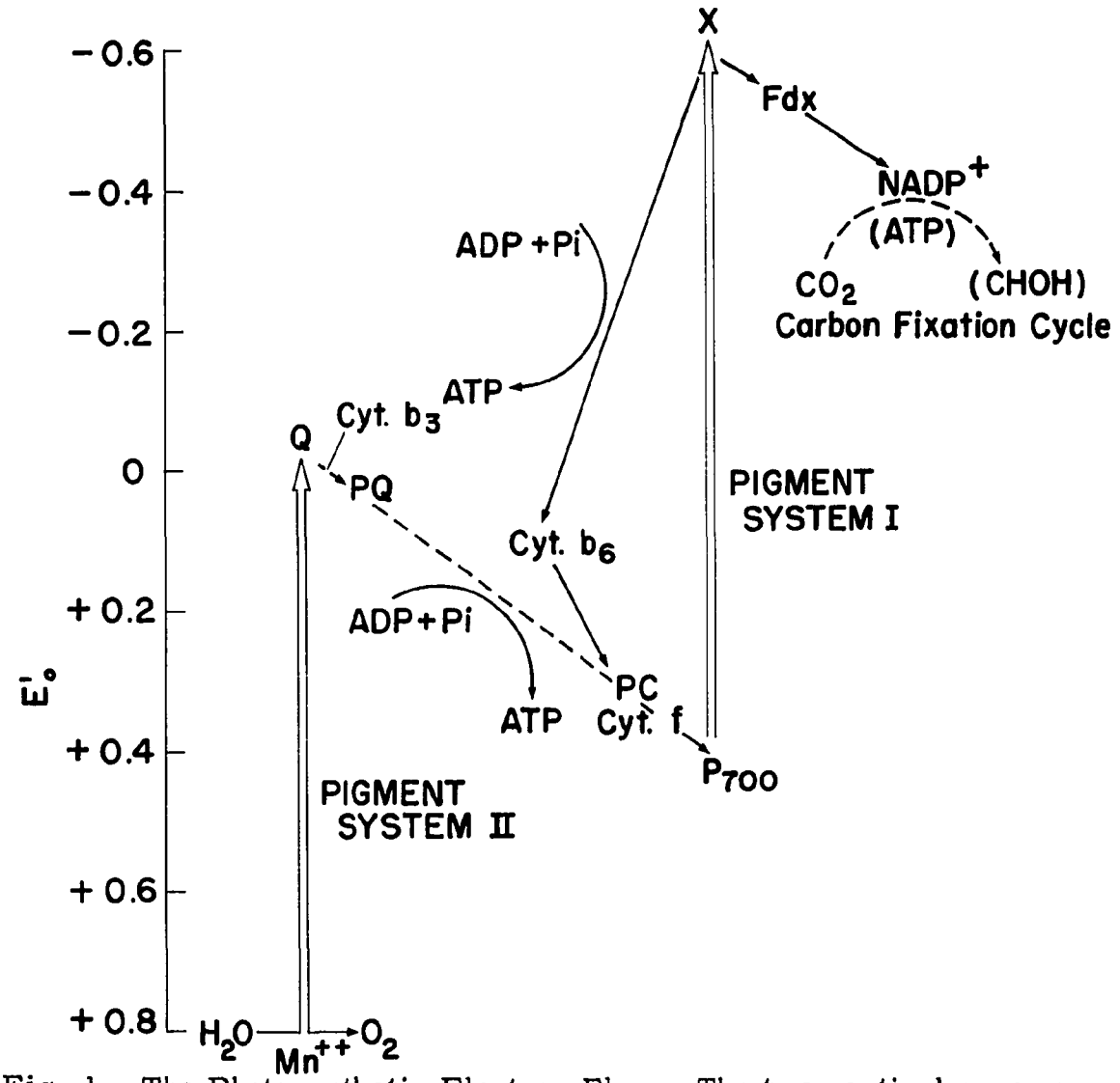

Fig. 1. The Photosynthetic Electron Flow. The two vertical arrows indicate light reactions; all others dark reactions. Electron transport from H_2O to $NADP^+$ is designated as the "non-cyclic" electron flow, the closed pathway involving system I only as the "cyclic" electron flow. Abbreviations used: Q, the primary oxidant of system II; PQ, plastoquinone; PC, plastocyanin; cyt b_3 cyt b_6 and cyt f, cytochromes b_3, b_6 and f; P_{700}, pigment absorbing at 700 nm, energy trap of system I; X, unknown electron acceptor of system I; Fdx, ferredoxin; $NADP^+$; nicotinamide adenine dinucleotide phosphate; ADP, ATP, adenosine di- and triphosphate, Pi, inorganic phosphate.

(or assimilating one CO_2) which corresponds to 600 Chl *a* molecules per transferred electron. These are apportioned between two functional units referred to as photosynthetic units, PSU_I and PSU_{II}, where the latin numeral subscript denotes the type of reaction they perform. Each PSU consists of a light energy collector, to which the majority of the pigments belong (bulk) and a light energy converter (energy trap or sink) which transforms the electronic excitation into chemical energy. Since each PSU also contains other accessory pigments besides Chl *a*, their total pigment complements are called pigment system I and pigment system II. These can be distinguished spectroscopically; pigment system II absorption bands are shifted toward shorter wavelengths of those of system I.

A sequence of dark redox steps involving a number of partially identified intermediates, connects the two light reactions. Some of the excess potential energy of an electron cascading along this pathway is conserved as ATP, the process being denoted as <u>non-cyclic photophosphorylation</u>. A second type of photophosphorylation, which is independent of H_2O as an electron donor and requires only the excitation of system I, is called <u>cyclic photophosphorylation.</u> In the latter, an electron raised to a higher oxidation potential (probably, $E_o^{'} = -0.6$ v) by light absorbed in system I, returns via a series of unidentified intermediates and cytochrome b_6 (Cyt b_6) into the chain of redox intermediates connecting the two primary photoreactions, with a concomitant conservation of some of its potential energy as ATP. A third type, which involves the reoxidation of a reduced intermediate by O_2, called <u>pseudocyclic photophosphorylation</u> is probably an accidental process.

2. Path of Energy.

The absorption of a light quantum raises a Chl a molecule into an excited state, with the electronic excitation spending most of its lifetime in the lowest excited singlet state because of rapid internal conversion of higher excited states into the lowest one. A Chl a lowest excited singlet state can be produced also by "sensitization" i.e., energy transfer from a previously excited Chl a molecule or by energy transfer from an accessory pigment molecule (homogeneous or heterogeneous excitation energy transfer). The high quantum efficiency of the primary photoreactions (the number of electrons transferred by each PSU er absorbed photon) is 0.95[5] indicates thatphotochemistry utilizes the major part of Chl a excitation quanta, only a small fraction is dissipated by fluorescence or thermal degradation. Actually, the quantum efficiency of Chl a fluorescence in vivo is of the order of 0.03[6,7], while that a Chl a in diethyl ether is approximately 0.33[6,8]. These two values cannot be compared, however, since the in vitro measurements refer to very dilute (10^{-6} M) solutions of Chl a, free of concentration quenching, while the concentration of Chl a in the chloroplast is of the order of 0.1 M[9]. Since a 0.1 M solution of Chl a has its fluorescence almost totally quenched[10,000], Duysens[12] concludes that one of the main functions of the lamellae on which the pigment molecules are organized is to keep them apart. This arrangement enables the energy migration to the reaction center to compete favorably with the radiative deexcitation. Changes in the lamellar geometry may manifest themselves as changes in the concentration quenching influencing in this manner the fluorescence quantum yield.

The fluorescence spectrum of Chl a in vivo consists of a band peaked at 685 ± 2 nm originating from a $\pi^* \rightarrow \pi$ transition whose dipole lies in the direction of the shorter axis of the conjugated porphyrin system[13]. There is evidence that this band does not come from a unique Chl a species, but is rather the envelope of more than one emission band, originating from various Chl a holochromic forms[14]. The fluorescence yield of photosynthetic organisms experiences characteristic, repeatable variations under continuous excitation, which may also lead to different spectral distributions of the fluorescence. These variations will be discussed in the following sections.

B. FLUORESCENCE INDUCTION

The Chl a fluorescence yield of photosynthetic organisms undergoes characteristic variations during a period of continuous illumination following a dark interval (fluorescence induction). Although the detailed kinetics of the fluorescence yield in a particular organism depend upon several experimental variables, the fluorescence induction curves can be classified into three general types. These are shown schematically in fig. 2, and they are labeled as type I, II, or III for the convenience of further discussion.

Type I. The time course consists of a rapid rise (O→P), followed by a slower and more extensive decay to a stationary level (S), which is attained within a few minutes from the onset of excitation. This type is characteristic of higher plants.

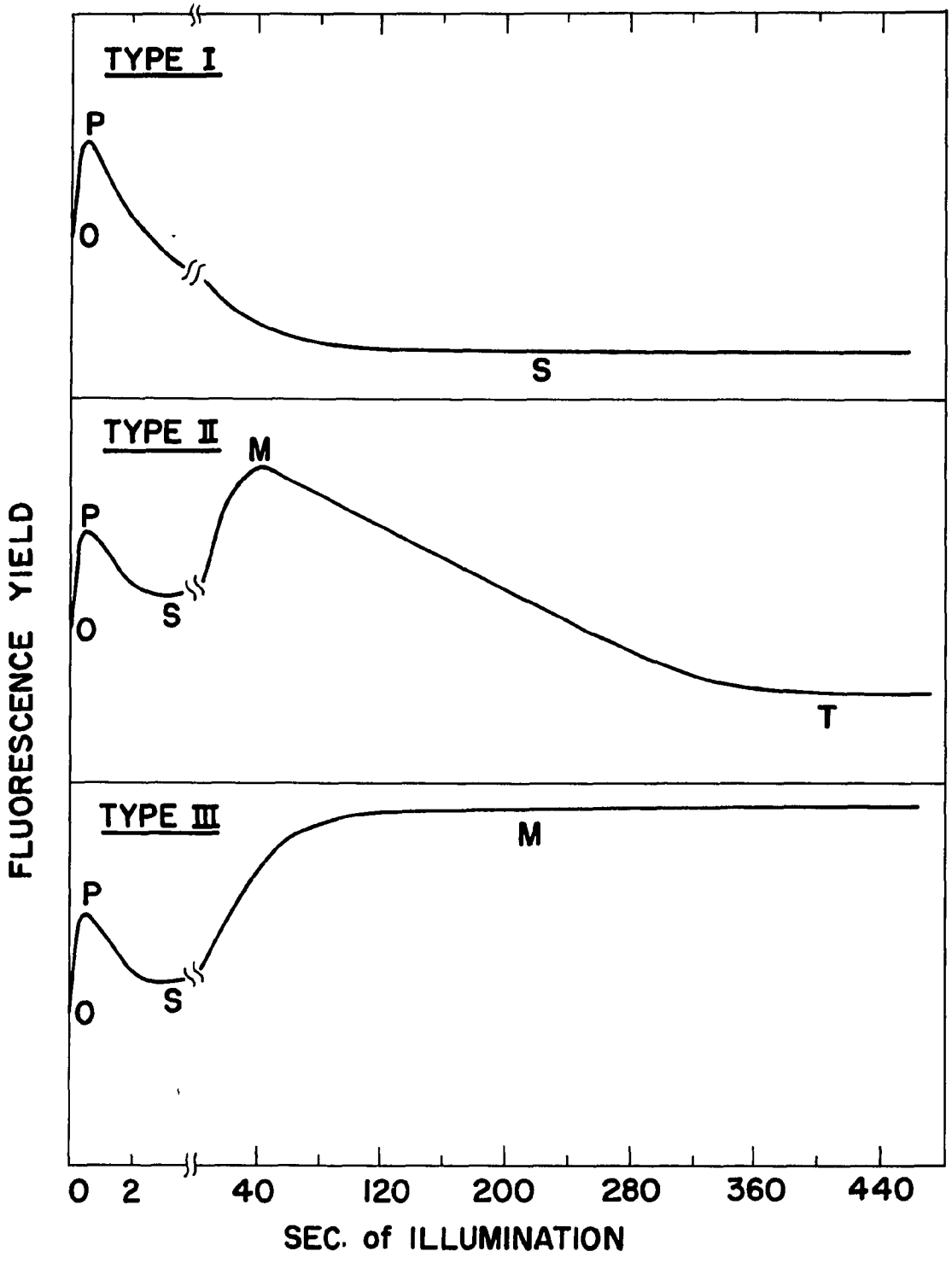

Fig. 2. Three types of fluorescence induction, I, II and III (schematic representation).

Type II. The fluorescence induction curve is composed of two successive waves. The first (O→P→S) is completed within a few seconds, while the second, (S→M→T), which represents a larger effect, is much slower. At the end of the induction phenomena, the fluorescence yield is constant and lower than the minimum between the first and the second wave (S). "Two-wave" time courses are typical of the green algae (e.g. Chlorella).

Type III. The fluorescence yield time course consists of a fast first wave (O→P→S), followed by an incomplete second one. In the latter, the fluorescence yield rises to a plateau (M), situated much higher than the minimum between the two waves (S). This type of fluorescence induction curve, typical of the blue-green alga, Anacystis nidulans, is described here for the first time.

The research on variations of the fluorescence yield under continuous illumination was initiated by Kautsky's[15] visual observation in 1931 of such phenomena in higher plant leaves. During the next two decades a large body of experimental evidence concerning these effects accumulated. Attempts to synthesize this information into a hypothesis[9,16] did not meet with success, mainly because of the diversity and divergence of the data and the lack of a unified theory for the mechanism of photosynthesis. The discovery of the two light reactions in the late fifties diverted the research interests toward more promising subjects and as a result the study of the fluorescence induction phenomena was rejected. In recent years, however, there is an increasing interest in this direction

and much valuable and consistent information has been obtained, especially about the first wave phenomena.

1. The First Wave of Fluorescence Induction

The first wave of fluorescence induction consists of a rapid fluorescence transient completed within a few seconds. On excitation (after a suitable dark period), the fluorescence yield rises instantaneously to an initial level 0, from where it proceeds biphasically to a maximum P, thereafter declining at a slower rate to the semi-stationary level S. The whole change O→P→S lasts approximately two seconds.

All the theories proposed to account for the first wave changes invoke a competition between chemical and radiative deexcitation processes. Thus, Kautsky and his co-workers[17] ascribed the first wave decay to quenching of chlorophyll a fluorescence by molecular oxygen or loose complexes of molecular oxygen, since according to their experimental evidence, the first wave failed to decay under complete anaerobiosis. A highly speculative hypothesis proposed by J. Franck and his co-workers[18-20] attributes the initial fluorescence rise (O→P) to a chemical inactivation (narcotization) of chlorophyll a via oxidized metabolic intermediates and the ensuing decay to a reactivation of chlorophyll a because of the depletion of the pool of the narcotics. An alternate hypothesis was proposed by Wassink and his co-workers.[21] This hypothesis, which approximates remarkably the currently held view, ascribes the fluorescence rise to a photochemical reaction which consumes a fluorescence quencher. The latter is regenerated by subsequent dark reactions, collectively

known as the Blackman reaction. An adaptation of the reaction sequence proposed is as follows:

$$\text{Chl} \xrightarrow{h\nu} \text{Chl}^* \longrightarrow A_o \text{ (quencher)} \longrightarrow \text{Blackman reaction}$$

where the arrows after Chl* represent electron transfer steps. A further improvement on the above scheme was proposed by Kautsky et al.[22]. According to their interpretation, the reoxidation of the quencher A_o involves a second light activated step coupled to the first by a non-photochemical (dark) reaction. The proposed kinetic scheme explained the biphasic fluorescence rise (O→P) but it did not account for the subsequent decay. (No attempt was made, at that time, to correlate the two light steps with the light reactions and the pigment systems of photosynthesis.)

A relationship between the fluorescence yield and the two light reactions of photosynthesis was first demonstrated by Govindjee et al.[23]. It was shown that the fluorescence excited with red (system II) light is quenched by far-red (system I) light, which by itself does not produce any fluorescence. The antagonistic effects of system II and system I excitations with respect to the fluorescence yield were also observed by Butler[24,25], who established that the maximum far-red light quenching is obtained at 705 nm. Although no time variable was included in these experiments, they do suggest a correlation of the fluorescence quantum yield with the rates of the two primary photoreactions of photosynthesis.[26]

The antagonistic effect of system II and system I excitation on the time courses of the first wave was also shown by Duysens and Sweers,[27] who found that system II excitation increases the fluorescence yield while system I light decreases it. To explain their results they postulated the existence of a photochemical quencher Q, which is reduced by system II into a non-quenching form QH and is reoxidized by system 1. An additional dark reoxidation path through a quenching but non-photoactive intermediate Q′ was included to account for the lower yield at the stationary level S as compared to the maximum yield at P. Duysens' reaction scheme is as follows:

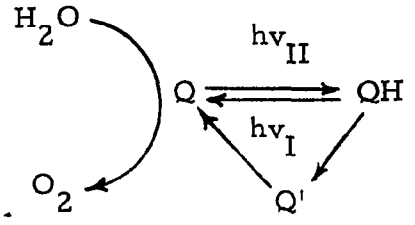

Simultaneous recording of the fluorescence and oxygen evolution kinetics by Joliot[28] showed that the long held view of the antiparallel course of these processes in the time interval of the first wave was correct except at the beginning of the light period. It was found that in the first phase of the fluorescence rise (activation phase) the fluorescence intensity and the oxygen evolution rate increase in parallel, while during the second rise phase they run in a complementary fashion. In order to explain his results, Joliot[28,29] assumed that (i) the first wave changes originate in system II and (ii) a photochemical quencher E is activated in two light steps. Joliot's reaction scheme can be written

as follows:

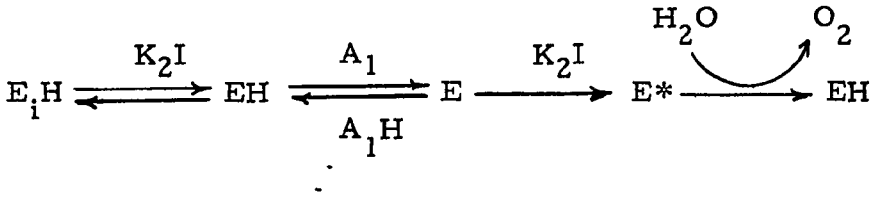

where E_1H and E can quench the Chl a fluorescence, while EH cannot. The couple A_1/A_1H represents a dark reaction partner whose redox state is determined by the light reaction of system 1.

Although these schemes do not specify the exact chemical nature of the quencher, they have been successful in correlating the early fluorescence kinetics with those of oxygen evolution and in explaining the antagonistic effect of the two light reactions. However, their application was not extended to the second wave of fluorescence induction phenomena, and probably they cannot account for them in view of the asynchrony in the time courses of fluorescence and oxygen evolution.

2. The Second Wave of Fluorescence Induction

The second wave of fluorescence induction refers to the fluorescence yield transient which follows the first wave. A typical second wave in a green alga consists of an increase of the fluorescence yield from the semi-stationary level S to a maximum M followed by a slower decay to a new terminal stationary level T (fig. 2, type II). We found that in blue-green algae the decay portion M→T is missing. The fluorescence yield in these organisms remains high for several minutes (fig. 2. type III), declining only after prolonged illumination.

The second wave kinetics depend upon experimental variables such as the incident light intensity, the temperature, the presence of

photosynthetic inhibitors, and the composition of the gas phase over the sample. Kautsky[30] has shown in the marine alga Ulva lactuca that increased light intensity accentuates the second wave transient and shifts its maximum towards shorter times of light exposure. The effects of the light intensity on the rise portion of the second wave was studied in detail by Wassink et al.[31] with KCN poisoned Chlorella. Above a certain concentration of this poison, which inhibits the carboxylation enzyme (ribulose diphosphate carboxylase),[32] the second wave decay disappears, and the rise can be studied without the complication of the reverse processes. It was found that the rise rate exhibits a light intensity optimum whose location is temperature dependent, being shifted towards lower intensities at lower temperatures. No correlation with light saturation of photosynthesis was given.

The rise rate of the second wave in CN^- poisoned Chlorella shows also an optimum temperature behavior for low light intensities, while at high light intensities the rise rate increases and then levels off, i.e., the temperature coefficient of the rise rate is always positive, approaching zero at higher temperatures.[31] Since increased temperature favors a faster decay of the second wave,[30, 33] the overall effect on the transient will be dependent on the temperature coefficients of both the fluorescence yield rise and the decay processes.

The second wave is remarkably inert with respect to the composition of the gas phase above the sample. Thus, Wassink[31] found that the rise rate in CN^- poisoned Chlorella is insensitive to oxygen

concentrations from 2-100%, while Kautsky[34] reported similar results in the case of Ulva lactuca. In oxygen-free nitrogen atmosphere both the second wave rise and the subsequent decay in Chlorella were enhanced, as compared to those in the aerobic samples. In addition, the fluorescence yield under nitrogen was higher throughout the two wave time course than it was for samples under air.[31] The relative insensitivity of the fluorescence time course with respect to oxygen concentration has a special significance since it appears to contradict the view held earlier by Kautsky, that the variations of the fluorescence yield reflect changes in the oxygen quenching of chlorophyll fluorescence.

Contrary to oxygen, carbon dioxide is essential for the development of the second wave, although the required concentration is different for different plants. Thus, McAlister et al.[35] have shown that one wave curves in wheat are converted in two wave curves in the range of 0.1-3% CO_2, while Franck et al.[18] obtained a similar result in Hydrangea. On the other hand, the normal two wave induction curve in Ulva changes to a one wave form in the total absence of CO_2[18]. Chlorella, however, shows a strong second wave even at CO_2 concentrations as low as those of atmospheric air (0.03%). (High abnormal concentrations of CO_2 may eliminate the first wave completely.[9])

Since CO_2 is the terminal oxidant in the photosynthetic process, complete absence of it will eventually result in inhibition of photosynthesis. Such a condition is impossible due to the production of CO_2 in respiration, but a low CO_2 concentration may inhibit drastically the

photosynthetic electron flow. In this respect, the effect of reduced CO_2 pressure on the second wave time course may be indirect. On the other hand, abnormally high CO_2 concentrations are likely to alter the ionic properties of the suspension medium (e.g., lower the pH) and upset the overall metabolism, introducing thus some non-specificity in the fluorescence transient data.

The comparison of fluorescence and gas exchange kinetics is of importance, since it may provide information about their relationship. A strict competition between the chemical and radiative deexcitation processes must in principle reveal itself as a complementarity in the time course of fluorescence and of the rate of oxygen evolution (or CO_2 assimilation). The complementarity requirement, however, can be violated for the following reasons: (i) In addition to the chemical and radiative processes, Chl a excitation can be dissipated also by thermal degradations, e.g., by transfer to non-fluorescing Chl a aggregates (or holochromes) absorbing at longer wavelengths. (ii) Every chemical deexcitation event at the Chl a site is not necessarily equivalent to a single step oxidation or reduction at the H_2O or CO_2 sites. For example, in the H_2O independent cyclic pathway, the light induced electron flow does not affect the end products of photosynthesis. Also, accidental autooxidations of reduced intermediates, as for example in the pseudocyclic pathway, disrupt the direct relationship between the chemical quenching of fluorescence and the oxygen evolution rate. (iii) The intervention of large pools of redox intermediates between the Chl a and the gas exchange sites

(especially for CO_2 assimilation) may not only disrupt the timing between the fluorescence and gas induction, but also lead to a complete damping of the latter. Because of the latter argument, fluorescence can be better correlated with the rate of oxygen evolution than with the consumption of CO_2.

On the basis of the above arguments, only the measurement of the change of a redox intermediate close to the energy trap (e.g., a cytochrome) can prove unambiguously the exact relationship between the fluorescence and chemical deexcitation events. Unfortunately, such experiments have not yet been carried out in the time interval corresponding to the second wave.

Simultaneous measurements of fluorescence and CO_2 uptake kinetcis, the latter by an infrared absorption method by McAlister et al.,[35] did not show a negative CO_2 wave corresponding to the positive second wave of fluorescence. Sometimes, an occasional antiparallel behavior was observed, but at other times both processes ran in parallel. Also, the time courses of oxygen evolution, measured with a polarographic technique with almost zero diffusion delay, does not show a negative effect in the time interval of the second wave.[36] Our results (Chapter III and IV) confirm the absence of any direct relationship between oxygen evolution and the second wave of fluorescence. We also observed that inhibition of photosynthesis does not impair the capacity of Anacystis nidulans to undergo prominent long term fluorescence changes. Rabinowitch,[9] reviewing the earlier results on the gas

exchange kinetcis, concludes: "Apparently, the transformation of the photosynthetic mechanism that gives rise to the second wave of fluorescence does not always affect the gas exchange equally strongly and may sometimes have no influence on this exchange."

Viewed in retrospect, the early theories proposed to account for the fluorescence transients appear highly speculative and off-pace with the currently held ideas. Kautsky[17] advanced a theory in which he formalized his belief about the quenching role of oxygen and of its molecular complexes on fluorescence. Without entering into detail, this theory can be discounted immediately, because it assumes carbonate as the source of the photosynthetically evolved oxygen.

The cornerstone of a theory formulated by J. Franck and his coworkers[18,20] is the idea that the fluorescence yield is determined by the ratio of the Chl a sites unavailable for photochemistry to those that are available to it. Chl a becomes photochemically inert by association with oxidized metabolic intermediates, presumably sugar photoperoxides, whose supply varies with the light history of the sample. Franck's theory can be discounted not only because it assumes direct reduction of CO_2 by Chl a and disregards the concept of a functional photosynthetic unit, but also because it takes for granted that lyophilic oxidized metabolites (sugar peroxides) can have access to the lipophilic Chl a sites. In addition, neither the existence nor the proposed role of the above-mentioned deleterious intermediates has ever been confirmed.

An alternate origin of the second wave fluorescence transient

can be inferred from the work of O. Kandler,[37] who demonstrated that the inorganic phosphate content (and inversely the ATP content) in Chlorella, shows a negative induction during a light period. In a subsequent dark interval, the change is reversed with the inorganic phosphate induction wave becoming positive. The negative induction lasted for 5 min., a duration typical also for the second wave of fluorescence in Chlorella. Kandler[38] also found that the CO_2 content has a negligible effect on the phosphate kinetics and that the light driven phosphorylation is independent of the presence of KCN.

Employing a more sensitive technique (ATP requiring luminescence of the firefly enzyme), Strehler[39] directly showed induction phenomena in the photosynthetic ATP production, in Chlorella, which he correlated with the fluorescence induction (fig. 3, left). In addition, the light intensity dependence of the steady state ATP content has an optimum, while its rate of formation follows a sigmoid saturation curve (fig. 3, right). Although the above results imply a relationship between photophosphorylation and the second wave of fluorescence induction, they do not, however, explain how it is achieved.

The fluorescence yield changes during the second wave may actually represent changes in the rate of internal conversion. That such processes occur is evident from the fact that complete inhibition of the photosynthetic electron flow raises the fluorescence yield only to 0.1. Since the amount of fluorescing pigments in a cell is, in all likelihood, constant during the experiment, a possible way by which the induction can

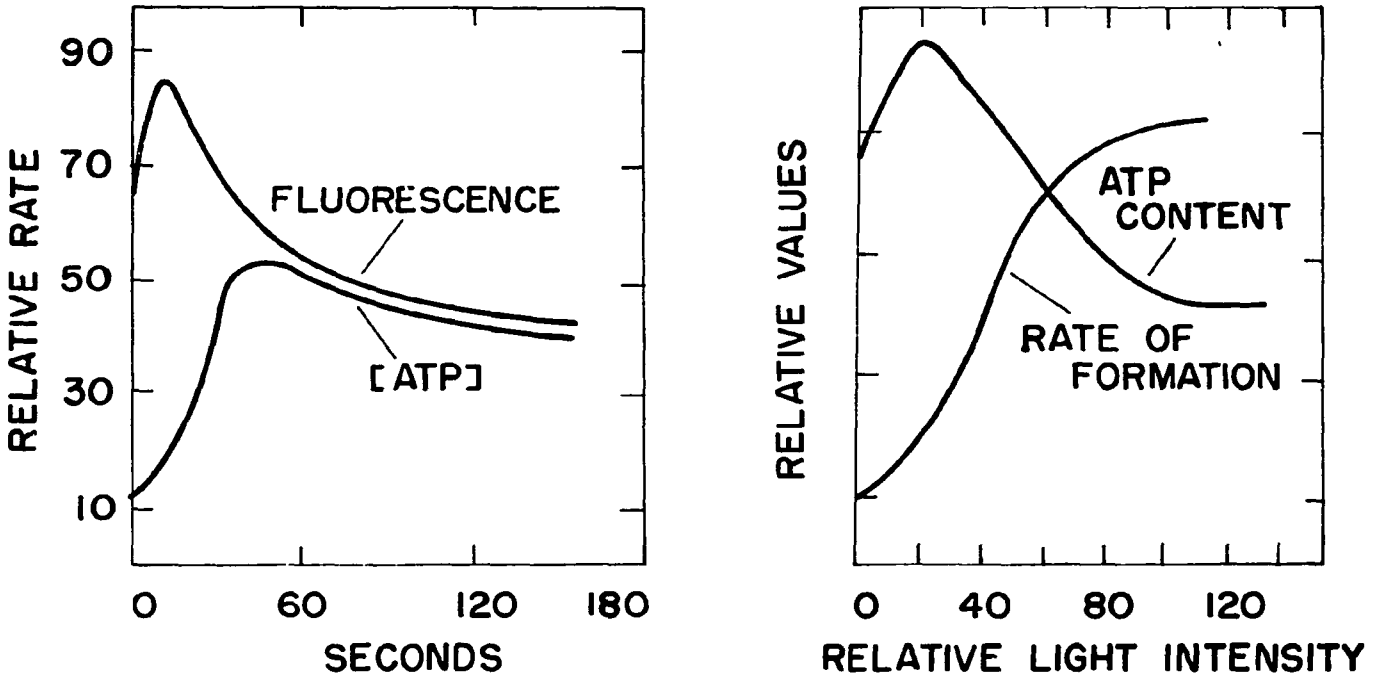

Fig. 3. Left: Time course of the fluorescence and ATP concentration in Chlorella. Right: Steady-state ATP content and initial rate of ATP formation in Chlorella; (redrawn from Strehler[39]).

occur is through a change in the spatial relationships between the pigment molecules, caused by light induced changes in the structure and the shape of chloroplast membranes; these changes will be referred to as "conformational" changes in this thesis. Such changes have been shown to occur and to be associated with the phosphorylation of ADP in both chloroplasts[40] and in mitochondria[41].

It is known that the terminal step of ADP phosphorylation in isolated chloroplasts is preceded by a light activated readjustment of the ionic equilibria between the suspension medium and the chloroplast. On illumination, an acidification of the chloroplast interior takes place increasing the pH of the medium.[42] The proton influx is followed with a somewhat slower cation (K^+, Mg^{++}) efflux,[43-45] by which the charge neutrality requirement is fulfilled, and by an even more slow H_2O efflux to establish the osmotic equilibrium. The concentration gradients formed in this manner provide, according to Mitchell's chemiosmotic hypothesis,[46] the required energy for the phosphorylation of ADP. Indeed, it has been shown that an ATP forming potential (X_E, high energy intermediate) is accumulated by illumination of chloroplasts at acidic pH, which on injection of the sample in the dark, into an alkaline medium, is converted into ATP.[47]

Whether X_E, which is supposed to denote a state of large concentration gradient, represents an intermediate in the reaction sequence which couples the electron transport to the terminal phosphorylation (energy conservation sequence) or a side effect, is not yet decided.

Because the rate of formation of X_E is smaller than that of ATP, Jagendorf[48] favors the second of the two possibilities given below.

(1) $\text{e-flow} \longrightarrow X_E \longrightarrow \text{ATP}$

(2) $\begin{array}{ccccc} \text{e-flow} & \longrightarrow & I & \longrightarrow & \text{ATP} \\ & & \upharpoonleft\!\downharpoonright & & \\ & & X_E & & \end{array}$

In the second scheme, X_E still has the character of an ATP forming potential, but now it exists as a storage reservoir operating through an unidentified non-phosphorylated intermediate I.

The light induced ionic shifts and the concomitant readjustment in the osmotic equilibrium are considered to be the causes for the "conformation" changes of the chloroplast lamellae and of the plastid as a whole, which occur in the transition from dark to light. Light induced chloroplast shrinkage manifests itself as increased light scattering, which was measured at a spectral region of minimal absorption.[49] The light induced scattering increase corresponds to gross deformations in the volume, shape, and the internal structure of the plastid.[45, 49, 50-52] Similar phenomena have also been observed with algal chloroplasts _in situ._[53] The correlation of the light induced structural changes with the ionic shifts that precede the terminal phosphorylation step is based on the following observations: (i) The kinetics of the acidification of the chloroplast interior, formation of X_E, and light scattering increase are similar.[45, 47, 54-55] (ii) Conditions unfavorable for X_E accumulation, such as high pH and optimal rate of ADP phosphorylation, suppress the scattering changes and _vice versa_.[47, 54] (iii) Compounds

which uncouple the photosynthetic electron flow from the energy conservation sequence (photophosphorylation uncouplers) abolish the scattering changes. Inhibition of the electron flow has the same effect.[54, 56-58]

The recent experimental evidence on the mechanism of photophosphorylation, reviewed in the preceding paragraphs, introduces a new possibility as to the origin of the second wave of fluorescence induction phenomena, namely their association with the "conformational" changes of the pigment carrying lamellae. The second wave changes of the green alga Chlorella pyrenoidosa and the long-term changes in fluorescence of the blue-green alga Anacystis nidulans and their dependence on the photophosphorylation have been examined in this work. The influence of experimental variables, such as the exciting light intensity, the pH of the medium, the presence of photosynthesis and phosphorylation inhibitors, was studied systematically. In addition, we investigated the relationship between the oxygen evolution kinetics and those of the second wave of fluorescence, as well as the effects of preillumination on the spectral distribution of the emitted fluorescence.

In spite of the established differences in the time course of fluorescence of these two algae, the evidence we obtained indicates that in both cases an indirect relation exists between the second wave fluorescence transients and photophosphorylation. (No direct measurements of the rate of phosphorylation were made.) In this respect, therefore, this work contributes to the understanding of the second wave changes of the fluorescence yield, first observed more than three decades ago and since then defying attempts for interpretation.

II. MATERIALS AND METHODS

A. THE ALGAE AND THEIR CHARACTERISTICS

1. Chlorella pyrenoidosa

Chlorella pyrenoidosa, a unicellular green alga (Chlorophyta) is the par excellence organism in photosynthesis research. The cell has an average diameter of about 5 μ, and contains a single cup-shaped chloroplast occupying most of the cellular volume. There are 32 layers (lamellae) running parallel to the chloroplast outer membrane on which the chlorophyll molecules are organized.[59] As shown in Table I, the estimated interfacial area available for each chlorophyll molecule is 95 $\text{A}^{\circ 2}$. Since the area of the rigid flat porphyrin ring is 225 $\text{A}^{\circ 2}$, the chlorophyll molecules must be tilted relative to the interface. Assuming no overlapping of the porphyrin rings, an inclination angle of 65° is estimated. Less steep positioning, of course, is possible in the case of some overlapping. Table I presents some characteristics of the Chlorella chloroplast.

The principal photosynthetic pigments of Chlorella are chlorophyll a (Chl a) and the accessory pigment chlorophyll b (Chl b). There is significant absorption by carotenoids in the blue end of the absorption spectrum of this alga. They appear, however, to be relatively inefficient in photosynthesis.[11, 60] Chl a exists in vivo in more than one, presumably holochromic or aggregated, forms[14] and is a member of both the photosynthetic pigment systems, while Chl b functions preferentially in pigment system II. The absorption spectrum of a Chlorella suspension in the visible range, shown in fig. 4, has the characteristic two-band

TABLE I

CHARACTERISTIC QUANTITIES OF THE CHLORELLA PYRENOIDOSA CHLOROPLAST*

PROPERTY	MAGNITUDE
Average chloroplast diameter	3.2 μ
Average chloroplast volume	1.2×10^{-11} cm^3
Total chlorophyll concentration in the chloroplast	7.2×10^{-2} M
Total number of chlorophyll molecules per chloroplast	5.5×10^{8}
Total interfacial area available to chlorophyll	510×10^{8} $\mathring{A}^2$
Interfacial area available per chlorophyll molecule	95 $\mathring{A}^2$
O. D. (at 680 nm) of a chlorophyll monolayer with 95 Å area per molecule	0.008

*Data from R. A. Olson and E. K. Engel.[59]

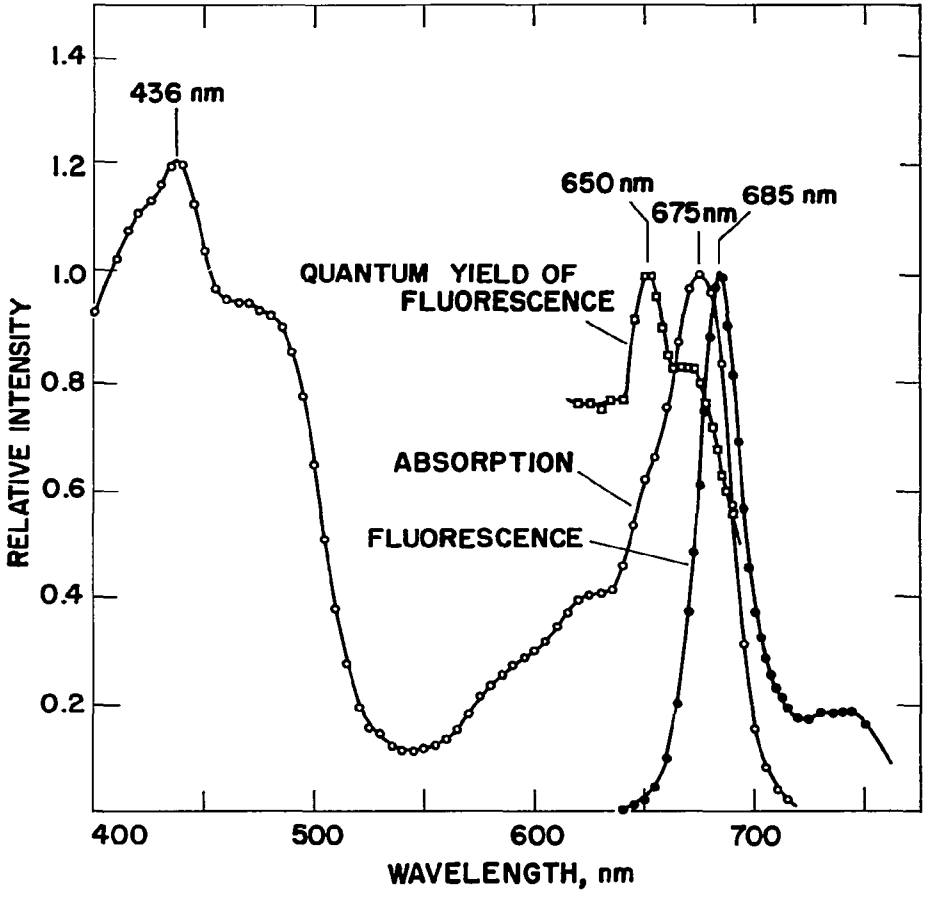

Fig. 4. Absorption and fluorescence spectra and the quantum yield of fluorescence as a function of the wavelength of excitation in Chlorella pyrenoidosa.

structure [blue (436 nm) and red (678 nm) absorption bands] of chlorophyll containing organisms. The fluorescence spectrum consists of the red Chl a emission band (685 nm); Chl b is non-fluorescent in vivo since it transfers its excitation to Chl a with high (~ 100 %) efficiency.[11] Thus, Chl a fluorescence can be excited either directly in the Chl a absorption bands or by sensitization through Chl b. The strong overlapping of the absorption spectra (of Chl b and Chl a) does not allow for exclusive direct excitation or sensitization.

It has been reported by Teale[61] that the quantum yield of Chl a fluorescence in Chlorella is constant in the spectral region 600 to 690 nm. We were unable to confirm this result, in a long series of experiments in which we employed narrow excitation bands (half-band width 6.6 nm) and a wide observation band (half-band width 26.4 nm) centered at 750 nm. Our results indicate (fig. 4) that the "red drop" of fluorescence begins at about 675 nm. In addition, the quantum yield spectrum has a maximum at 650 nm, where Chl b has its absorption maximum. This would be explained if a fraction of the Chl a complement of the alga is non-fluorescent, while Chl b tranfers its excitation preferentially to the fluorescent form. Similar results have been obtained also by Govindjee[62] in Chlorella and by Litvin and Sineschekov[63] in Elodea.

The absorption and emission spectra of Chl a and Chl b in solution are shifted toward shorter wavelengths and have narrower half-band widths than that of Chlorella.[9] The exact location of the band maxima depends on the polarity of the solvent; solvents with high dielectric constants

displace the maxima toward the blue.[9, 64, 65] The shape of these spectra is almost Gaussian. The absorption spectra of various photosynthetic organisms have been analyzed[66, 67] by assuming that the in vivo spectra of chlorophyll a forms are also Gaussian. In Chlorella, three forms of Chl a (characterized by their absorption maxima), Chl a 670, Chl a 680, and Chl a 694, have been identified.

2. Anacystis nidulans

Anacystis nidulans, a unicellular blue-green alga (Cyanophyta), is the second photosynthetic organism we employed in this investigation. The cell lacks a chloroplast having only three incomplete concentric lamellae running parallel to the cell wall on which the photosynthetic pigments are organized. As shown in table II, the available interfacial area per Chl a molecule is 272 $\mathring{A}^2$, sufficient to accommodate the porphyrin ring at 0° angle to the lamellar plane. Table II lists some characteristics of Anacystis nidulans cells.

Typical of the pigment composition of this alga is the absence of Chl b, its function being taken by the biliprotein (phycobilin) phycocyanin (PC). The absorption spectrum (fig. 5) shows the phycocyanin band peaked at 625 nm and the two Chl a bands. The shoulder at the long wavelength side of the blue band is due to carotenoids. The ratio of Chl a to phycocyanin content is determined by the intensity of the light provided to the cells during culturing.[68] Strong illumination suppresses the phycocyanin band, so that its height becomes smaller than that of Chl a, while weak illumination has the reverse effect. We characterize the two types of

TABLE II

CHARACTERISTIC MAGNITUDES OF ANACYSTIS NIDULANS CELLS*

PROPERTY	MAGNITUDE
Average cell length	$2.67 \pm 0.82\ \mu$
Average cell diameter	$0.22 \pm 0.01\ \mu$
Average cell volume	$1.58 \times 10^{-12}\ cm^3$
Chlorophyll a concentration in the cell	1.44×10^{-2} M
Phycocyanin concentration in the cell	$3.44 - 6.88 \times 10^{-4}$ M
Number of chlorophyll a molecules per cell	1.3×10^{7}
Number of phycocyanin molecules per cell	$3.27 - 6.54 \times 10^{5}$
Pigmented cortical volume	$6.43 \times 10^{-13}\ cm^3$
Cortical chlorophyll a concentration	3.55×10^{-2} M
Cortical phycocyanin concentration	$4.24 - 8.52 \times 10^{-4}$ M
Total interfacial area available to chlorophyll a	$1.83 \times 10^{9}\ \text{Å}^2$
Interfacial area available per chlorophyll a molecule	$272\ \text{Å}^2$

* Data from J. A. Bergeron,[74]

cultures as "high light" and "low light" Anacystis. Actually, it is impossible to provide homogeneous illumination to all the cells of a culture; in particular, a "high light" sample is a mixture of high light and low light cells. Predominantly low light Anacystis was used in all the experiments that we performed.

The shape of the fluorescence spectrum of Anacystis nidulans depends primarily on the absorption band in which it is excited. Excitation in the blue gives an almost pure Chl a emission band, while excitation in the orange (phycocyanin absorption) results in emission from both phycocyanin and Chl a (fig. 5). The shape of this spectrum depends on the light history of the sample and the integrity of the photosynthetic process. Low light cells are characterized by increased Chl a fluroescence as compared to high light cells.[68] Strong variations in the time course of fluorescence will be described in the experimental part (Chapter IV, Section B). Finally, poisoned Anacystis is characterized by a dominant Chl a fluorescence band.

To obtain the absorption and emission spectra of phycocyanin in solution, a crude extract in 0.05 M phosphate buffered at pH = 4.7, was twice purified by precipitation with $(NH_4)_2SO_4$ at half saturation.[69] The purified phycocyanin was readily soluble in the phosphate buffer. For the fluorescence measurements the optical density of the sample was adjusted to 0.50 (0.05 for 1 mm path in the sample holder). The absorption and emission spectra of phycocyanin are shown in fig. 6. The location of the absorption band is almost identical with that in Anacystic cells.

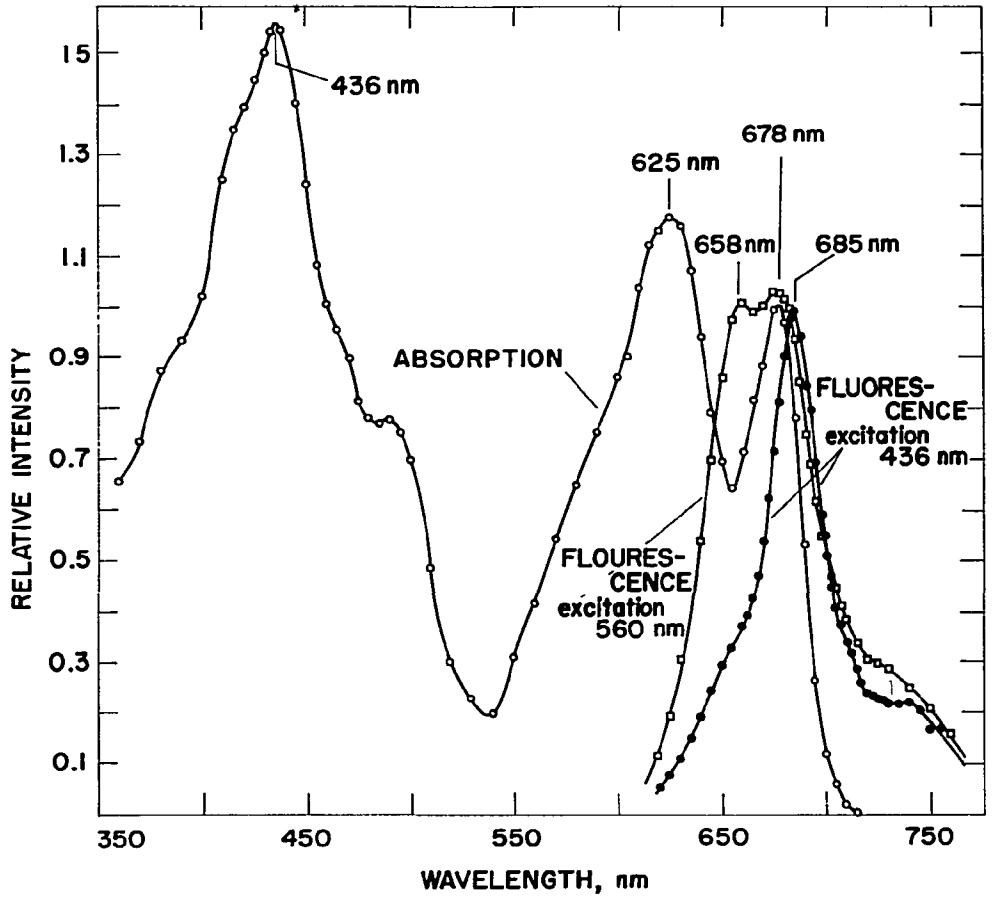

Fig. 5. Absorption and fluorescence spectra of Anacystis nidulans. Fluorescence spectra excited at 560 nm (in the phycocyanin absorption band) and at 436 nm (in the Chl a absorption band); the fluorescence bands have been adjusted to equal heights at 685 nm; the spectra were recorded with different samples.

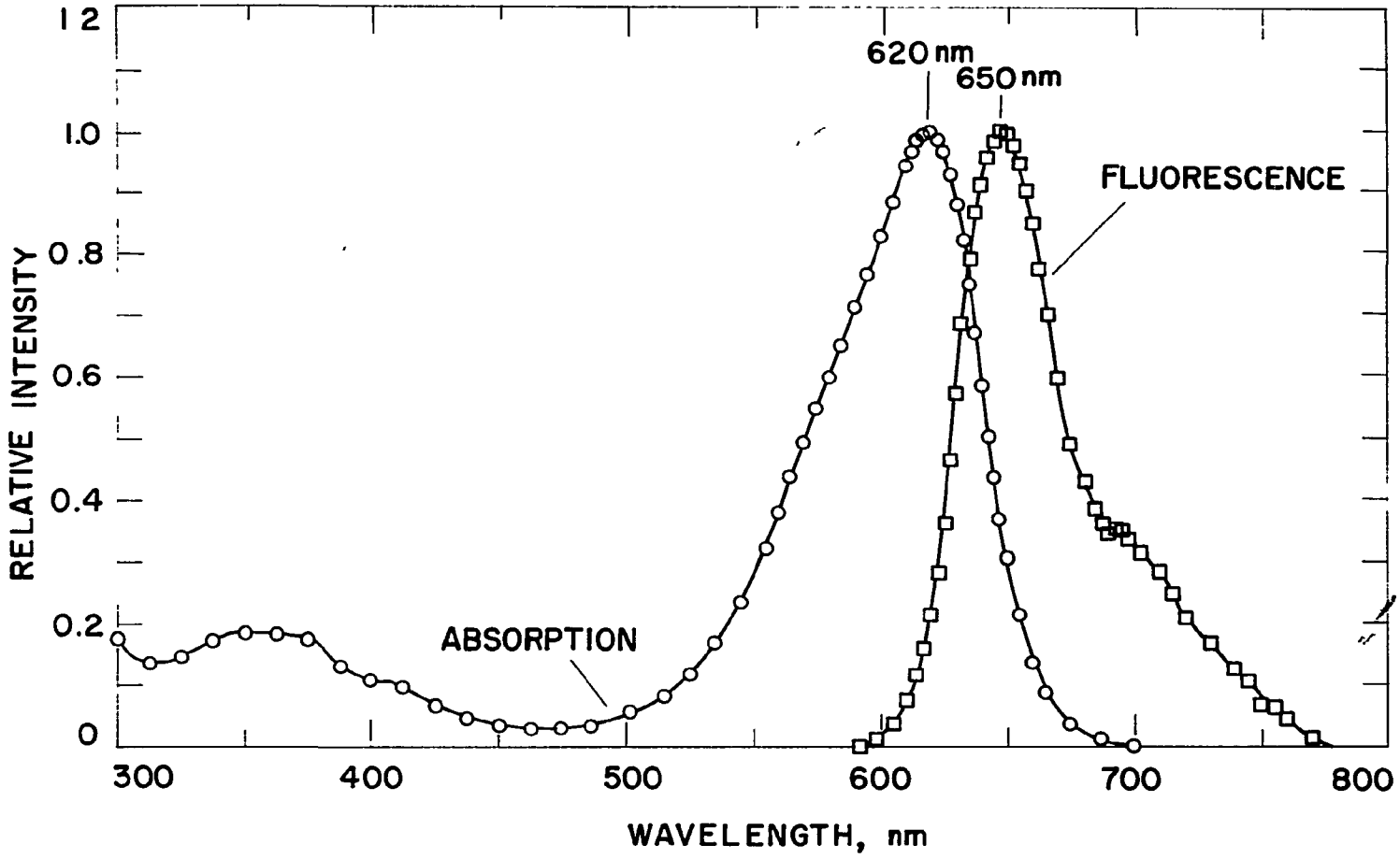

Fig. 6. Absorption and emission spectra of pure phycocyanin.

B. CULTURING OF ALGAE AND SAMPLE PREPARATION

Chlorella pyrenoidosa and Anacystis nidulans were cultured under white light in inorganic media as described by Govindjee and Rabinowitch.[70] Three to six-day-old cultures were transferred into a tris-amino methane HCl, 0.02 M, NaCl 0.04 M (Tris-NaCl) buffer and their optical densities were adjusted to 0.5 units at the red Chl a absorption maximum for 1 cm path. This medium was selected because of its good buffering capacity in the pH range 6.5 to 9.0. Unless otherwise specified, the pH of the samples was 8.0. The surface to volume ratio of the sample, in the sample holder, was about 10, this allows a fast equilibration with the atmospheric air and the alkaline pH is favorable for CO_2 absorption. Various additions were made at least 15 min. prior to the measurements. A dark interval of 15 min. preceded all measurements. This was essential not only for the establishment of dark steady-state conditions in each sample, but also to allow for the completion of the sedimentation of the cells in the sample holder. The total chlorophyll content of our samples measured according to the method described by McKinney[71] was 18 μg Chl/ml (approximately 2×10^{-5} M) in Chlorella and 8 μg Chl a/ml (approximately 8.0×10^{-5} M) in Anacystis. Unless otherwise stated all experiments were done at room temperature.

C. INSTRUMENTATION

The absorption spectra were measured with a Bausch and Lomb

double beam recording spectrophotometer (Spectronic 505) equipped with an Ulbricht integrating sphere in which both the sample and the reference are placed. The sphere is coated on the inside with MgO, whose diffuse reflection insures that all the scattered light will eventually reach the photodetector (see Appendix I). The instrument provides a measuring beam of 5 nm half-band width. The absorption spectra of phycocyanin in solution were measured with a Model 14 double beam Cary Spectrophotometer, provided with a double monochromator (prism and grating) and having variable entrance and exit slits ($0 \rightarrow 3.0$ nm).

The fluorescence measurements were carried out with the recording spectrofluorometer described by Govindjee.[72] The instrument shown in fig. 7 consists of two large Bausch and Lomb grating monochromators (3.3 nm half-band width per mm slit aperture) equipped with mechanical drives for the automatic scanning of the excitation and the emission spectra. The light source is a 6v, 18 amp, tungsten (W) ribbon filament lamp; monochromatic light (for excitation) is obtained by passing the light through the "excitation" monochromator. A second, 750 watt excitation lamp may be used as an additional light source, in conjunction with Corning colored glass or narrow band interference filters (Farrand Optical Co., Inc., New York, N.Y. or Baird-Atomic, Inc., Cambridge, Mass.).

The optical arrangement of the instrument is such that a "front-face" collection of the emitted fluorescence is achieved. This arrangement, as well as the low optical density of the samples (0.05 units for

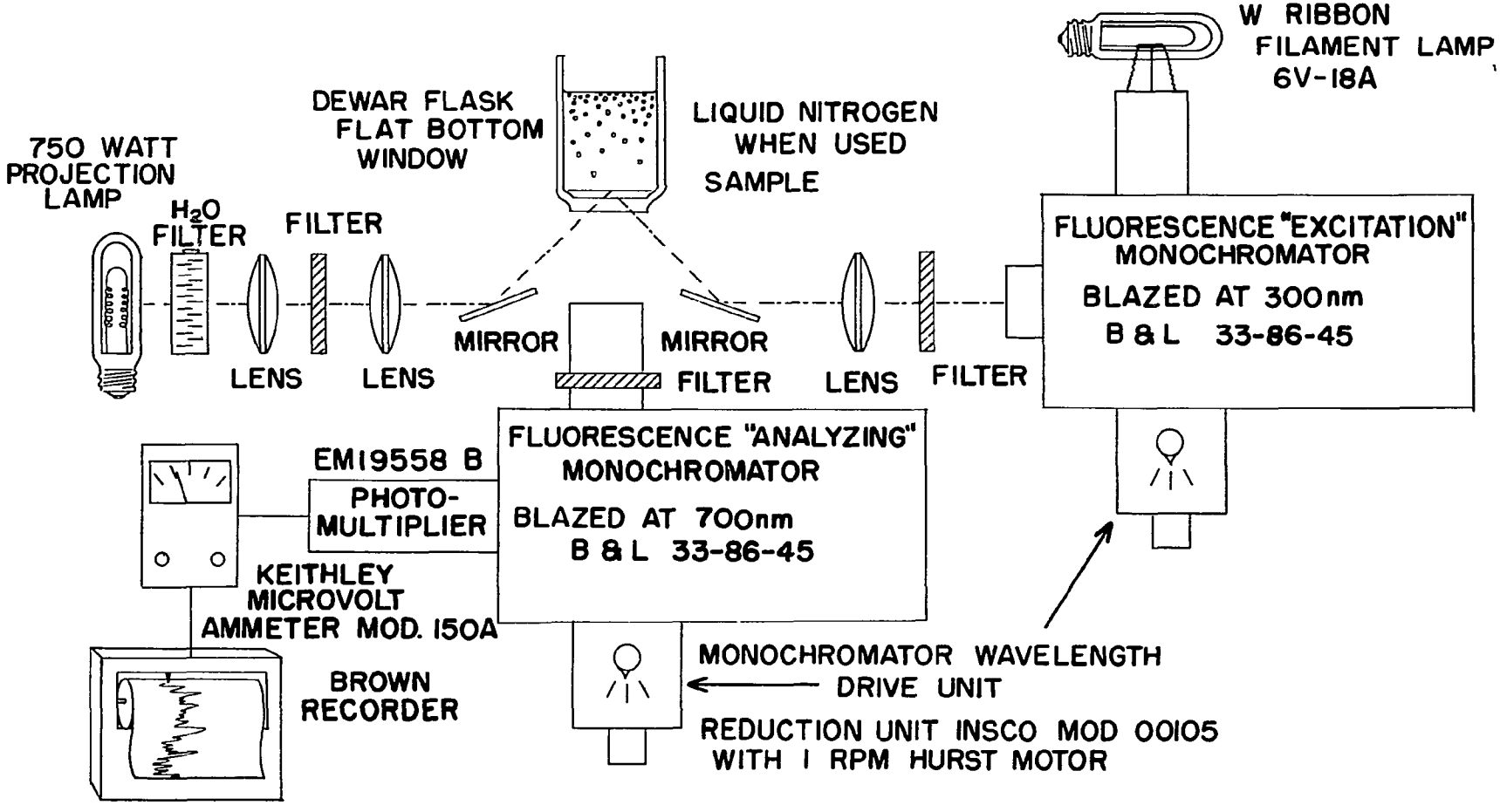

Fig. 7. Fluorescence instrument: Block diagram (not drawn on scale).

1 mm thickness) are advantageous because they minimize the reabsorption of fluorescence (See Appendix II). Reabsorption within the cell, however, possible because of the high Chl a concentration in the chloroplast, is always an undetermined factor in the spectroscopy of cell suspensions.

The fluorescence is scanned by the "analyzing" monochromator. Admission of the exciting light in this monochromator was prevented by appropriate colored glass sharp cut-off filters. The selected fluorescence band was detected by an EMI 9558B photomultiplier (Electra Megadyne Inc., New York, N.Y.) and the electric signal was amplified by a model 150A Keithley microvolt ammeter (Keithley Instruments, Cleveland, Ohio) and finally recorded with a Brown recorder (Brown Instrument Division, Minneapolis-Honeywell Reg. Co., Philadelphia, Pa.) equipped with a variable chart speed (Insco Corp., Groton, Mass.) attachment.

Light intensity was measured with a Bi/Ag Eppley thermopile (the Eppley Laboratory, Inc., Newport, R.I.). The reduction of the excitation intensity to a given fraction was accomplished with Balzer's neutral density filters (Geratebauanstalt, Balzers, Furstentum, Liechtenstein). The transmittance of these filters was always determined before the fluorescence measurements.

Oxygen evolution measurements were performed with the Pt-electrode polarograph described by Bannister and Vrooman.[73] The instrument consists of a flat Pt cathode, on which the cell paste is deposited and a large area Ag/AgCl reference anode. The two electrodes were immersed in an electrolyte solution (tris-NaCl buffer, pH = 8.0),

stirred constantly by a stream of 5% CO_2 in air. The sample was excited by monochromatic light from a Bausch and Lomb grating monochromator. The current, generated by a negative potential of 0.55 v applied to the Pt cathode, and amplified by a model 150A Keithley microvolt ammeter was recorded with a Varian G10 chart recorder (Varian Associates, Palo Alto, Calif.). The current is proportional to the rate of oxygen delivery to the cathode, where it is reduced to H_2O. Because of the immediate contact of the sample with the electrode diffusion delays were minimal. The rate of the photosynthetically evolved oxygen is proportional to the difference of the electric signals obtained in the presence and in the absence of exciting illumination, the latter being taken as correction for the respiratory oxygen uptake,

The pH of the sample was measured with a Beckman glass electrode pH meter (Beckman Instruments, Inc., S. Pasadena, California).

D. PRESENTATION OF THE EXPERIMENTAL RESULTS

Only a small fraction of the total emitted fluorescence enters the analyzing monochromator. Because of the light scattering, the profile of the emitted fluorescence is not spherical. Consequently, it is difficult to measure the fluorescence per spectral interval in absolute energy units and thus the fluorescence intensities are given in relative units. However, the relative emission spectra are corrected for the wavelength dependence of the photomultiplier sensitivity and the transmission efficiency of the analyzing monochromator. For reasons

given in Appendix II, no correction for the reabsorption of fluorescence is needed.

The results of the fluorescence intensity time course experiments are given in terms of the ratio $f = F_t:F_3''$, where F_t and F_3'' correspond to the intensity values at t and 3 seconds of total light exposure. F_3'', which is our first recorded signal, corresponds to the S level of the first wave. Since the absorbance of the sample is invariable during the experiment (the pigment content is the same), the ratio f is a measure of the relative fluorescence yield and can be set equal to $\Phi_t:\Phi_3''$. This representation was selected because the relative yield values are independent of such factors as the exact number of the cells in the light field and the precise positioning of the sample.

Oxygen evolution rates are also presented in relative units.

Spectral data, such as wavelengths and band widths of excitation and observation, filters and excitation intensities and the concentrations of compounds added to the samples, are all given in the legends of the figures.

III. THE LONG-TERM FLUORESCENCE INDUCTION IN CHLORELLA PYRENOIDOSA: RESULTS AND DISCUSSION

A. FLUORESCENCE INDUCTION IN CONTINUOUS AND FLASHING LIGHT

The time course of fluorescence in Chlorella pyrenoidosa corresponds to the type II of fig. 2. A typical second wave induction curve (illumination, 436 nm) is shown in fig. 8. On excitation, the relative fluorescence yield f (F_t:F_3'') rises rapidly to a maximum M, thereafter declining at a much slower rate to a terminal stationary level T. At that stage, the fluorescence yield is lower than the minimum between the two waves (S level). The rise portion S→M of the second wave is clearly biphasic (cf. insert in fig. 8), consisting of an initial minor rise phase and a second more extensive one. We observed similar fluorescence time courses with Chlorella suspended in a variety of buffers, including carbonate-bicarbonate, tris-aminomethane hydrochloride (tris-HCl) and phosphate buffers. For the experiments to be presented in this chapter, the tris-HCl, NaCl medium, described in Chapter II, was employed.

The second wave is perfectly reproducible in a given sample, provided an adequately long dark period is interposed between two successive light exposures. This observation led us to investigate the behavior of the relative fluorescence yield during a dark interval which succeeds a light period. The relative yield values were calculated as the ratios of the fluorescence intensity recorded by the flash over that at 3 sec of light exposure in the beginning of the experiment. We checked the possibility of distortions introduced by the brief light interruptions, (1) with low

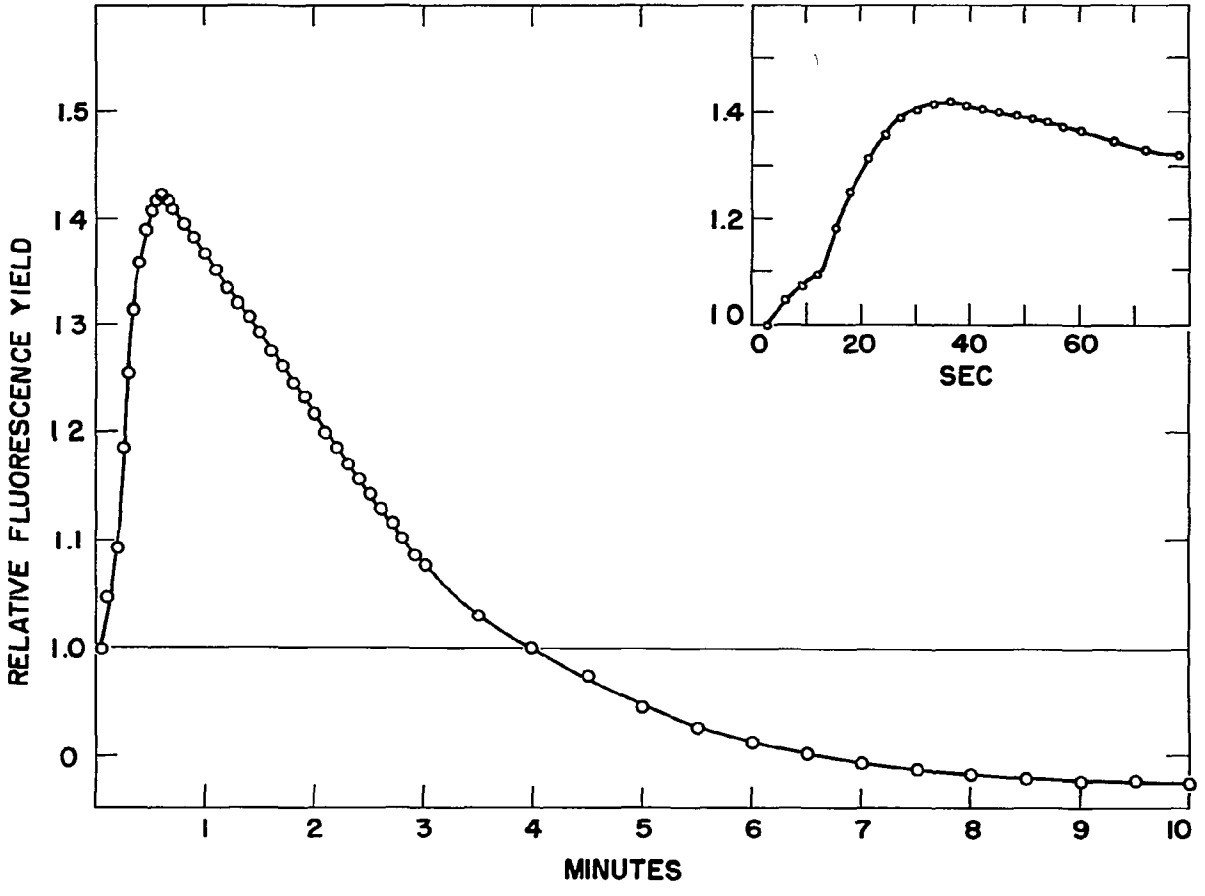

Fig. 8. Time course of the relative fluorescence yield ($f = F_t : F_3''$) in Chlorella Pyrenoidosa. Excitation: λ = 436 nm; half-band width, 10 nm; incident intensity, 10^3 ergs. cm.$^{-2}$ Observation: λ = 685 nm; half-band width, 16.5 nm; Corning filter, C.S. 3-69. Insert: Data up to 80 sec. drawn on an expanded time scale.

intensity (5-10% of the intensities in the preceding light period) flashes and (ii) by varying the spacing between the flashes in consecutive experiments so that different light doses were given to the sample in each case. The very nearly identical fluorescence time courses obtained with either of the two procedures indicate that the brief light interruptions do not alter significantly the values of the relative fluorescence yield in the dark interval.

Fig. 9 shows the kinetics of the relative fluorescence yield in the dark (curves A, B, C), and the typical second wave of the sample in light (curve W). It is apparent that the time course depends on the length of the preceding light exposure. After 20 sec illumination, i.e., in the fast rising phase of the second wave, shutting off the excitation results in an abrupt decrease of the fluorescence yield followed by a slower decay to a minimum, after which it rises slowly and approaches the level at S. Similar results are obtained when the second wave is interrupted in the decay portion M-T (curve B). Since curves A and B are almost superimposed, we conclude that a brief light exposure (e.g., 20 sec as for A) is sufficient to trigger a light independent process which effects a decrease in the fluorescence yield. This change is opposed by a second dark process, as a result of which the fluorescence yield attains a minimum value in the dark, thereafter increasing toward the S level. Very short flashes (2-3 sec), interrupting a long dark period, were found insufficient to trigger the dark induction phenomena. When the excitation is removed at the completion of the second wave, only an increase of the fluorescence yield during the subsequent dark interval

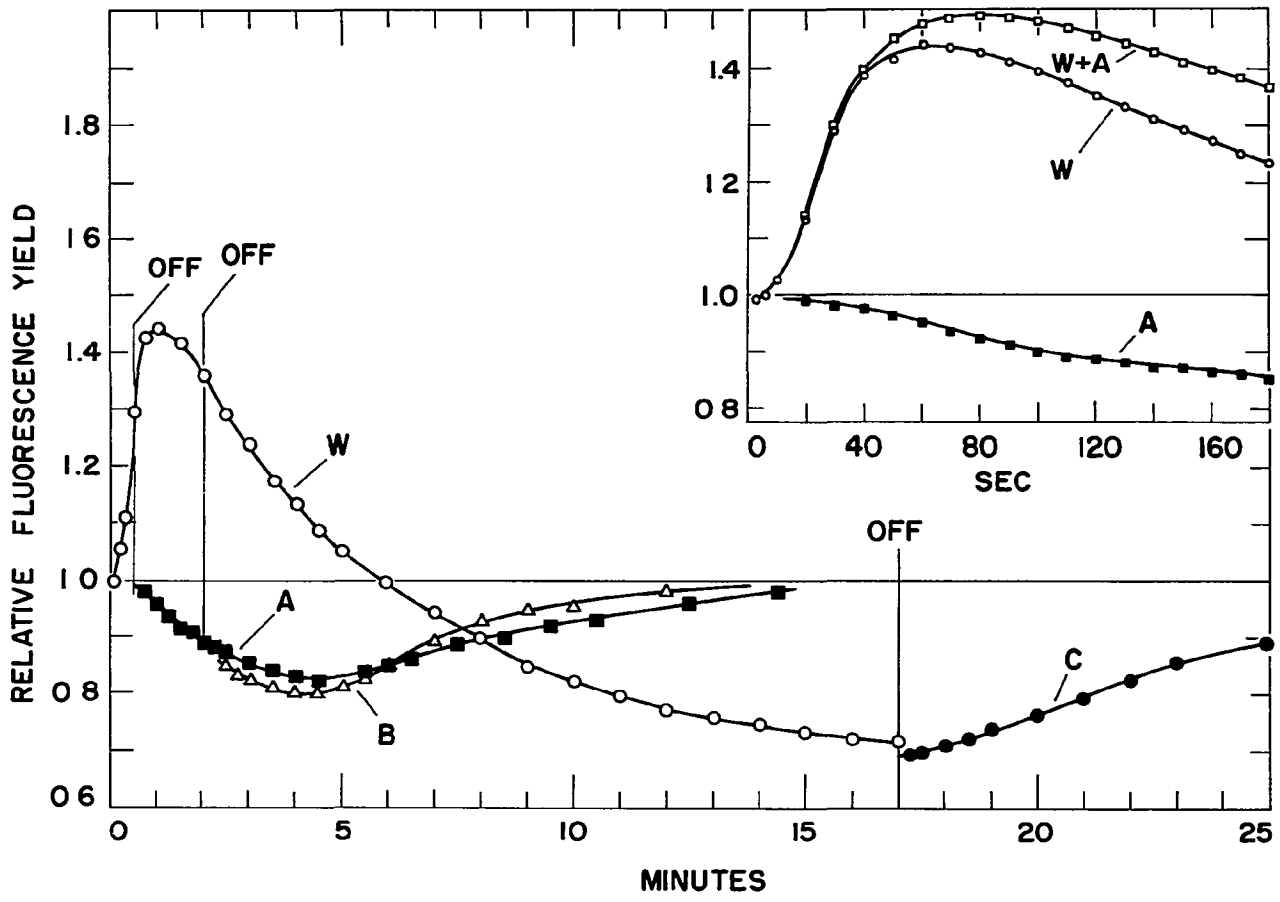

Fig. 9. Time course of the relative fluorescence yield in continuous and in flashing light in Chlorella. In continuous light (W); in the dark, measured with light flashes (A, B and C). Excitation: Blue band, Corning filter, C.S. 5-56; half-band width, 130 nm; incident intensity, 2.5×10^3 ergs. $cm.^{-2}$ $sec.^{-1}$ Observation: λ = 685 nm; half-band width, 16.5 nm; Corning filter, C.S. 2-60. Insert: Data up to 3 min. drawn on an expanded time scale (W and A); fluorescence induction in the absence of dark changes (W + A).

is registered (curve C), indicating that the light triggered decay of the yield has been completed.

The foregoing discussion suggests that continuous illumination of Chlorella induces not only the known light dependent increase but also a light triggered dark decrease in the fluorescence yield. To answer the question whether the overall second wave time course is determined by the interplay of these two processes, we plotted the sum W + A (fig. 13, insert). This plot corresponds to a second wave transient which is independent of the light triggered dark process. The decay of the curve W + A suggests the possibility of a photochemical process which effects a decrease in the fluorescence yield.

Our results, therefore, indicate that a minimum of four processes participate in the second wave of fluorescence induction. Two of them are light-dependent, having opposing effects on the fluorescence yield. A third one requires a minimum of light dose, but proceeds in the absence of simultaneous excitation and it is opposed by the fourth dark process. The triggering of the dark induction changes is reminiscent of the post-irradiation overshoot of the pH of the suspension medium[57] and of the light scattering increase in chloroplasts.[47] Both these changes exhibited typical induction curves consisting of an increase to a maximum and a subsequent decay. Prolonged illumination suppressed any post-irradiation overshoot of the pH.

The important feature of the changes in the fluorescence yield in the dark is their occurrence in the absence of sustained photosynthetic

electron flow. It could be argued that the second wave originates from a gradual shift of the oxidation potential of a pool of intermediates to more negative values, as a result of which the probability of photochemical quenching of the Chl a excitation will be diminished. The light dependent decay of the fluorescence yield, however, cannot be accounted for by this interpretation; neither can the increase in the dark (fig. 13, curve C). Additional evidence will be presented later (section G) in support of our contention that there is no direct correlation between the rate of the photosynthetic electron flow and the second wave fluorescence transients.

B. CHANGES IN THE EMISSION SPECTRUM DURING THE FLUORESCENCE INDUCTION

In 1956, Rabinowitch[9] (p. 1376) wrote: "Nothing is known so far of the changes in the fluorescence spectrum of chlorophyll, which are not impossible, if the chemical structure of chlorophyll itself, or of its associates in the 'photosensitive complex', undergoes changes in the transition from darkness to light and back". Since then, it has been established that during the first wave the fluorescence varies more at 685 nm (main Chl a emission maximum, primarily system II emission) than at 716 nm where the contribution of system I is significant[75-77]. Nothing, however, was reported up to now about the changes in the fluorescence spectrum during the second wave. Since more than one form of Chl a contributes to the red emission band, we investigated the spectral changes during the second wave in the hope that we would

identify the variable fluorescent component.

We employed a special technique to record the emission spectra at the various second wave stages because of the rapidity with which the fluorescence yield changes. However, in the terminal stationary state T, where the fluorescence yield remains constant, the spectrum was recorded automatically. Spectra corresponding to the level S and the maximum value M were constructed from the fluorescence induction curves observed at different wavelengths Dark intervals of adequate length were interposed between two successive observations and the return of the system to the dark steady level (S) was assured by following the dark time course of the fluorescence yield with widely spaced excitation flashes.

The fluorescence spectra at the second wave stages S, M and T (fig. 10) are typical Chl a emission bands, having their maxima at 686 nm and half-band widths of 22 nm. The same peak location and half-band width characterize the difference spectra S-T, M-T and M-S, given in the insert of fig. 10.

C. INTENSITY OF EXCITATION

The second wave transient in Chlorella is obtained only when the organism is capable of photosynthesis, since addition of inhibitors which block the non-cyclic electron flow results in the obliteration of the fluorescence change (section E). The dependence of the second wave on the rate of the photosynthetic electron flow can be explored by varying the excitation intensity since these quantities are interrelated. It is

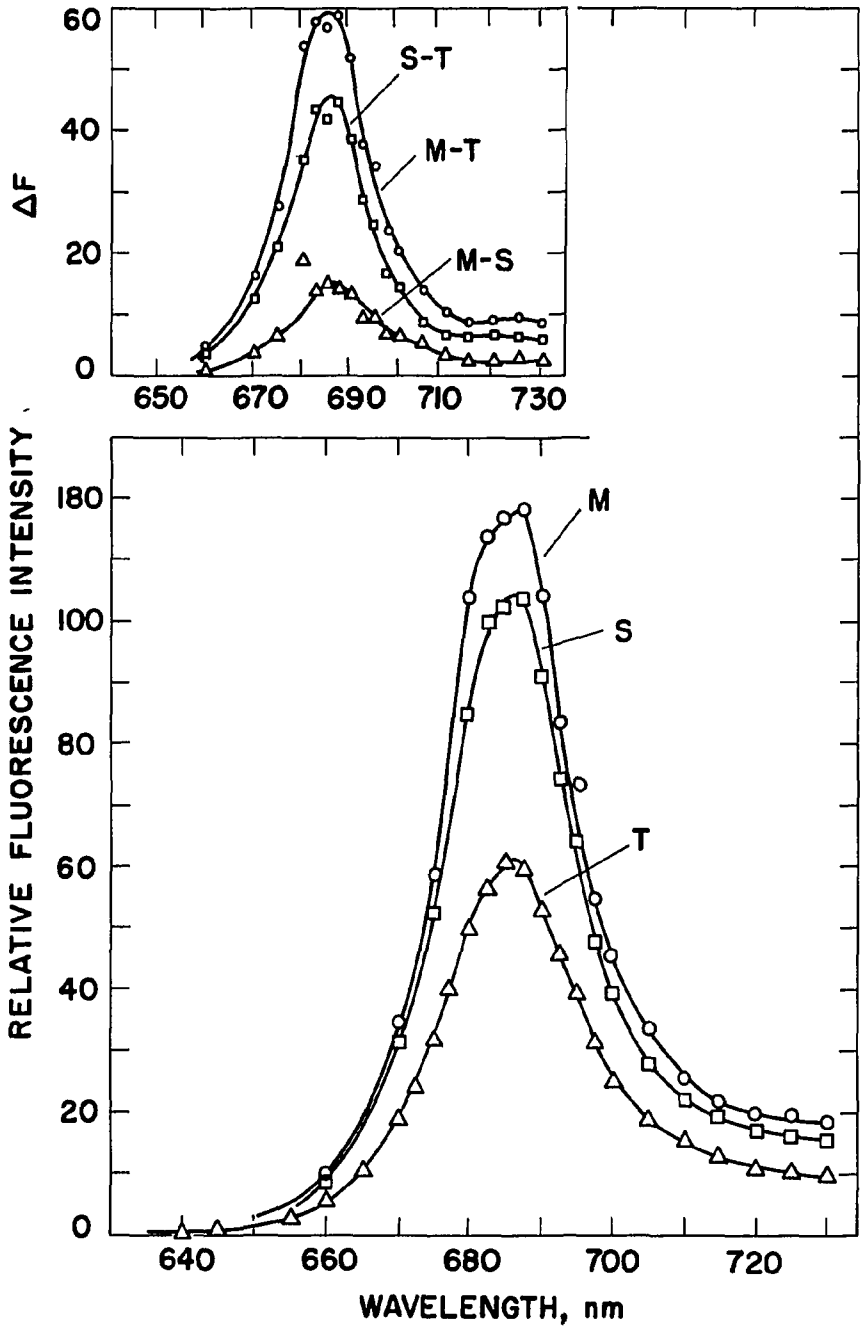

Fig. 10. Emission spectra of Chlorella at 3 sec. (S), 40 sec. (M) and 12 min. (T) of light exposure. Excitation: λ = 480 nm; half-band width, 10 nm, incident intensity, 1.4×10^{3} ergs. cm.$^{-2}$ sec.$^{-1}$ Observation: Half-band width, 6.6 nm, Corning filter, C.S. 2-63. Insert: Difference emission spectra (M - S, M - T, S - T).

known[9] that the rate of photosynthesis is proportional to the exciting light intensity at low values of the latter ($R \propto I$) and independent of it at high values (saturation); this is so because at weak intensities it is the rate of light absorption and at strong intensities, it is the rate of dark enzymatic reactions, which limit the overall rate of photosynthesis. In weak light, the fluorescence yield is low and constant, above saturation, however, this fluorescence yield more than doubles. Therefore, a plot of the steady-state fluorescence intensity, F, against the exciting light intensity, I (fluorescence light curve) consists of two linear portions; the second is twice as much inclined to the abscissa as the first. Light curves of this type, in which the fluorescence intensity corresponds to the terminal stationary level, were used to ascertain the establishment of the saturation of photosynthesis.

The above described behavior of the fluorescence yield is due to the dissipation of the Chl a electronic excitation by a set of mutually independent processes. Denoting the emission rate constant as K_f, the bimolecular rate constant of photochemical quenching as $K_c[Q]$ and the rate constant of internal conversion as K_r, the fluorescence yield (Φ_f) can be expressed as follows:

$$\Phi_f = F/I_{abs} = K_f/K_f + K_r + K_c [Q]$$

Here, F and I_{abs} stand for the numbers of emitted and absorbed photons per unit time while Q is the primary oxidant of system II. The fluorescence is generally assumed to originate mostly from pigment system II.

Q is reduced by the light reaction II to the non-quenching form Q^- which, in turn, is reoxidized by the light reaction I, through a series of enzymatic reactions. In weak light, it is the rate of the photon absorption that determines the rate of photosynthesis. With such excitation, the observed quantum yield of fluorescence is low and constant, while that of photosynthesis is high and constant; this implies a high and constant concentration of Q. At high excitation intensities the rate of the enzymatic reoxidation reaches a limit and fails to keep up with the photochemical reactions. The quantum yield of fluorescence at these intensities is known to be high and constant, implying a low and constant concentration of Q.

In weak light, the quantum yield of fluorescence is 0.03 while the quantum yield of the primary photoreduction of Q to Q^- (Φ_p) is high and can be set equal to 0.95. From the ratio $\Phi_f:\Phi_p$ and the natural fluorescence lifetime of Chl *a* (τ = 15.2 nsec) the rate constant of the photochemical quenching is calculated to be, $K_c[Q] = 1.44 \times 10^9$ sec^{-1}. At strong excitation a doubling of the fluorescence yield is observed. (This is an experimental fact[113] and not predicted by the equation on the last page.) Assuming that the rate of thermal deexcitation, K_r is invariable, we obtain $K_c[Q] = 0.68 \times 10^9$ sec^{-1}, which indicates a lower concentration of Q. (The doubling of the fluorescence yield in the transition from weak to strong excitation requires that the primary photochemical yield will be reduced from 0.95 to 0.90.)

Besides the above-mentioned effect of the exciting intensity on

the absolute Chl a fluorescence yield at the stationary state, the excitation intensity affects the fluorescence time course, but in a different way. Fig. 11 shows that the wave amplitude increases with the exciting light intensity, the second wave being hardly discernible for weak excitation. There is a biphasic rise at low intensities, which becomes monophasic at strong excitation and an initial short-lived negative induction appears. When the second wave is plotted in terms of the relative yield magnitudes (i.e., normalized at 3 sec illumination) as in fig. 12, an optimum excitation intensity for its amplitude is seen. The rise and the decay rates also exhibit a similar dependence on the light intensity.

Since the individual processes involved in the second wave cannot be isolated and studied separately, we chose to examine only the light intensity dependence of the terminal change, $f_3'' - f_T$. In fig. 13, $f_3'' - f_T$ is plotted against the exciting intensity, together with the fluorescence light curve F = f(I) at T. $f_3'' - f_T$ appears to increase with the exciting intensity in the range where photosynthesis and fluorescence are proportional to it. At saturating intensities, $f_3''-f_T$ declines, so that its light curve shows an intensity optimum.

The optimum intensity relationships described above, resemble similar observations on the second wave rise rate[31] and the steady-state ATP content[39] (Chapter I, section B). Our results suggest that greater terminal changes may be related to an increased ATP content or an immediate precursor of it such as X_E. The important feature is that $f_3''-f_T$ is variable even in the range of exciting intensities where

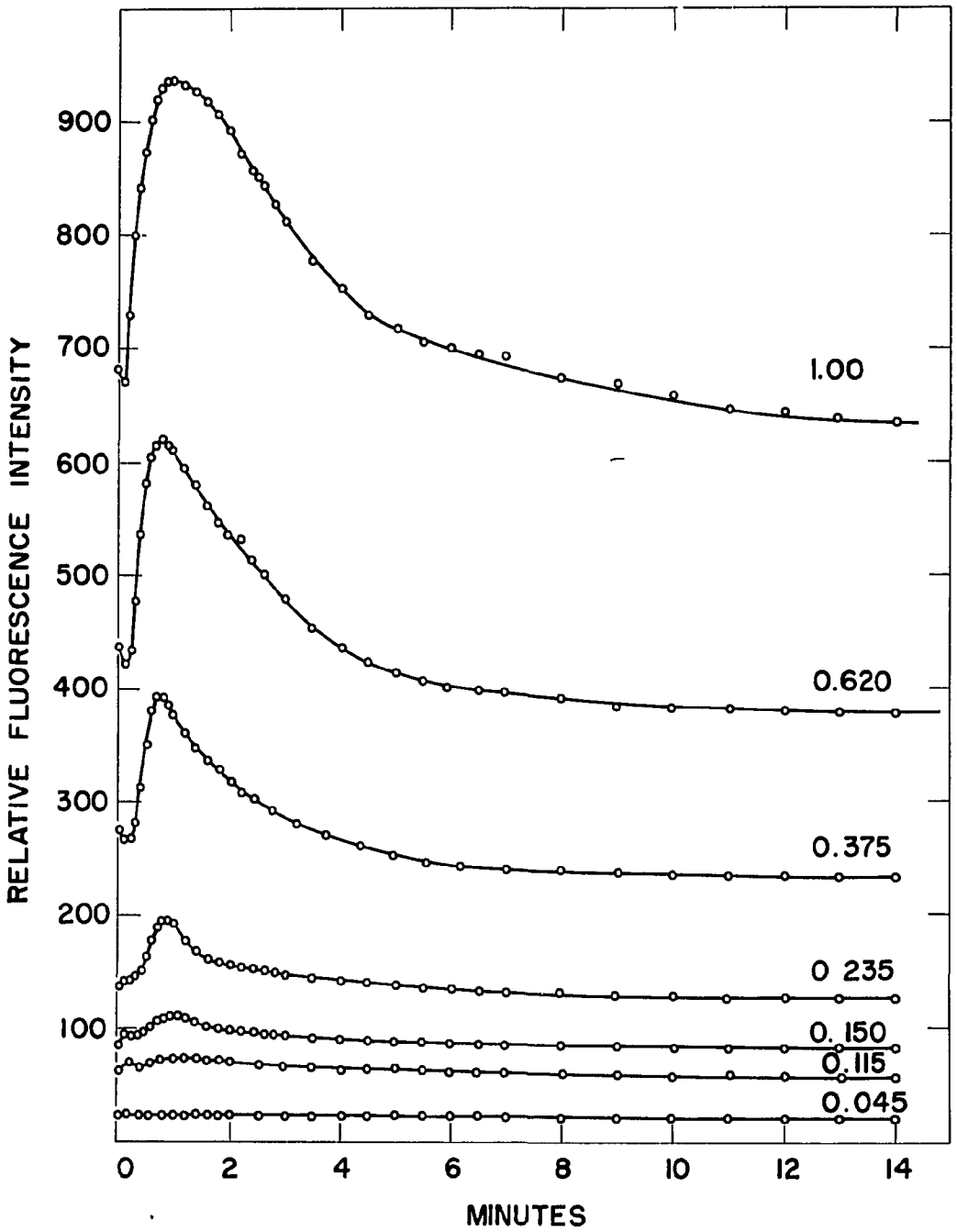

Fig. 11. Time course of the fluorescence intensity (F) in Chlorella at different exciting intensities. Intensity (indicated on the graph), 1.00 = 6.6 x 10^3 ergs. cm.$^{-2}$ sec.$^{-1}$ Excitation: Blue band, Corning filter, C.S. 5-60; half-band width, 100 nm. Observation: λ = 685 nm; half-band width, 16.5 nm, Corning filter, C.S. 2-60.

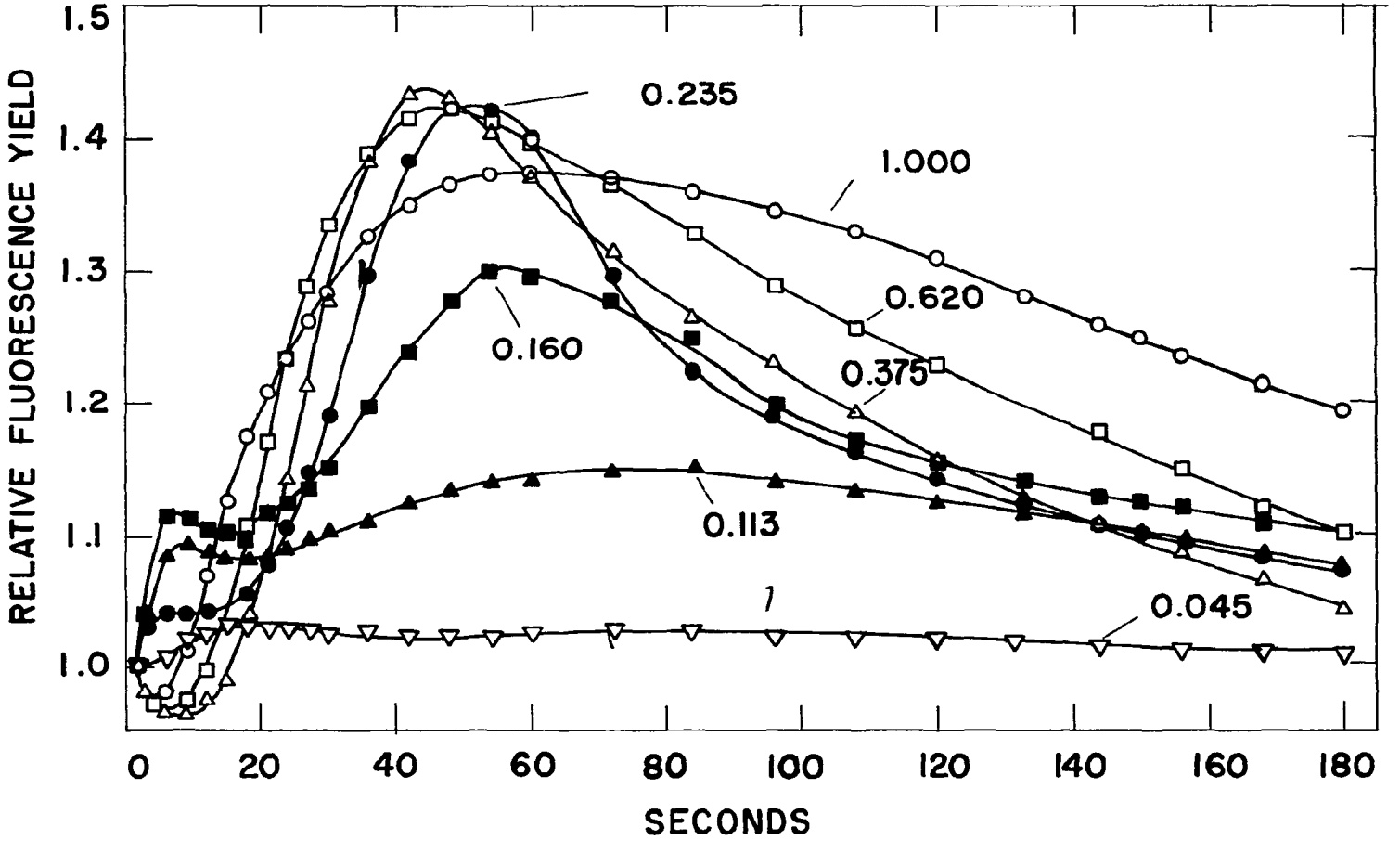

Fig. 12. Time course of the relative fluorescence yield ($f = F_t:F_3''$) at different exciting intensities, details as in fig. 11.

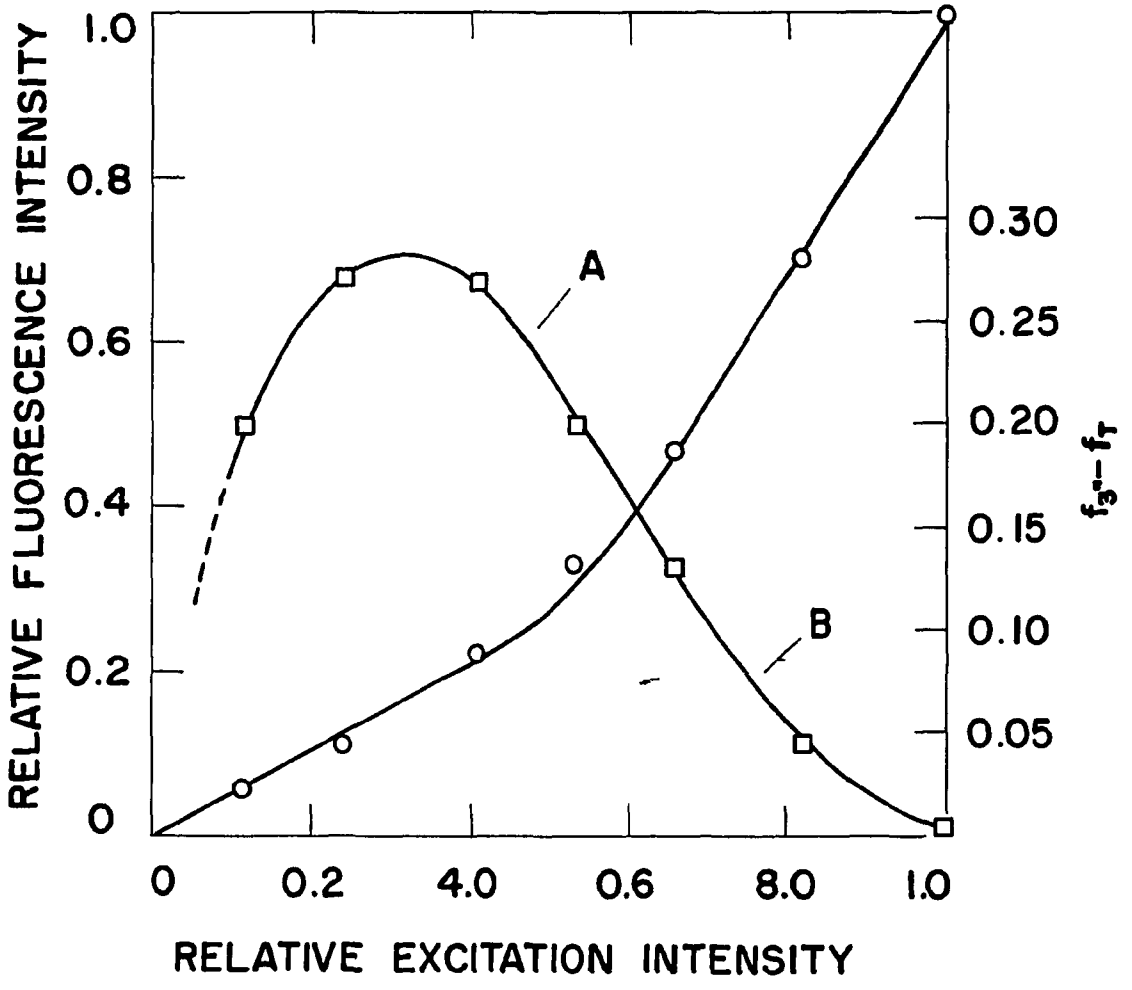

Fig. 13. The fluorescence change $f_3'' - f_T$(A) and the fluorescence intensity at T (B) as a function of the incident light intensity in Chlorella. Intensity 1.0 ≡ 25.5 x 10^3 ergs. $cm.^{-2}$ $sec.^{-1}$. Excitation· Blue band, Corning filter, C.S. 4-72, half-band width, 150 nm; Observation: λ = 685 nm, half-band width, 16.5 nm; Corning filter C.S. 2-60.

photosynthesis yield is constant. This suggests that continuous high intensity illumination affects the fluorescence yield although the rate of photochemistry remains constant.

To obtain the high exciting intensities needed for these experiments a wide blue band (transmitted by Corning glass filter C.S. 5-60) was used. Narrow band excitations at 436 nm and 480 nm gave similar results as the polychromatic one, although the correspondence was restricted to the low intensity values of it. To answer the question whether both system I and system II can support the second wave change, we constructed the action spectrum of the terminal change ($f_3'' - f_T$) observed at 720 nm (fluorescence from both system I and II) fig. 14 . Since the terminal change does not vary linearly with the exciting light intensity, we maintained a constant intensity of excitation at each wavelength. (By aligning the two monochromators and replacing the sample by a reflector, we could assess the light intensity values from the photomultiplier signal.) By regulating the current through the light source we could adjust the exciting light intensity to a predetermined value.

The action spectrum of fig. 14 indicates that the second wave can be excited in the entire blue absorption band of Chlorella. The effective overlap of system I and system II absorption bands do not allow us to clearly distinguish whether the one of the two photochemical systems is more important than the other. However, the sharp drop of the effectiveness at wavelengths longer than 680 nm, where the system I absorption band is located, indicates that the second wave phenomena are caused

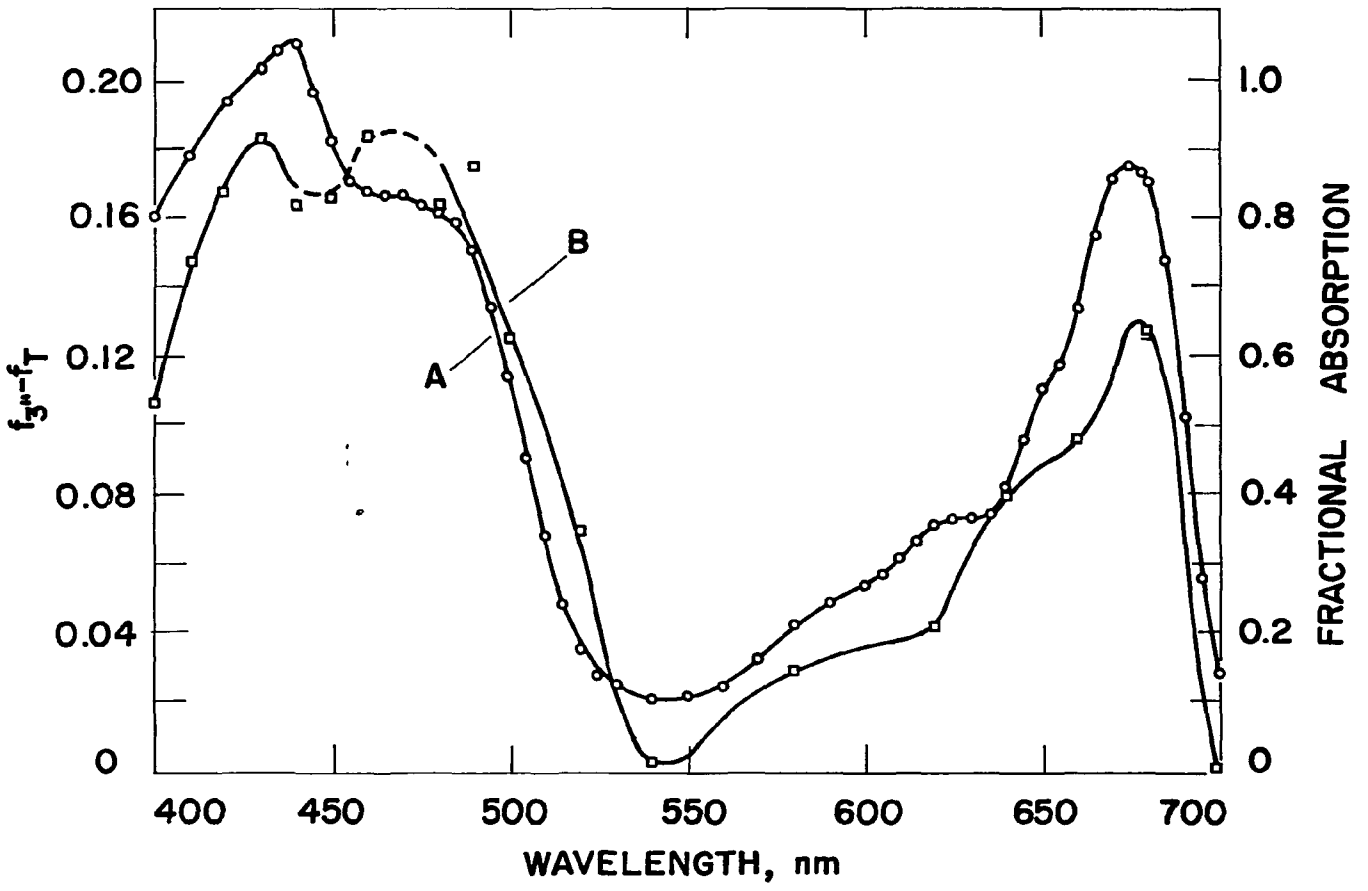

Fig. 14. Fractional absorption spectrum (A) and the action spectrum of the change $f_3'' - f_T$ (B) in Chlorella. Excitation: Half-band width, 6.6 nm. Observation: λ = 730 nm; half-band width, 10 nm; Corning filter, C.S. 7-69.

predominantly by system II. This statement is supported also by the fact that the ratio of the fractional absorption at 480 nm (mainly Chl b) to that at 440 (mainly Chl a) is 0.76, while the same ratio in the action spectrum is approximately 1.0, suggesting increased effectiveness of system II (Chl b). It will be seen later (Chapter IV) that the fluorescence transient in normal Anacystis nidulans also requires system II excitation.

D. HYDROGEN ION CONCENTRATION

In the preceding section we suggested that the second wave is the net effect of a set of enzymatic processes. We would then expect that the pH of the system will exert an influence on the rates of the individual processes and thus on the second wave. It is known[42,45] that the accumulation of ionic gradients, in the transition from dark to light, has an optimum at pH 6-7, in the alkaline region the increased photophosphorylation rate prevents this accumulation. Starting, therefore, from the premise that the second wave is related to the "conformation" changes produced as a consequence of the light induced ionic shifts, we investigated its dependence on the hydrogen ion concentration.

Since the immediate environment of the Chlorella chloroplast is not the suspension medium but the surrounding cytoplasm, with its own buffering capacity, the question arises whether the chloroplast pH will respond to the pH changes in the medium. We consider that such a correspondence was established, since the suspensions retained their pH for long times and since the pH effects on the second wave were

reproducible when the direction of the pH change in the medium was reversed. The pH of the samples was measured before and after each fluorescence measurement; it remained constant. (It was not possible to determine the pH inside the chloroplast and therefore the interpretation of the pH experiments must be considered tentative.)

The influence of proton concentration on the second wave is shown in fig. 15. While the rise phase appears to be insensitive to the pH variations outside the cells, the decay phase is much slower in the alkaline region. The effects on the second wave amplitude and peak location can be explained on the basis of the pH dependence of the rates of the rise and the decay processes. Reduced decay allows the forward change to proceed further and achieve higher amplitude transients, while with increased decay the opposite is true.

An optimum pH behavior of the second wave decay rate can be seen in fig. 16. Similar effects are also true for the terminal stationary level T (not shown in fig. 15). When the second wave is allowed to proceed to completion, the magnitude of the terminal change $f_3''-f_T$ is pH dependent in the manner shown in the fig. 16 (left). The pH curve of the second wave decay rate is given in fig. 16 (right). Since the decay process cannot be isolated from the fluorescence rise, we chose as a measure of the decay rate the inverse of the time interval in which the transient crosses the f = 1.00 value of the ordinate.

Since the terminal stationary fluorescence yield reflects the balancing of the various processes which affect the second wave

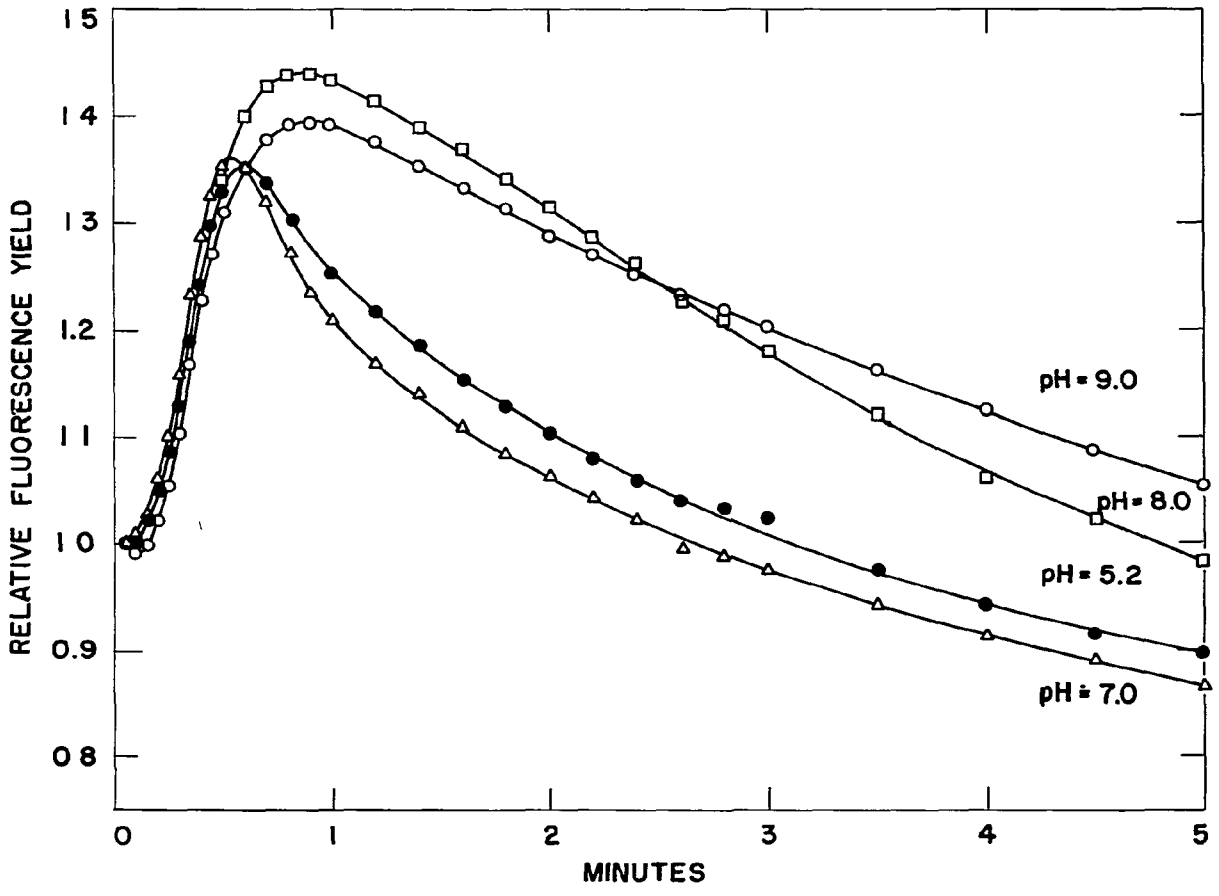

Fig. 15. Time course of the relative fluorescence yield ($f = F_t:F_3''$) at different pH in Chlorella. The indicated pH is of the medium and not of the chloroplasts. Excitation: λ = 480 nm; half-band width, 6.6 nm; incident intensity, 650 ergs. $cm.^{-2}$ $sec.^{-1}$ Observation: λ = 685 nm; half-band width, 16.5 nm; Corning filter, C.S. 2-62.

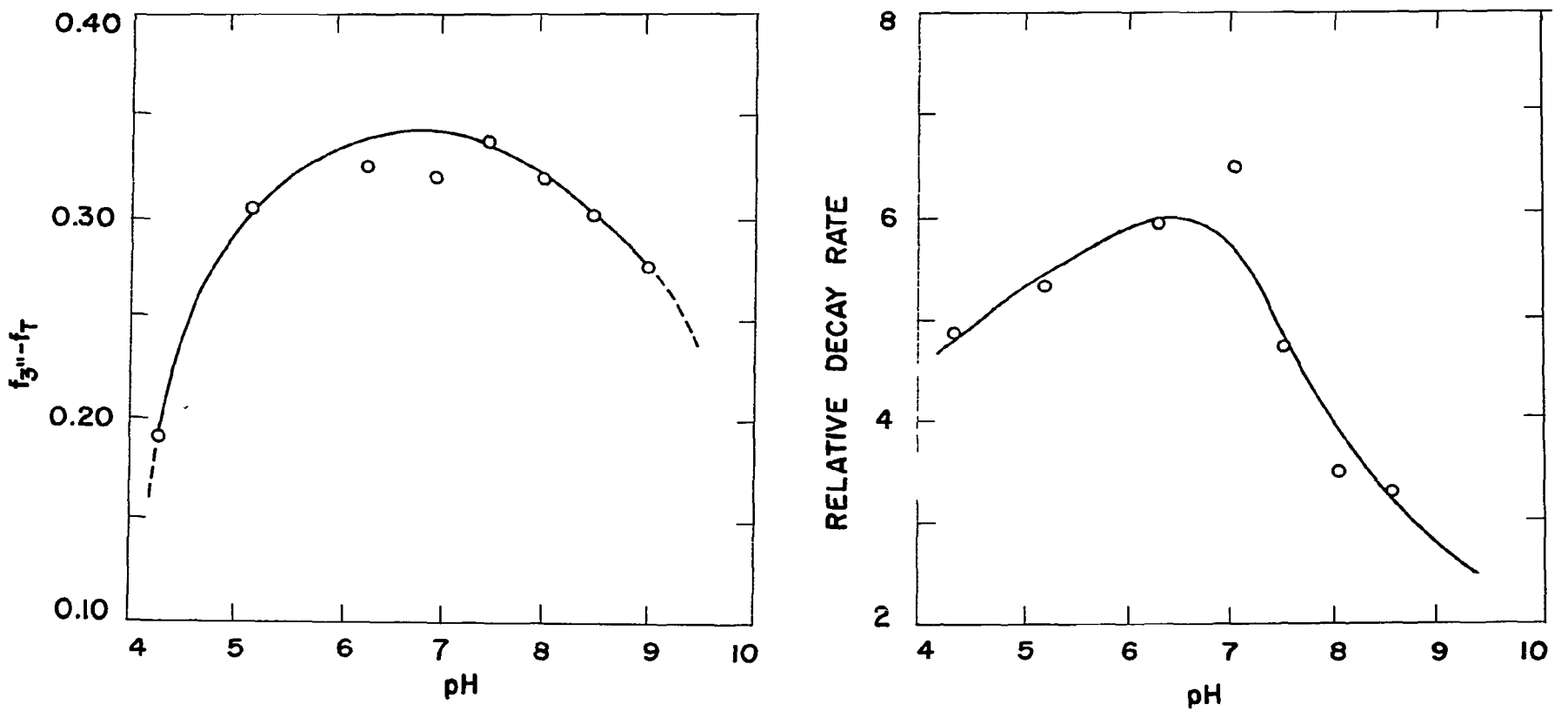

Fig. 16. The fluorescence change $f_3'' - f_T$ (left) and the decay rate of the fluorescence time course (right) in Chlorella as a function of the pH of the suspension medium; details as in fig. 15.

phenomena, we consider that the similarity of the pH curves in fig. 16 is not coincidental. The increased decay of the second wave is expected to lead to lower terminal stationary levels and vice versa. On the other hand, the similarity of the pH curves of the second wave and of the ionic shifts and the associated "conformational" changes observed in chloroplasts may be indicative of their interrelationship. Shrinkage, for example, caused by the light induced cation efflux, may enhance the non-photochemical radiationless quenching of excited Chl a, decreasing the fluorescence yield.

E. INHIBITION OF PHOTOSYNTHESIS

The sharp decline in the effectiveness of light beyond 680 nm (fig. 14) to support the second wave transient hints to the requirement of an intact non-cyclic photosynthetic electron flow. Additional evidence for this is provided by the direct inhibition of photosynthesis with poisons such as 3-(3,4-dichlorophenyl)-1,1-dimethylurea (DCMU) and o-phenanthroline. DCMU blocks the photosynthetic electron flow at a site between the two primary photoreactions.[78] The site of inhibition of o-phenanthroline is not known and it seems that it does not chelate the well protected Mn of the oxygen releasing enzyme. However, it is, like DCMU, a system II inhibitor. Both poisons inhibit the oxygen evolution.

As shown in fig. 17, the interruption of the photosynthetic electron flow obliterates the typical second wave transients. Instead of a well-formed second wave, poisoned samples exhibit a slow increase of the fluorescence yield to a stationary level. The absolute magnitude of

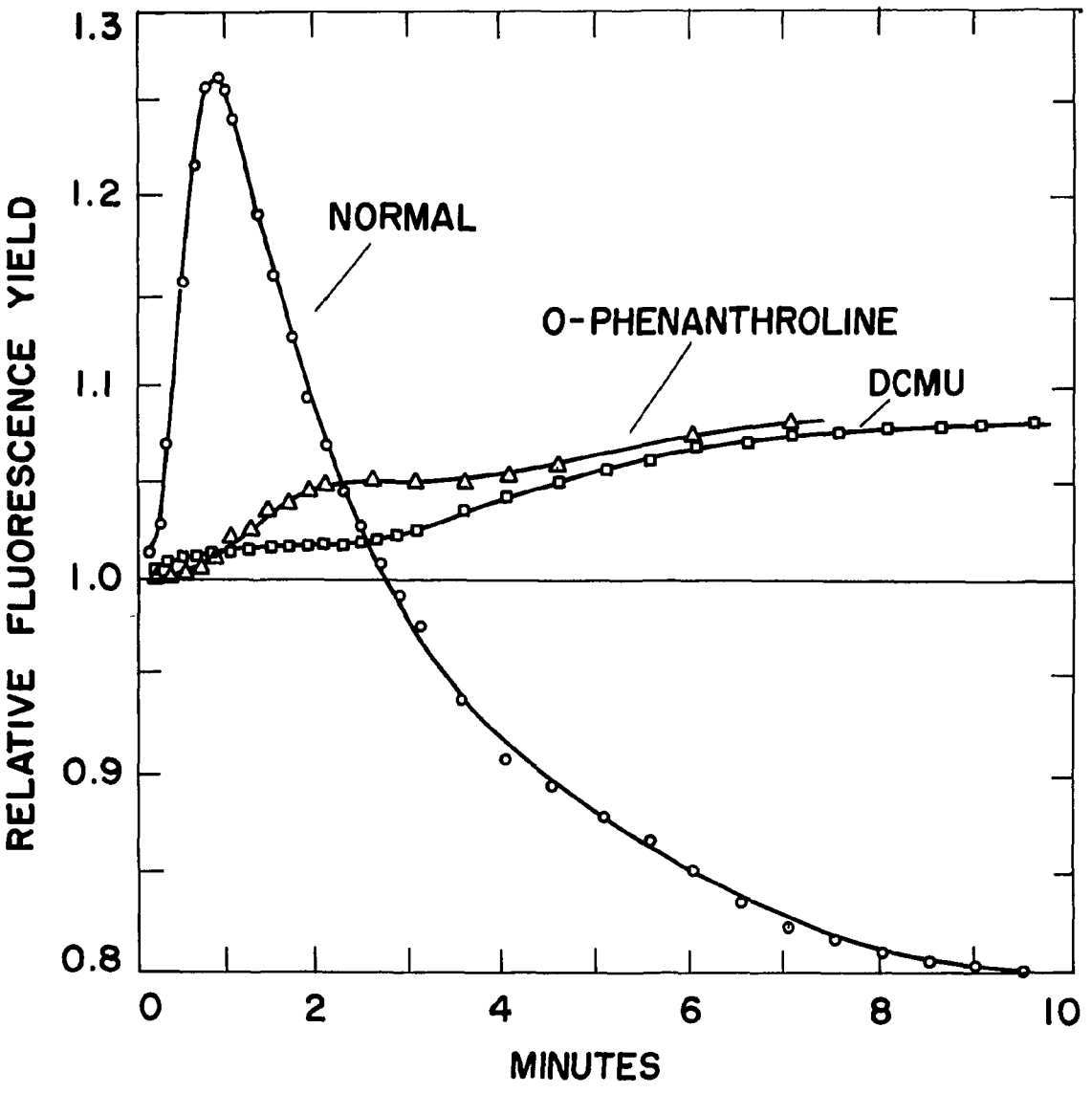

Fig. 17. Time course of the relative fluorescence yield ($f = F_t:F_3''$) in Chlorella. Control; with DCMU, 5×10^{-5}M; with o-phenanthroline, 5×10^{-4}M. Excitation: λ = 436 nm, half-band width, 16.5 nm; incident intensity, 2.1×10^3 ergs. cm.$^{-2}$ sec.$^{-1}$ Observation: λ = 685 nm, half-band width, 16.5 nm; Corning filter C.S. 2-60.

this slow change is much smaller than that of a normally photosynthesizing sample. At a subsequent dark period the small increment of the fluorescence yield disappears. The slow increase in the relative fluorescence yield of a poisoned sample rules out the accumulation of the reduced form of the primary photochemical quencher (QH) as a cause, since this is completed within one second after the onset of illumination. As to the origin of this increase we speculate that it may be related to electron flow pathways which are not affected by the photosynthetic poisons or to the low non-cyclic electron flow.

F. UNCOUPLING OF PHOTOPHOSPHORYLATION

Unlike the inhibitors described above, the effects of the phosphorylation uncouplers are less specific, since they may inhibit not only the photophosphorylation but the mitochondrial oxidative phosphorylation as well. Such an uncoupler will introduce an ATP deficiency thus affecting a variety of the cell functions. As an example, we may consider the inhibition of the CO_2 fixation cycle in ATP deficient systems, which will, in principle, reduce the rate of the photosynthetic electron flow because of the lack of an adequate pool of terminal electron acceptors.

The above considerations require the establishment of a set of criteria by which we may decide that the uncoupler exerts a recognizable direct effect on the main photosynthetic electron pathway, distinguishable from the indirect influences, due to the overall ATP deficiency. The reversibility of a particular effect in the second wave transients, in

successive light and dark exposures, may be taken as indicative of its independence of the dark biochemical pathways in the cytoplasm and in the chloroplast, since these would have a unidirectional influence rather than a light dependent reversible one. On the other hand, indirect inhibition of photosynthesis due to the inability of the cell to provide ATP to the CO_2 fixation cycle, is expected to increase the fluorescence yield in the same manner as the photosynthetic poisons and saturating light intensities do. Indeed, since the photochemical deexcitation of Chl a is by far the predominant fluorescence quenching process, any change in its rate will be reflected by a change in the quantum yield of fluorescence. Lastly, since we found that the addition of DCMU abolishes all the modified second wave changes in the presence of the photophosphorylation uncouplers and approximately doubles the fluorescence yield we have to accept that the ATP deficiency did not impair significantly the photosynthetic electron flow in our samples.

1. FCCP

Halogenated derivatives of the phenylhydrazone of ketomalonylnitrile [CCP] are potent uncouplers of both the oxidative and photophosphorylation.[79] In chloroplast suspensions they minimize the light

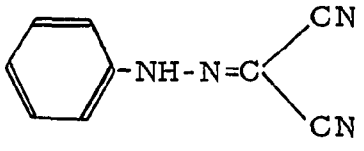

CCP

induced ion fluxes.[40, 57] The p-trifluoromethoxy-derivative of CCP (FCCP) is the most potent inhibitor of photophosphorylation and oxidative phosphorylation known. In photophosphorylation, both the non-cyclic and cyclic types of it are inhibited, although the second to a lesser extent.[80, 81] The photophosphorylation inhibition is accompanied by the suppression of the light induced scattering increase in chloroplasts[56, 82] and the abolition of the cation fluxes. In the absence of light, FCCP accelerates the dissipation of the ionic gradients formed during a preceding light period.[40] The inhibition with FCCP is reversed by 1, 2 and 1, 3 aminothiols,[79] suggesting that the uncoupler acts as a sulfhydryl reagent.

In spite of the expected severe inhibition of the photosynthetic electron transport in Chlorella, FCCP had a small effect on the fluorescence yield S, even at relatively high concentrations (10^{-5}M). This effect due to a reduction in the rate of electron transfer -- also observed by a reduction in the rate of oxygen evolution -- did not effect our conclusion because we normalized the normal and the FCCP curves at S and then studied their differences. With continuous illumination, the time courses of fluorescence yield of the normal and of the FCCP inhibited sample are different (fig. 18); the normal sample exhibits the regular type of second wave transient while the FCCP treated sample shows a very slow decay of the second wave. Thus, after the establishment of the terminal stationary state, the absolute fluorescence yield of the control sample is significantly lower ($\sim$40%) than that of the FCCP containing one; a portion of this effect is due to the reduction in the rate of electron

transport. On addition of 10^{-3} M cysteine (1,2-aminothiol) to the FCCP inhibited sample the second wave change is reinstated (fig. 18).

The effectiveness of different concentrations of FCCP to reduce the decay rate of the second wave ($f_{20}' - f_3''$) was studied (fig. 19). The concentration for half-maximal inhibition of the second wave decay was found to be 4.5×10^{-6} M, which is close to the value of 1×10^{-6}M for half-maximal inhibition of chloroplast photophosphorylation[80] and 2×10^{-6}M for ^{54}Mn incorporation into manganese deficient Ankistrodesmus.[83] This similarity suggests a common inhibition site for all three processes.

The light induced fluorescence increase in the FCCP treated sample is reversed in a subsequent dark interval. On shutting off the excitation the fluorescence yield (as measured with light flashes) drops sharply below the f = 1.0 value and then slowly approaches the S level. These changes are reproducible in subsequent light-dark cycles, which indicates that they are not due to an overall ATP deficiency, but they are associated with processes requiring light activation.

Inhibition of the second wave decay with FCCP is particularly pronounced at low light intensities as it is also the uncoupling of chloroplast photophosphorylation.[82] This is shown in the fig. 20 (left), where the relative yield at 4 min (f_4') illumination is plotted against the incident exciting intensity. Very low light intensities cannot support the second wave increase and in consequence a low f_4' value is obtained. At high intensities the increased decay of the curve (corresponding to

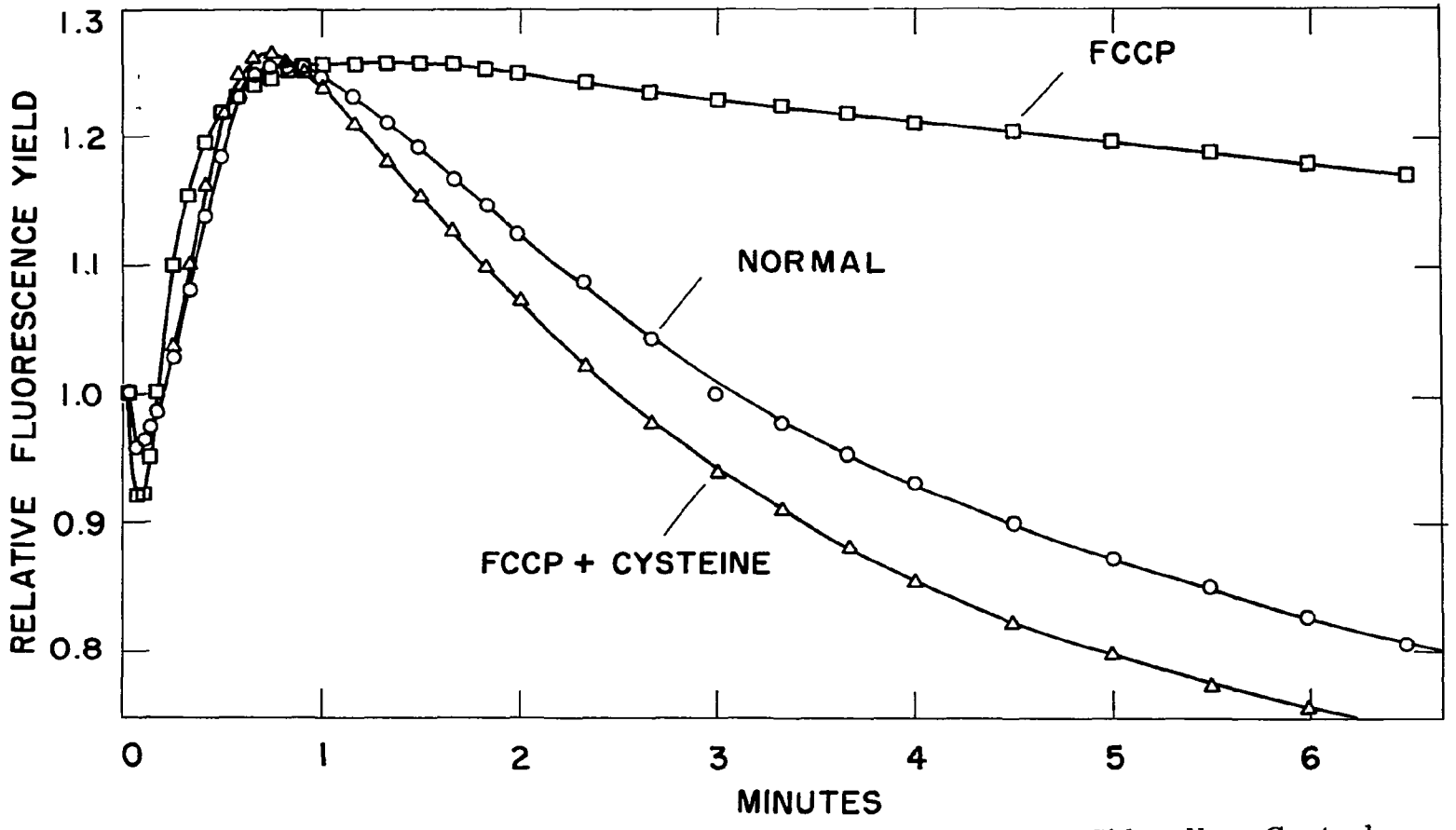

Fig. 18. Time course of the relative fluorescence yield ($f = F_t:F_3''$) in Chlorella. Control; with 10^{-5} M F C C P, with 3×10^{-5} M FCCP, and 10^{-3} M cysteine. Excitation: λ = 480 nm; half-band width, 10 nm, incident intensity, 1.4×10^3 ergs. cm.$^{-2}$ sec.$^{-1}$ Observation· λ = 685 nm; half-band width, 11.6 nm, Corning filter, C.S. 2-60. (Additions were made at least 30 minutes prior to illumination).

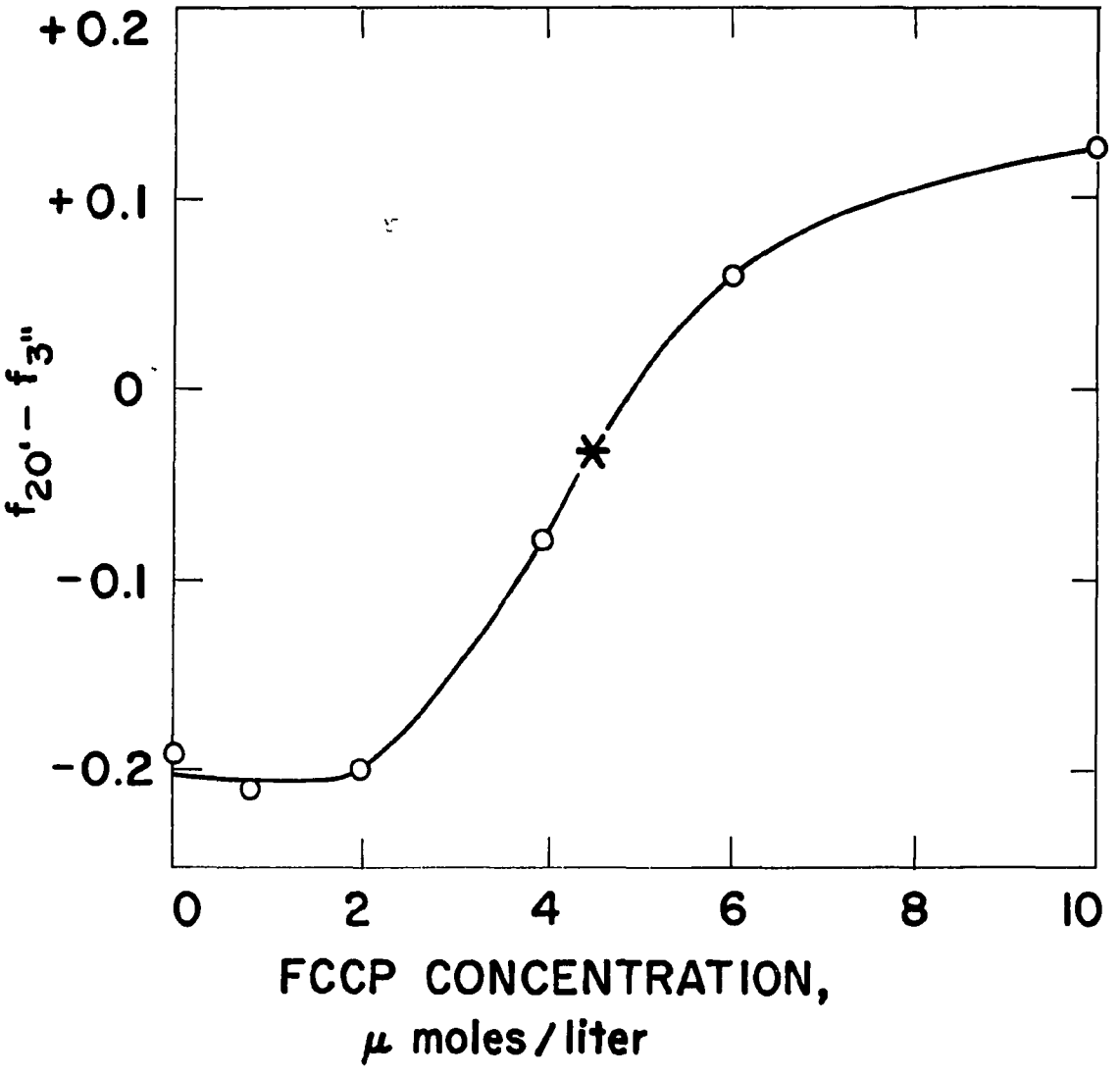

Fig. 19. The fluorescence change $f_{20}' - f_3''$ as a function of the FCCP concentration in Chlorella. Excitation: λ = 480 nm; half-band width, 16.5 nm' incident intensity, 3.1×10^3 ergs. cm.$^{-2}$ sec.$^{-1}$ Observation: λ = 685 nm; half-band width, 16.5 nm; Corning filter, C.S. 3-69.

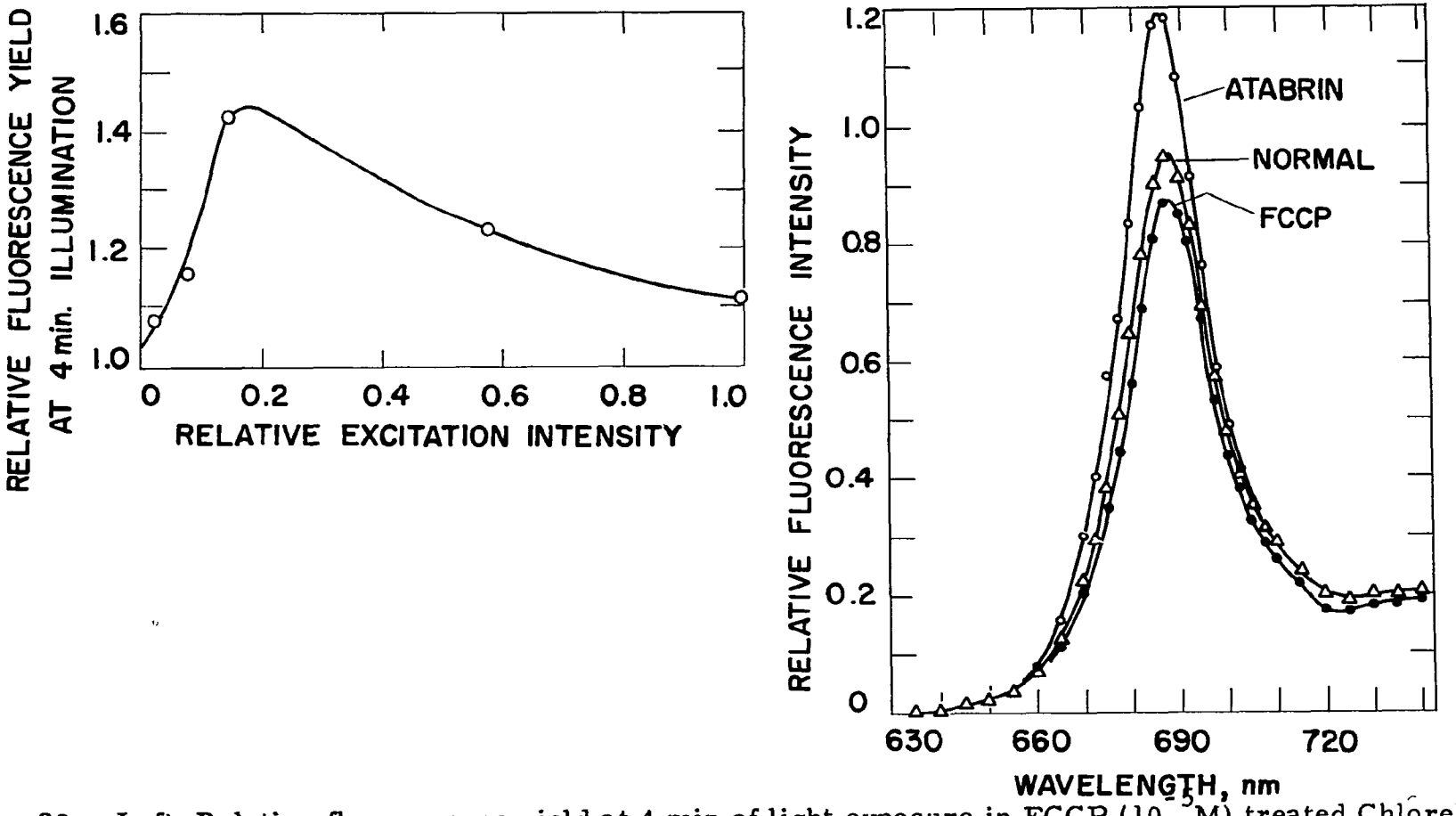

Fig. 20. Left: Relative fluorescence yield at 4 min of light exposure in FCCP (10^{-5} M) treated Chlorella as a function of the incident light intensity. Intensity 1.00 ≡ 9 4 x 10^{3} ergs. cm.$^{-2}$ sec.$^{-1}$ Excitation: Blue band, Corning filter, C.S. 5-56; half-band width, 130 nm. Observation: λ = 685 nm, half-band width, 10 nm; Corning filter, C.S. 2-60. Right: Emission spectra of Chlorella. Control: with 10^{-5}M FCCP; with 3 x 10^{-5}M atabrin. Excitation: λ = 485 nm; half-band width, 10 nm, incident intensity, 1.4 x 10^{3} ergs. cm.$^{-2}$ sec $^{-1}$ Observation. half-band width, 6.6 nm, Corning filter, C.S. 3-69.

decreased FCCP inhibition) also results in low f_4' values. Finally, the emission spectra of the normal and FCCP treated samples, recorded at the respective stationary states, were found to be nearly identical [fig. 20 (right)].

2. Atabrin

A photophosphorylation uncoupling agent which acts on a late stage of the energy conservation sequence is atabrin (quinacrine).

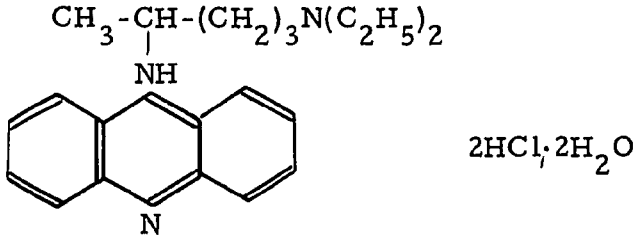

Atabrin

Atabrin is a powerful uncoupler of the photophosphorylation[84] and a weak one for the oxidative phosphorylation.[85] The location of its pH optimum at alkaline values shows that it is rather the free base which is active although at high pH it may also inhibit the photosynthetic electron transport.[40] In chloroplasts it promotes the light induced shrinkage[54] and it accelerates the cation efflux.[86]

Since atabrin absorbs strongly in the blue (absorption maximum at 422 nm) we employed monochromatic excitation at 485 nm where its absorption is negligible (molar absorption coefficient at 485 is $\sim$ 330 lit/mole · cm, while for Chl b it is of the order of 10^4 lit/mole · cm). The fluorescence yields of the atabrin treated samples were found to be

nearly identical to those of the controls in the S level. Addition of DCMU, however, more than doubled the fluorescence yield of the atabrin containing samples. These results indicate that there is no significant inhibition in the electron transport, either by direct atabrin poisoning or because of the induced ATP deficiency.

Atabrin suppresses both the forward fluorescence yield increasing process and the decay of the second wave transient (fig. 21). A small slow increase of the fluorescence yield to a level about 5% higher than that at 3 sec is evident. This increase is reversed in the dark. At lower atabrin concentrations than the one given in fig. 21, a second wave transient of smaller amplitude and with higher terminal stationary value develops. The emission spectra of atabrin treated samples observed at the stationary state were similar to those of the controls, taken after the completion of the transient fig. [20(b)].

3. Phlorizin

In contrast to the strong effects of FCCP and atabrin on the second wave of fluorescence induction, the uncoupler phlorizin had no appreciable influence. The latter compound, a glucoside, is known as a terminal inhibitor of the energy conservation sequence[87] acting presumably on a phosphorylase.[88]

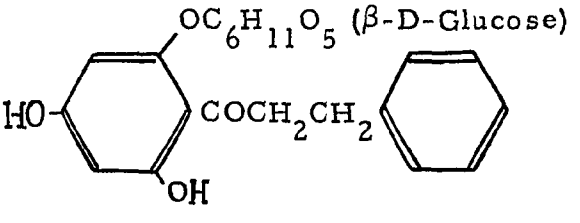

Phlorizin

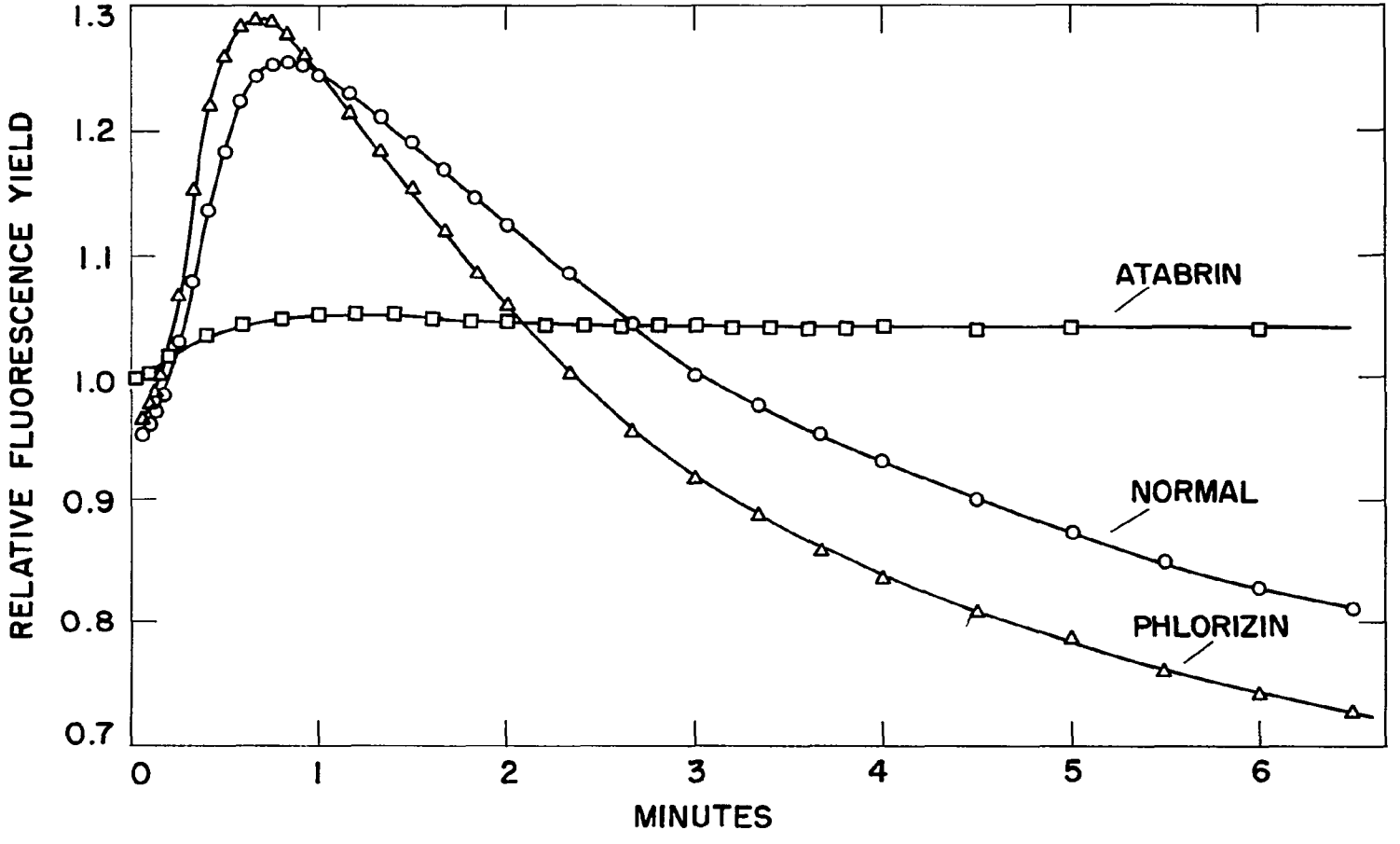

Fig. 21. Time course of the relative fluorescence yield f = F_t:F_3" in Chlorella. Control, with 3×10^{-5}M atabrin, with 2×10^{-3}M phlorizin. Excitation: λ = 480 nm; half-band width; 10 nm, incident intensity, 1.4×10^{3} ergs. cm.$^{-2}$ sec.$^{-1}$ Observation: λ = 685 nm; half-band width, 11.6 nm; Corning filter, C.S. 2-60.

Both the photophosphorylation and the oxidative phosphorylation[89] are inhibited. Phlorizin accelerates both the rise and the decay of the second wave fig. 21 . Our results with phlorizin indicate that the second wave originates from events that precede the terminal phosphorylation step; and since inhibition of the noncyclic electron flow abolishes completely the fluorescence transient, we believe that the origin of the second wave is in the reaction sequence which couples the electron flow with the phosphorylation of ADP.

G. FLUORESCENCE INDUCTION AND OXYGEN EVOLUTION

It was pointed out in the introduction (Chapter I, section B) that the photosynthetic oxygen evolution is not always in direct competition with fluorescence. In order to establish the relationship between these two processes during the time interval of the second wave, two samples prepared from the same stock suspension, were tested. Care was taken so that equal numbers of photons were absorbed by each sample.

A total absence of any correlation in the rate of oxygen evolution and fluorescence was found (fig. 22). On excitation both quantities increase in parallel. However, while the fluorescence yield experiences the typical second wave change, the rate of oxygen evolution tends to a high stationary level. Significantly, the fluorescence yield decays even after the rate of oxygen evolution has attained a constant magnitude. The insert in fig. 22 shows the time course for both processes on an expanded time scale.

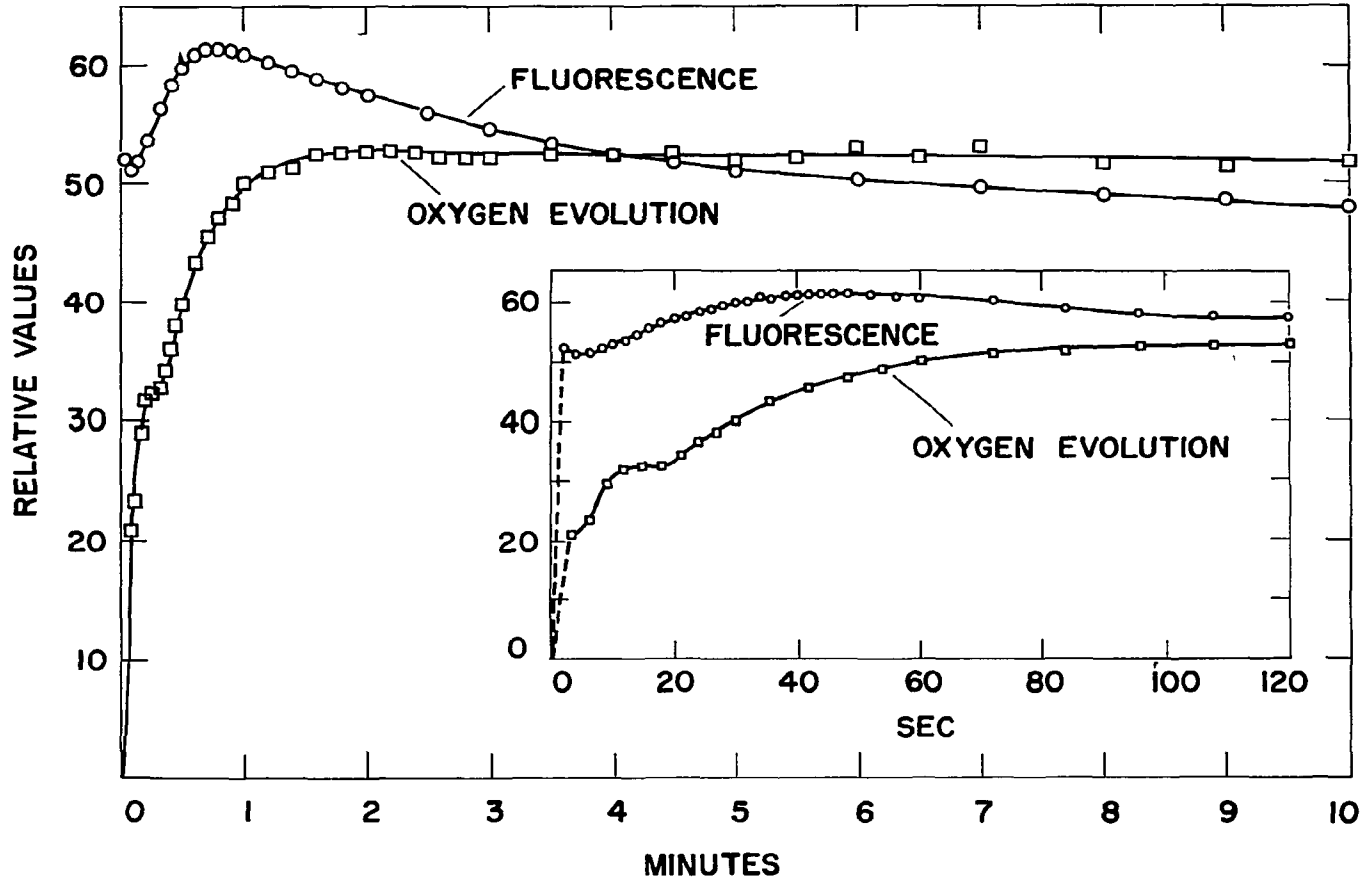

Fig. 22. Time course of the fluorescence intensity and of the rate of oxygen evolution in Chlorella. Excitation: λ = 480 nm; half-band width, 16.5 nm; incident intensity, 3.1×10^{3} ergs. cm.$^{-1}$ Observation: λ = 685 nm; half-band width, 16.5 nm; Corning filter, C.S. 2-60. Insert: Data up to 2 min. on an expanded time scale.

H. THE SECOND WAVE OF FLUORESCENCE INDUCTION IN CHLORELLA: CONCLUSIONS

The experimental results described in the preceding sections indicate that the second wave of fluorescence induction in Chlorella pyrenoidosa is the net effect of at least four processes. Two of them are photochemical, requiring simultaneous excitation, while the other two are triggered by light and proceed in the dark. The existence of two opposing photochemical processes is inferred (see fig. 9, insert) from a comparison of the second wave time course and the fluorescence induction in the dark (measured with light flashes).

The participation of non-photochemical components in the second wave rules out its complete dependence on the rate of primary photochemistry. Support for this argument is provided by the absence of correlation between the second wave of fluorescence and the rate of oxygen evolution (fig. 22). Moreover, it is shown in fig. 13 that the second wave terminal change ($f_3''-f_T$) decreases in the range of intensities at which photosynthesis is saturated. Nevertheless, the second wave events are not completely independent of the photosynthetic electron flow since inhibition of photosynthesis by DCMU and o-phenanthroline abolishes the fluorescence transient (fig. 17). The requirement of an intact non-cyclic photosynthetic electron flow is also supported by the fact that excitation at wavelengths shorter than 680 nm, which is distributed in both the photosynthetic systems, is effective in promoting the second wave change, but far red light ($\lambda > 680$ nm), absorbed primarily by system I, is not (fig. 14).

Powerful uncouplers of photophosphorylation, such as FCCP and atabrin, exert a strong effect on the second wave (fig. 18, 21). FCCP, which uncouples the energy conservation sequence at a site near the photosynthetic electron flow, delays the second wave decay. Its effect is reversed by cysteine. Atabrin, which may uncouple at a later stage than FCCP, suppresses both the rise and the decay of the second wave. Both uncouplers, however, lead to a higher terminal fluorescence yield in comparison with normal Chlorella; part of this is due to reduction in the rate of electron transport.

Contrary to the results obtained with FCCP and atabrin, the phosphorylase inhibitor phlorizin (fig. 21) allows the second wave to proceed in the normal manner, except for an accelration of the rise and decay phases. These results appear to localize the origin of the fluorescence transient at a site between the non-cyclic electron pathway and the terminal ADP phosphorylation. Accordingly, the second wave may indeed be related to the accumulation of X_E and the associated "conformational" changes. Since the latter correspond to chloroplast shrinkage, the low terminal stationary yield represents a state of increased concentration quenching of the fluorescence. The similarities of the pH curves (although we have some reservation for this effect) for the terminal change (fig. 16) and the accumulation of X_E[42, 45] is in favor of this correlation.

A relationship between the second wave in Chlorella and the light driven ATP formation has been suggested previously[39] on the basis of the similarity of the respective time courses. In addition, the steady-

state ATP level was found to obey an optimum intensity light curve (fig. 3, right); our results also show such an intensity dependence for the terminal change. It appears, however, that the low stationary yield may represent an accumulation of an immediate precursor (X_E) of ATP (cf. table III).

In conclusion, we may say that the experiments we presented suggest an indirect correlation between the second wave changes in Chlorella and the rate of photosynthesis. The possibility of a connection with the light induced cation transport and its associated effects has been explored. Our data show positively that the second wave fluorescence transient must be related to the events which lead to energy conservation as ATP.

TABLE III

EFFECTS OF PHOTOSYNTHETIC INHIBITORS AND PHOTOPHOSPHORYLATION UNCOUPLERS ON THE LIGHT INDUCED ION FLUXES AND THE ASSOCIATED PROCESSES

Additions	Chloroplasts or Chloroplast Fragments					Chlorella
	Photophosphorylation	Cation Fluxes*	X_E Formation	Volume Changes	Light Scattering	Fluorescence Yield Difference: $f_{10min} - f_{3sec}$
Control	Normal	$-K^+$, $-Mg^{++}$, $+Na^+$, $+H^+$ $+Ca^{++}$ [42, 44, 92]	Normal[56]	Shrinkage[50, 58, 82]	Increases[49]	
DCMU	Inhibited[91]	-	Inhibited[57]	None[49, 82]	No Change[49, 54]	No Change
FCCP or CCCP**	Inhibited[79]	Inhibited[86]	Inhibited[56, 57]	None[50, 58, 82]	No Change[54, 56, 82]	Positive
Atabrin	Inhibited[84]	Accelerated Efflux	Inhibited[56, 57]	None[58]	Increases[54, 56]	No Change
Phlorizin	Inhibited[87, 90]	-	-	-	-	Negative

*Efflux toward the medium is denoted by a (-) sign before the cation and the influx toward membrane bound spaces by a (+) sign.

**m - Cl - CCP

IV. THE LONG-TERM FLUORESCENCE INDUCTION IN ANACYSTIS NIDULANS: RESULTS AND DISCUSSIONS

The blue-green alga Anacystis nidulans was selected as an additional organism for our investigation, because of the better spectral separation of the photosynthetic pigment systems I and II in comparison to the green alga Chlorella. This property facilitates the preferential excitation of either pigment system I or II. System I can be excited in the blue band of Chl a while system II in the green-orange absorption band of phycocyanin. A complication, however, arises due to the overlap of the emission spectra of phycocyanin and Chl a. Thus narrow measuring band widths were used to insure that we observe preferentially either Chl a or phycocyanin fluorescence.

A. FLUORESCENCE INDUCTION IN CONTINUOUS AND FLASHING LIGHT

With continuous system II excitation (λ = 590 nm) a gradual increase of the Chl a fluorescence yield to a higher stationary level, M, is observed (fig. 23, curve A). In a subsequent dark interval the fluorescence yield decays and approaches the initially recorded level S (curve B). This decay was followed with short flashes as it was done in Chlorella (Chapter III, section A). Continuous excitation with a broad blue band (system I light) results in a much suppressed fluorescence yield rise (curve C). Since the phycocyanin absorption in the blue is negligible we conclude that only excitation in the system II absorption band can support the Chl a fluorescence increase in normal Anacystis.

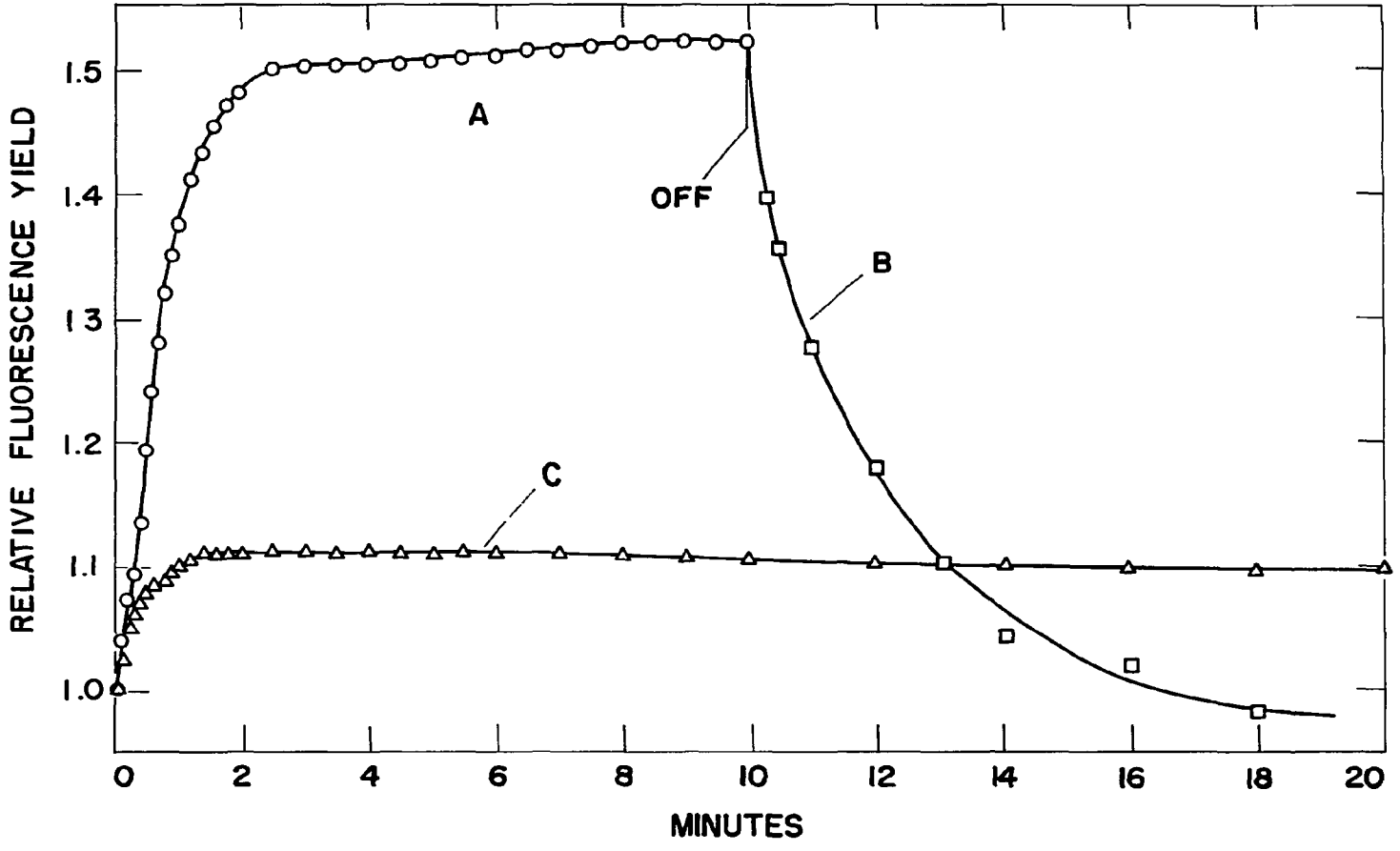

Fig. 23. Time course of the relative fluorescence yield ($f = F_t:F_3''$) in normal Anacyst is nidulans (A). Excitation: λ = 590 nm, half-band width, 16.5 nm; incident intensity, 4.1×10^3 ergs. cm.$^{-2}$ sec.$^{-1}$ Observation: λ = 685 nm, half-band width, 13.2 nm; Corning filter, C S. 2-60. Dark decay (measured with light flashes) of the relative fluorescence yield (B). Time course of the relative fluorescence yield with blue excitation (C). Excitation. Blue band, Corning filter, C.S. 5-60; half-band width, 100 nm; incident intensity, 9.4×10^3 ergs. cm.$^{-2}$ sec.$^{-1}$ Observation as for (A).

It will be shown later (section C) that system I excitation is capable of inducing considerable changes in DCMU poisoned Anacystis nidulans.

The rise of the Chl a fluorescence yield appears to be biphasic. The first phase is completed within a few seconds while the second and more extensive one lasts for several minutes (fig. 23, curve A). Both the fluorescence rise during the light interval and the decay in the succeeding dark do not obey any elementary kinetic law. In what follows, we will consider that the fluorescence yield time course is the net outcome of two processes, a photochemical one leading to increased fluorescence and an opposing non-photochemical process.

Interruption of the photosynthetic electron flow with DCMU results in an increase of the yield of Chl a fluorescence. Contrary to the results obtained with Chlorella, poisoned Anacystis nidulans is capable of an extensive induction in the fluorescence yield, which is readily reversed in a subsequent dark period (fig. 24, curves A and B). As with normal cells, the fluorescence rise in the poisoned samples is biphasic. The initial minor rise phase is clearly seen with weak excitation. In general, poisoned Anacystis undergoes a more extensive fluorescence induction change than the normally photosynthesizing cells. On occasion, the fluorescence increase amounted to more than 100% relative to the yield at the 3 sec illumination level (S).

When the fluorescence is observed at 645 nm (mainly phycocyanin emission) only a slight increase of the yield is registered (fig. 24, curve C). Taking into consideration that a fraction of this increase

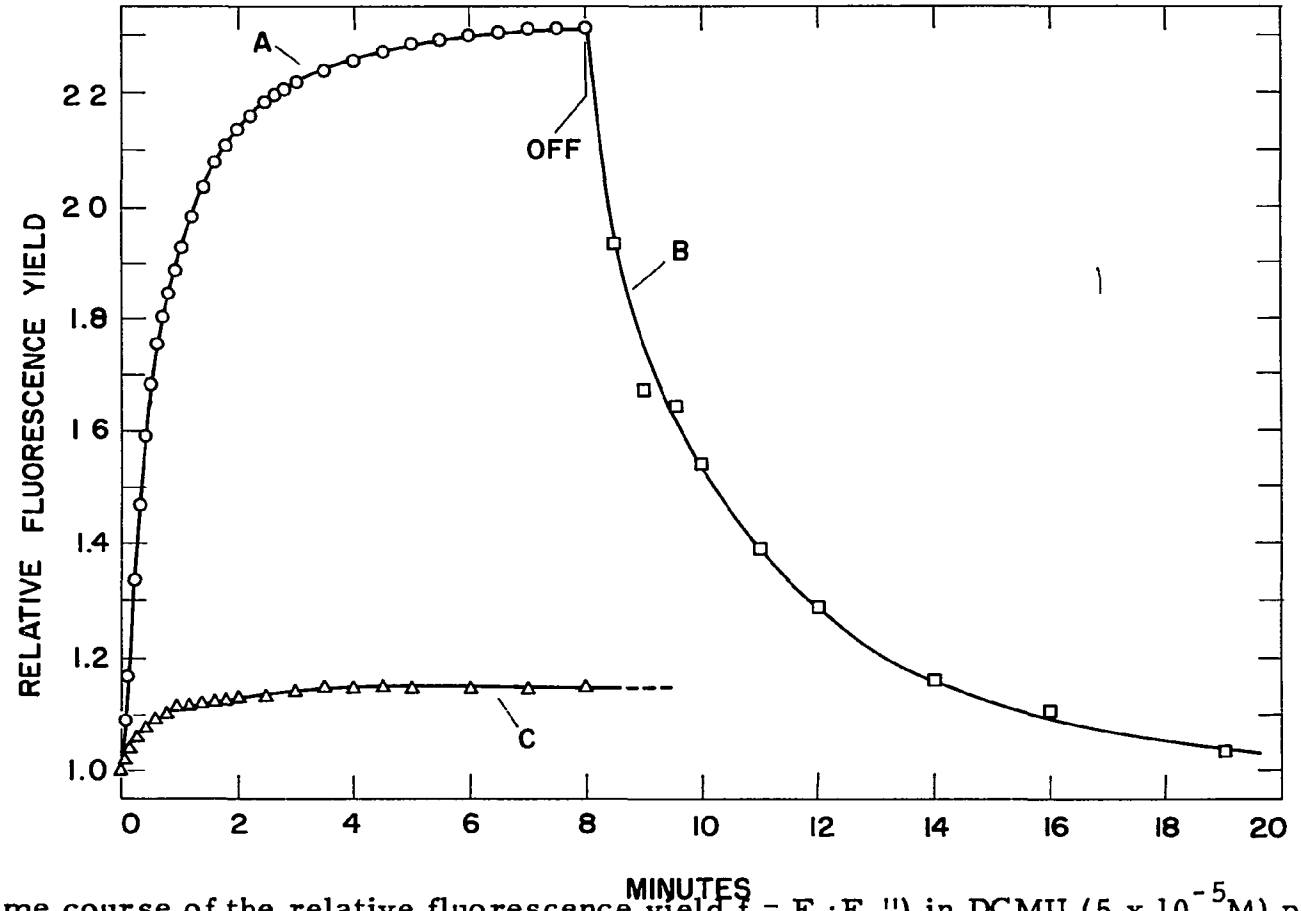

Fig. 24. Time course of the relative fluorescence yield ($f = F_t:F_3''$) in DCMU (5×10^{-5} M) poisoned Anacyst is (A). Excitation: λ = 590 nm; half-band width, 16.5 nm; incident intensity, 4.1×10^3 ergs. cm.$^{-2}$ sec.$^{-1}$ Observation: λ = 685 nm; half-band width, 6.6 nm; Corning filter, C.S. 2-58. Dark decay (measured with light flashes) of the relative fluorescence yield (B). Time course of the phycocyanin fluorescence (C). Excitation as for (A). Observation: λ = 645 nm; half-band width, 8.3 nm; Corning filter, C.S. 2-63.

may be attributed to the short wavelength tail of the Chl a emission band, we conclude that there is very little if any induction of the phycocyanin fluorescence. This result is significant in the sense that if the increase were the result of a higher energy transfer efficiency from phycocyanin to Chl a in system II, we would expect a concomitant decrease in the fluorescence yield of phycocyanin itself. We must therefore accept that the variable quantity is the quantum yield of Chl a fluorescence and not the efficiency of excitation energy transfer from phycocyanin to Chl a in system II.

B. CHANGES IN THE EMISSION SPECTRUM DURING THE FLUORESCENCE INDUCTION

Large changes in the spectral distribution of the Anacystis fluorescence accompany the fluorescence induction phenomena. The emission spectra at the stationary state were recorded automatically, while the spectrum at 3 sec of excitation was recorded point by point with short flashes. An adequate dark interval was interposed between each two successive flashes to insure the independence of each individual measurement.

The emission spectra of normal Anacystis, excited at 590 nm (system II) and measured at the beginning and at the stationary state (M) of the induction time course are shown in fig. 25 (curves S and M, respectively). (Both spectra have been corrected for the photomultiplier sensitivity and measuring monochromator transmission.) In the 3 sec fluorescence spectrum, the phycocyanin emission band is higher than

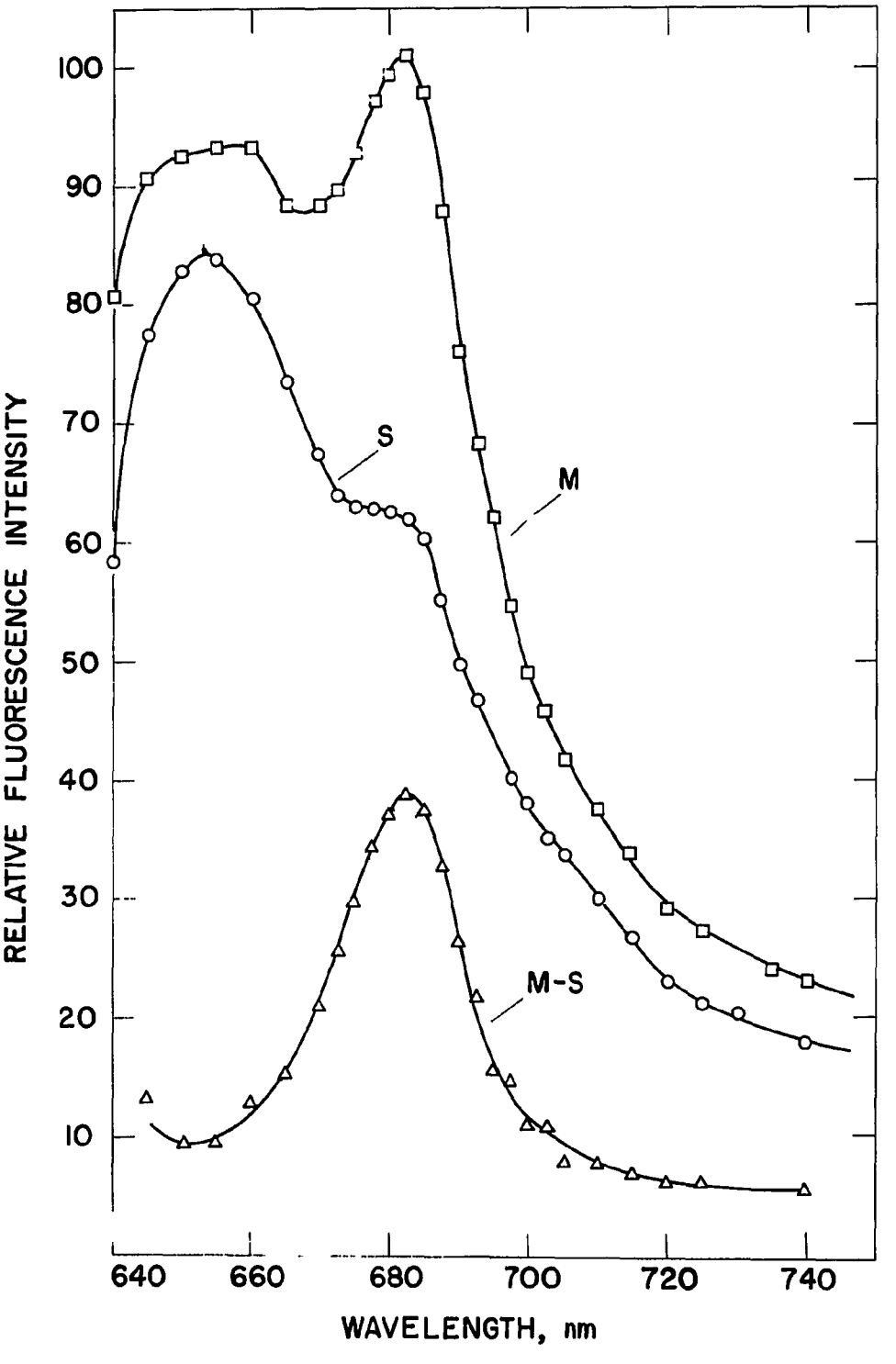

Fig. 25. Emission spectra of normal Anacystis at 3 sec (S) and 10 min (M) of light exposure; M - S the difference emission spectrum. Excitation as in fig. 24. Observation: Half-band width, 8.3 nm; Corning filter, C.S. 2-63.

that of Chl a. At the end of the induction change, however, a large increase of the Chl a fluorescence yield is observed, while that of the phycocyanin has increased considerably less. The difference spectrum obtained by subtracting curve S from M corresponds to a typical Chl a fluorescence band, peaked at 684 nm and having a half-band width of 22-23 nm. These values are identical with those obtained by exciting the Chl a fluorescence at 440 nm. Such an excitation yields an almost pure Chl a fluorescence band with negligible, if any, phycocyanin fluorescence (fig. 5).

Similar results were obtained with DCMU poisoned Anacystis. Fig. 26, curve S, shows the emission spectrum which corresponds to the 3 sec light exposure and curve M to the spectrum at the stationary state. Again, the fluorescence yield increase is in the Chl a emission. This is clearly seen in the difference spectrum M-S which has a maximum of 685 nm and a half-band width of 25 nm. The stationary state fluorescence spectra of both normal and DCMU poisoned Anacystis are typical of those reported in the literature. In the S spectrum an additional band seems to be present at about 710 nm. The invariability of the phycobilin fluorescence yield of marine red algae under continuous illumination was first reported by French and Young.[93]

The Chl a fluorescence increase can be interpreted either as an increase of the Chl a fluorescence yield or as an increased excitation energy transfer from phycocyanin. Changes of the energy transfer from phycocyanin to the strongly fluorescent Chl a of system II and the weakly

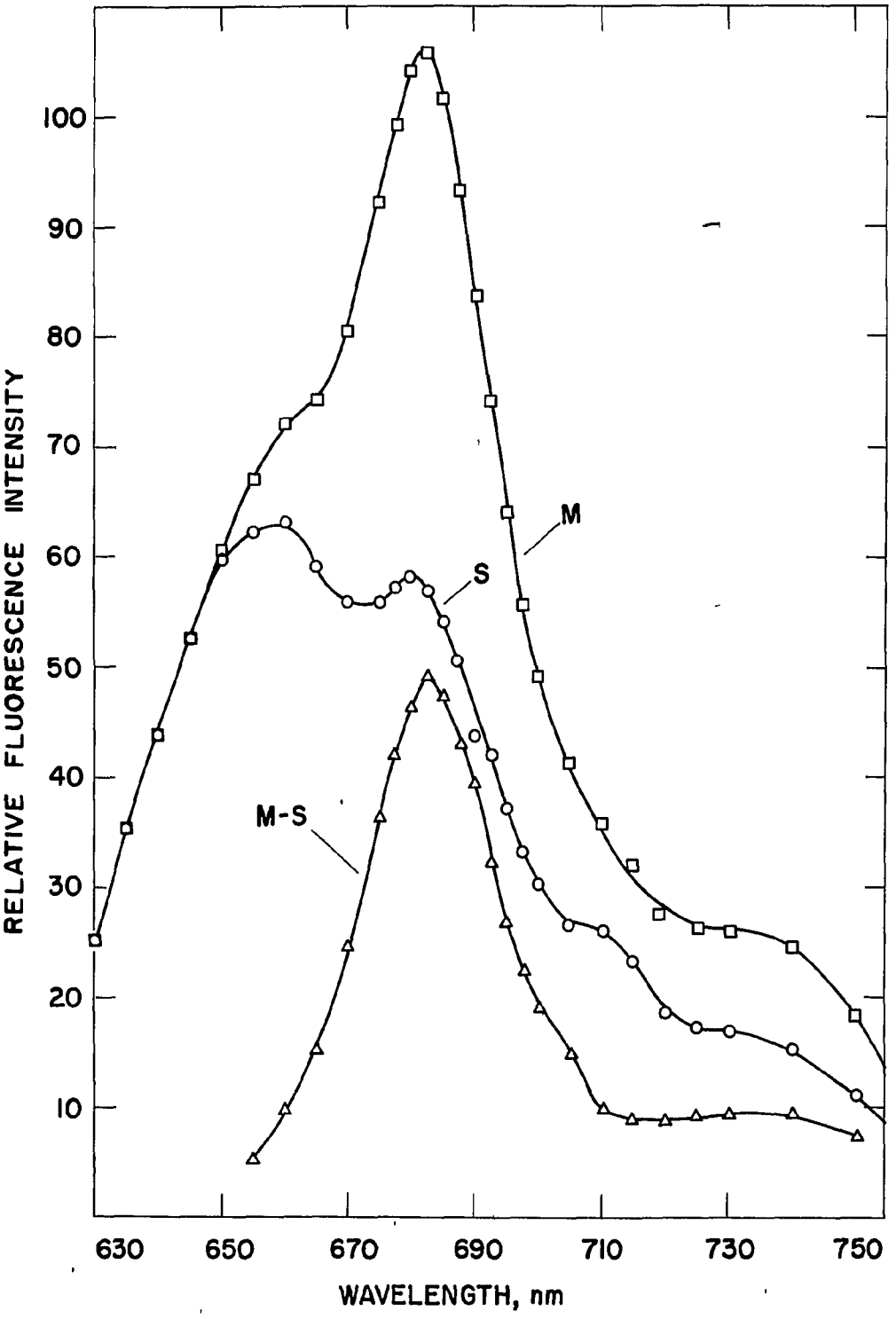

Fig. 26. Emission spectra of DCMU (5×10^{-5} M) poisoned Anacystis at 3 sec (S) and 10 min (M) of light exposure, M - S, the difference spectrum. Excitation as in fig. 24. Observation: Half-band width, 7.6 nm; Corning filter, C.S. 2-63.

fluorescent Chl a of system I have been invoked by Ghosh and Govindjee[68] for the interpretation of the low stationary state Chl a fluorescence of Anacystis grown in "high light". We believe, however, that in our experiments the changes observed originate mostly from the light induced increase of the Chl a fluorescence yield because (i) we did not observe a decrease in the phycocyanin fluorescence, as it would be expected for increased energy transfer and (ii) the fluorescence increase in the DCMU poisoned Anacystis can also be effected by direct excitation of Chl a (section C).

C. FLUORESCENCE INDUCTION WITH PROLONGED ILLUMINATION*

The high fluorescence yield at M which was taken in the preceding sections to indicate the end of the induction change in Anacystis, experiences a slow decay when the continuous excitation is extended to longer times (up to 90 min). Prolonged system II excitation of normal Anacystis (590 nm), suspended in carbonate-bicarbonate buffer (K_2CO_3, $NaHCO_3$, $[CO_3^{=}] = 9.2$ M, pH = 9.2) results in a gradual decline of the Chl a fluorescence yield (fig. 27, curve A), while the phycocyanin yield observed at 650 nm (curve B) remains steady. A similar and more extensive decline of the Chl a fluorescence was observed also with DCMU poisoned Anacystis (curve C). As in the case

*Results presented in this section were reported by the author at the Symposium on Energy Conversion by the Photosynthetic Apparatus held at the Brookhaven National Laboratory, Upton, L.I., N.Y. (June 1966) and in his paper in the Biophysical Journal 7, 375 (1967).

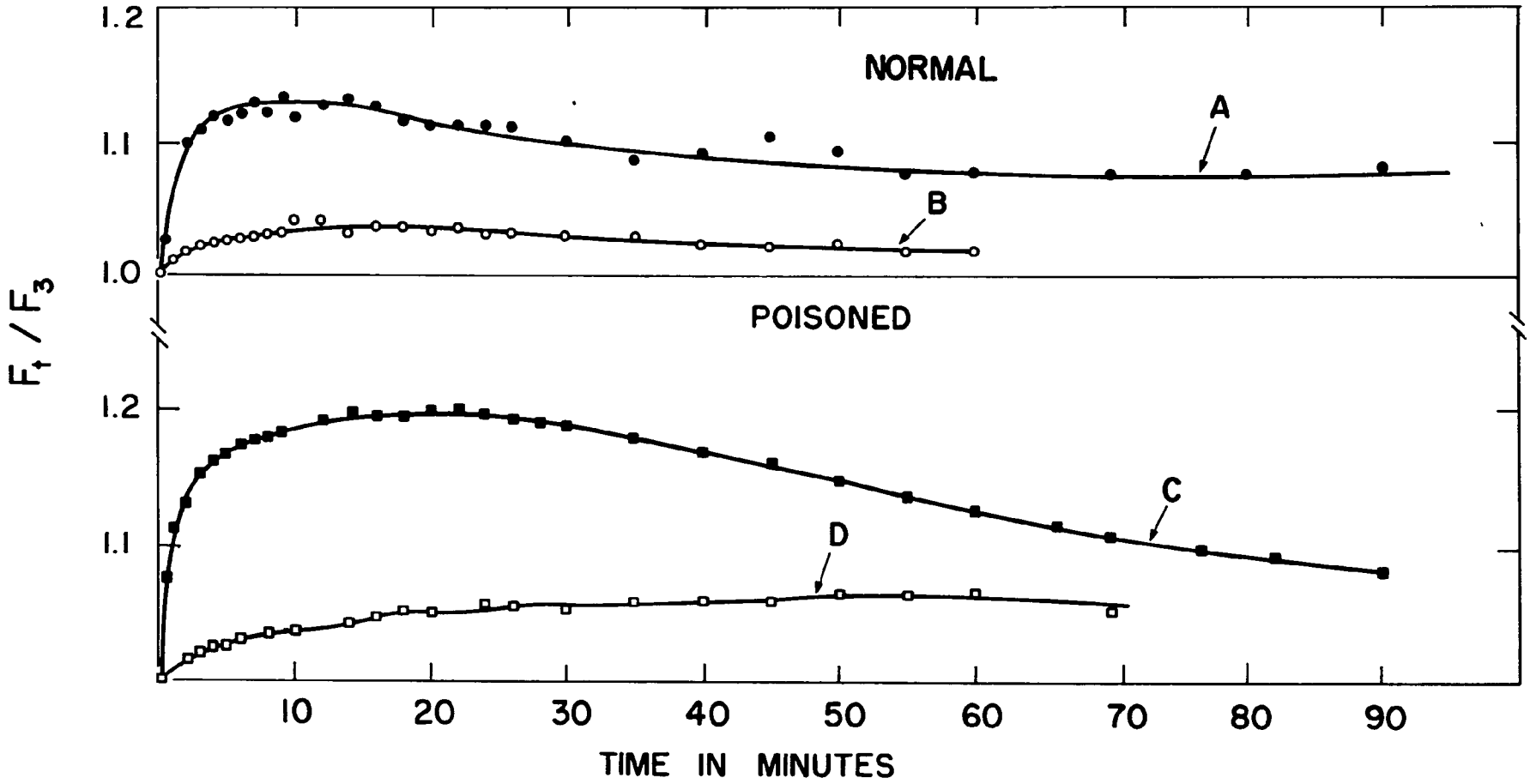

Fig 27 Time course of the relative fluorescence yield ($f = F_t \cdot F_3''$) in normal and DCMU (5×10^{-5} M) poisoned Anacystis for prolonged illumination A and C Excitation: λ = 590 nm; half-band width 20 nm, intensity 4.9×10^3 ergs cm.$^{-2}$ sec.$^{-1}$ Observation: λ = 685 nm (Chl a); half-band width, 6.6 nm, Corning filter, C.S 2-58 B and D Excitation: λ = 580 nm, half-band width, 20 nm; incident intensity, 4.9×10^3 ergs. cm^{-2} sec^{-1} Observation. λ = 650 nm (phycocyanin); half-band width, 6.6 nm; Corning filter, C.S. 2-58 (redrawn from ref 94)

of normal Anacystis, the fluorescence yield of the poisoned samples at 650 nm experiences a much smaller change consisting of a rise to a low plateau (curve D). For reasons given before (section A), the actual increase in the phycocyanin fluorescence may even be smaller.

Fig. 28 shows the emission spectra, excited at 590 nm, of normal and DCMU poisoned Anacystis nidulans at two different times of light exposure. Curves A and D correspond to spectra recorded 15 min after the onset of illumination, while curves B and E after 90 min. The Chl a emission has decreased throughout the spectral region of observation. Difference spectra constructed by subtraction of the emission intensity values at 15 min from those at 90 min (curves C and F) show that there are two regions within the Chl a emission band where the changes are maximal, one at 685 nm, the other at 693 nm. The doublet character of the difference spectra has been observed repeatedly with cultures of varying ages, optical densities and with different illumination intensities. The short wavelength peak varied between 683 and 687 nm and the long wavelength one between 692 and 699 nm.

It was stated before (section A) that direct Chl a excitation does not support fluorescence induction in normal Anacystis. DCMU poisoned cells, however, are capable of an extensive fluorescence increase when they are subjected to continuous blue illumination (fig. 29). Contrary to the results obtained with system II light, the high stationary yield persists for a long time with no indication for a decay. The different responses of the normal and DCMU poisoned Anacystis to

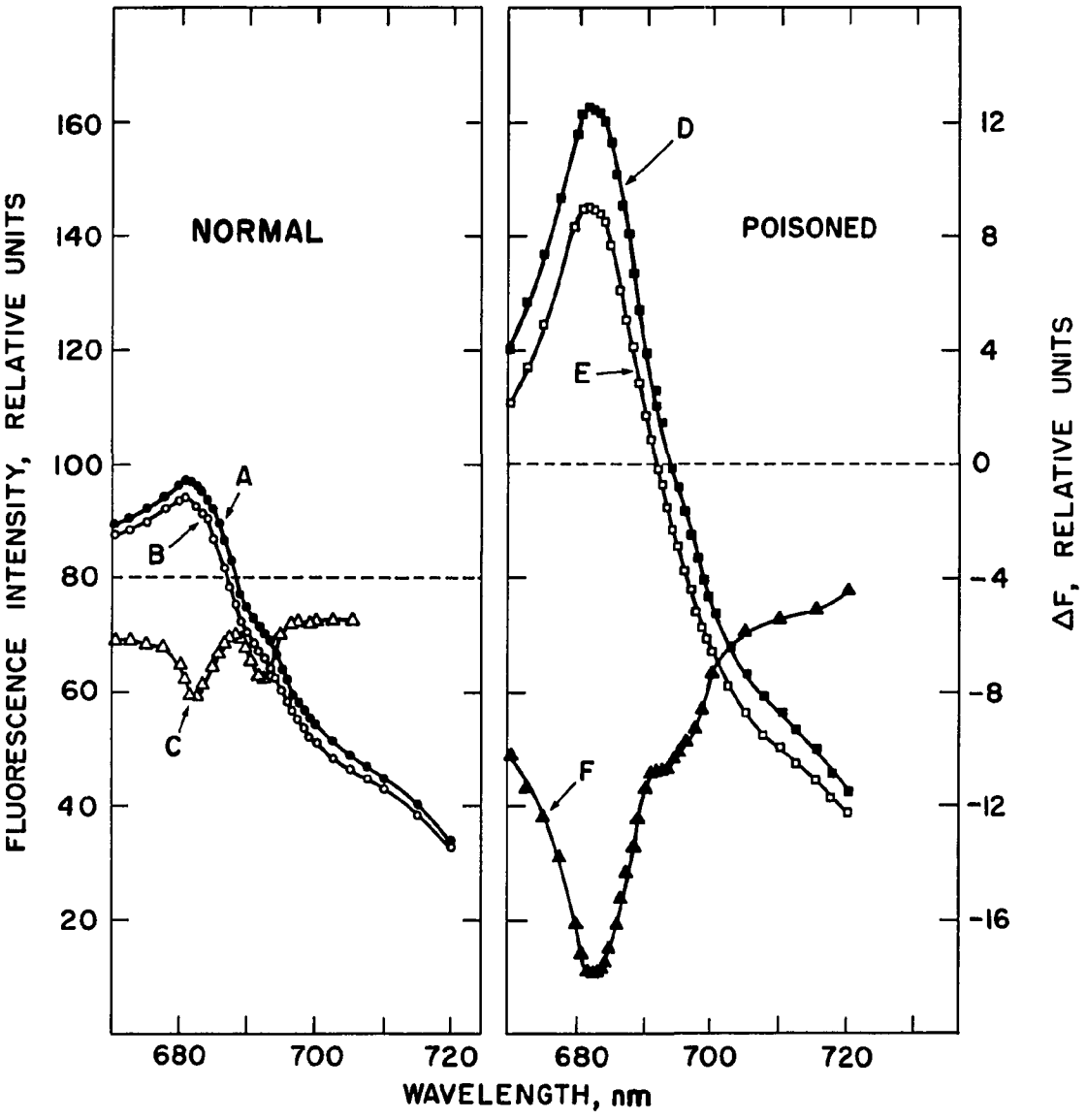

Fig. 28. Emission spectra of normal and DCMU (5×10^{-5}M) poisoned Anacystis. A and D, at 15 min. B and E at 90 min of light exposure; C = B - A and F = E - D, the difference spectra. Excitation as in fig. 27. Observation: Half-band width, 2.5 nm; Corning filter, C.S. 2-59 (redrawn from ref. 94).

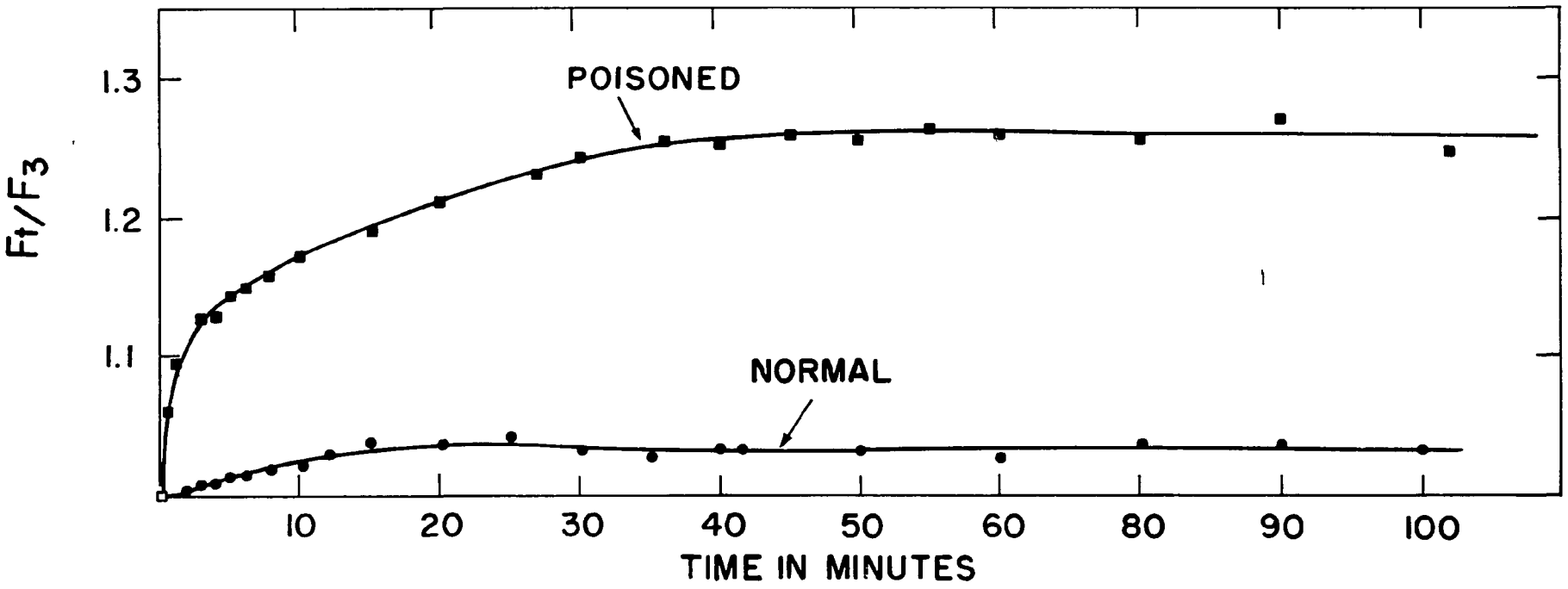

Fig. 29. Time course of the relative fluorescence yield ($f = F_t:F_3''$) in normal and DCMU (5×10^{-5}M) poisoned Anacystis for prolonged illumination. Excitation: λ = 440 nm; half-band width, 20 nm; incident intensity, 2.4×10^{3} ergs. cm.$^{-2}$ sec.$^{-1}$ Observation: λ = 685 nm; half-band width, 25 nm, Corning filter, C.S. 2-58 (redrawn from ref. 94).

direct Chl a excitation indicate that different mechanisms may be involved. For example, inhibition of system II with DCMU may result in enhanced electron flow involving only system I. It will be shown later that uncoupling of the photophosphorylation and variations of the suspension pH also elicit different responses in the second wave of normal and poisoned samples.

The slow variation of the fluorescence yield of a poisoned sample after 5 min of blue light illumination (cf. fig. 29) allows the automatic recording of the emission spectra (scanning time ~1 min). Fig. 30 shows such spectra taken at 5 min (curve A) and 60 min (curve B) of total exposure to blue light. The positive difference spectrum (curve C; B-A) is again characterized by two maxima located by 684 and 694 nm.

The existence of a minor Chl a emission band (at 694 nm) appearing on the far red side of the main band (at 685 nm) is not a novel result obtained for the first time in the course of this investigation.[94] Its occurrence was first reported by Krey and Govindjee[95] in the difference spectrum of Porphyridium cruentum, constructed by subtracting the emission values excited with non-saturating light from those obtained with saturating excitation. The multiplet band structure of Chl a in vivo fluorescence was also suggested by Govindjee and Yang[96] for chloroplasts and by Brody and Brody[97] for Euglena as a result of the application of Weber's[98] matrix method for the resolution of a mixture of fluorescence components. More recently, Williams et al.,[99] using the same approach, identified a weakly fluorescent component in Chlorella emitting near 700 nm. Whether the 692-699 nm emission band observed in the present work

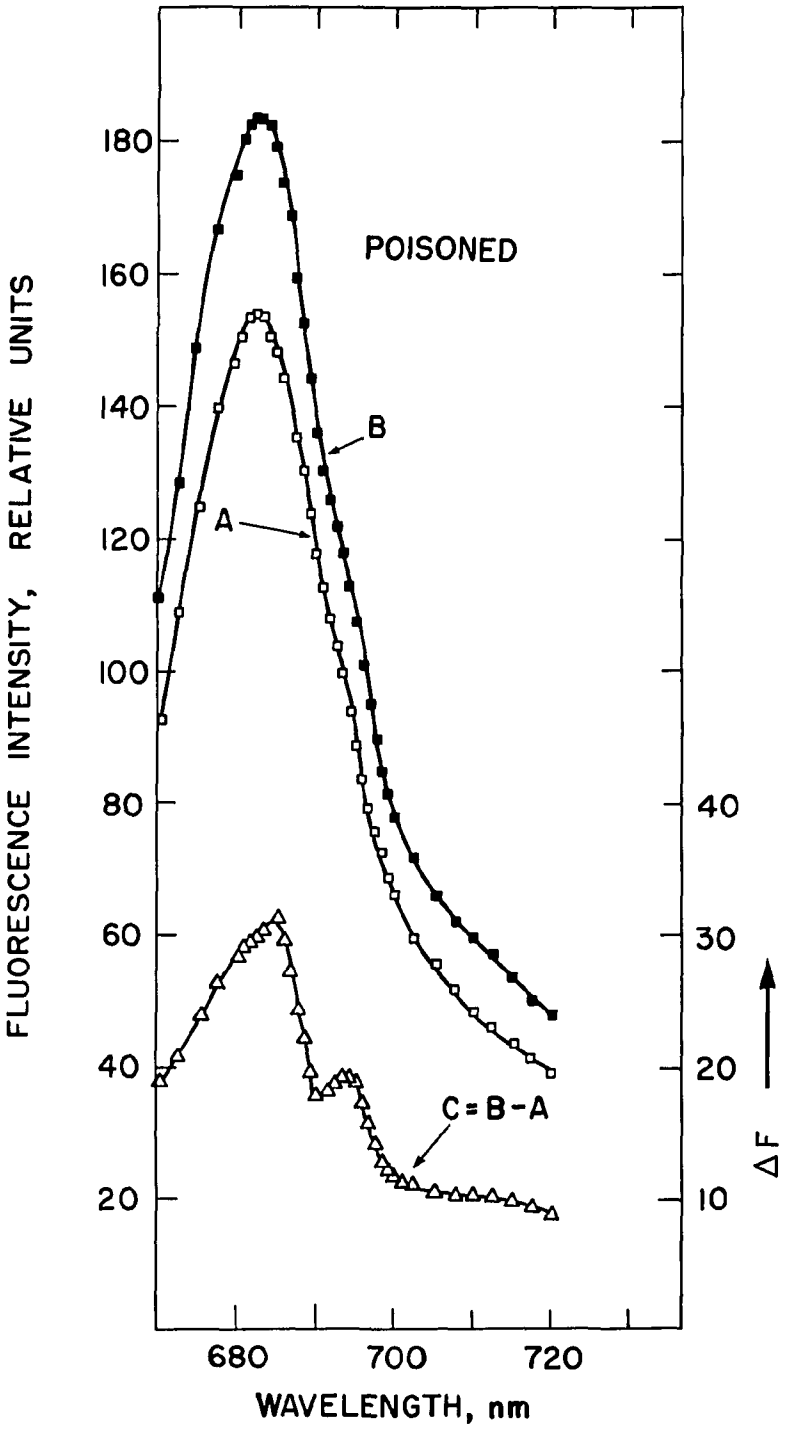

Fig. 30. Emission spectra of DCMU (5×10^{-5}M) poisoned Anacystis at 5 min (A) and at 60 min (B) of light exposure; C = B - A, the difference spectrum. Excitation, as in fig. 29. Observation: Half-band width, 3.3 nm, Corning filter, C.S. 2-58 (redrawn from reference 94).

originates from a system II or a system I Chl a form is not unequivocally decided. Since these changes are caused by system II excitation it is likely that this band originates from that system.

The most convincing proof for the multiplicity of Chl a fluorescence was, however, provided by the low temperature (77°K; liquid nitrogen) spectroscopy. The higher yields and the band sharpening which characterize the low temperature emission spectra are certainly advantageous for the detection of minor fluorescent components. The Chl a emission at these temperatures consists of three separate bands located at 685, 697 and 716 nm.[96, 100, 101] The different temperature dependence of their yields in the range 4°K to 300°K [96, 102] indicates that these bands originate from distinct Chl a forms (holochromes or aggregates) having presumably different roles in the photochemical utilization of the electronic excitation.[14] These results will be discussed fully by F. Cho.[102]

D. INTENSITY OF EXCITATION

The rate and the magnitude of the increase in the Chl a fluorescence yield of Anacystis nidulans are functions of the exciting (absorbed) light intensity. The time course of the fluorescence intensity of a normal Anacystis sample for a number of incident intensities at 620 nm (phycocyanin absorption peak) are given in fig. 31. In fig. 32, relative yield, $f = F_t:F_3''$, is plotted. Very weak excitation causes only a slight increase, starting after a lag phase. With increasing exciting intensity both the maximal change $f_M - f_3''$ (height of the plateau of the f vs time curve) and

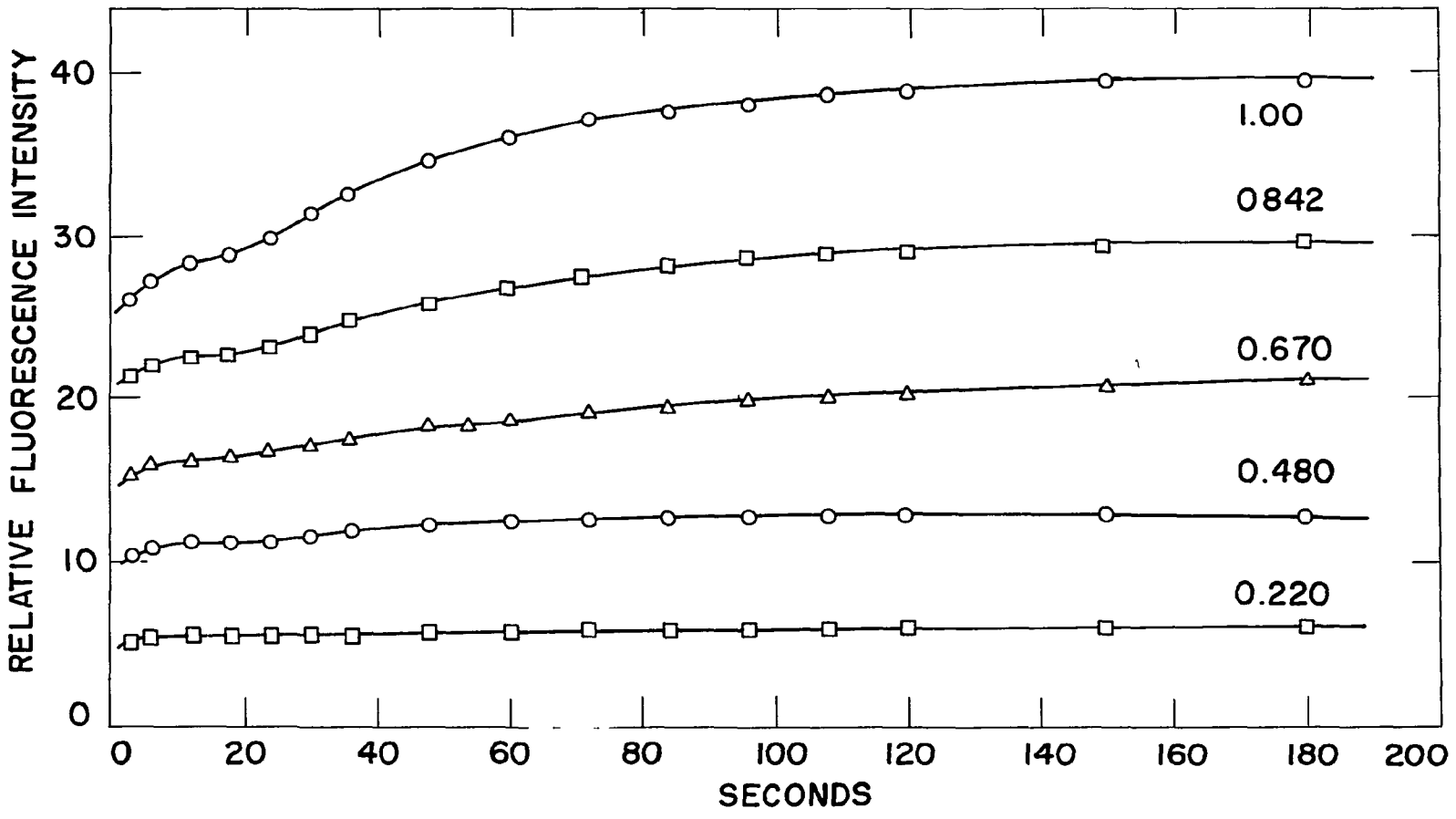

Fig. 31. Time course of the fluorescence intensity of normal Anacystis at different exciting intensities. Intensity 1.00 ≡ 4 1 x 10^3 ergs. cm.$^{-2}$ sec.$^{-1}$ Excitation· λ = 590 nm, half-band width, 16.5 nm. Observation λ = 685 nm, half-band width, 13.2 nm, Corning filter, C S. 2-60.

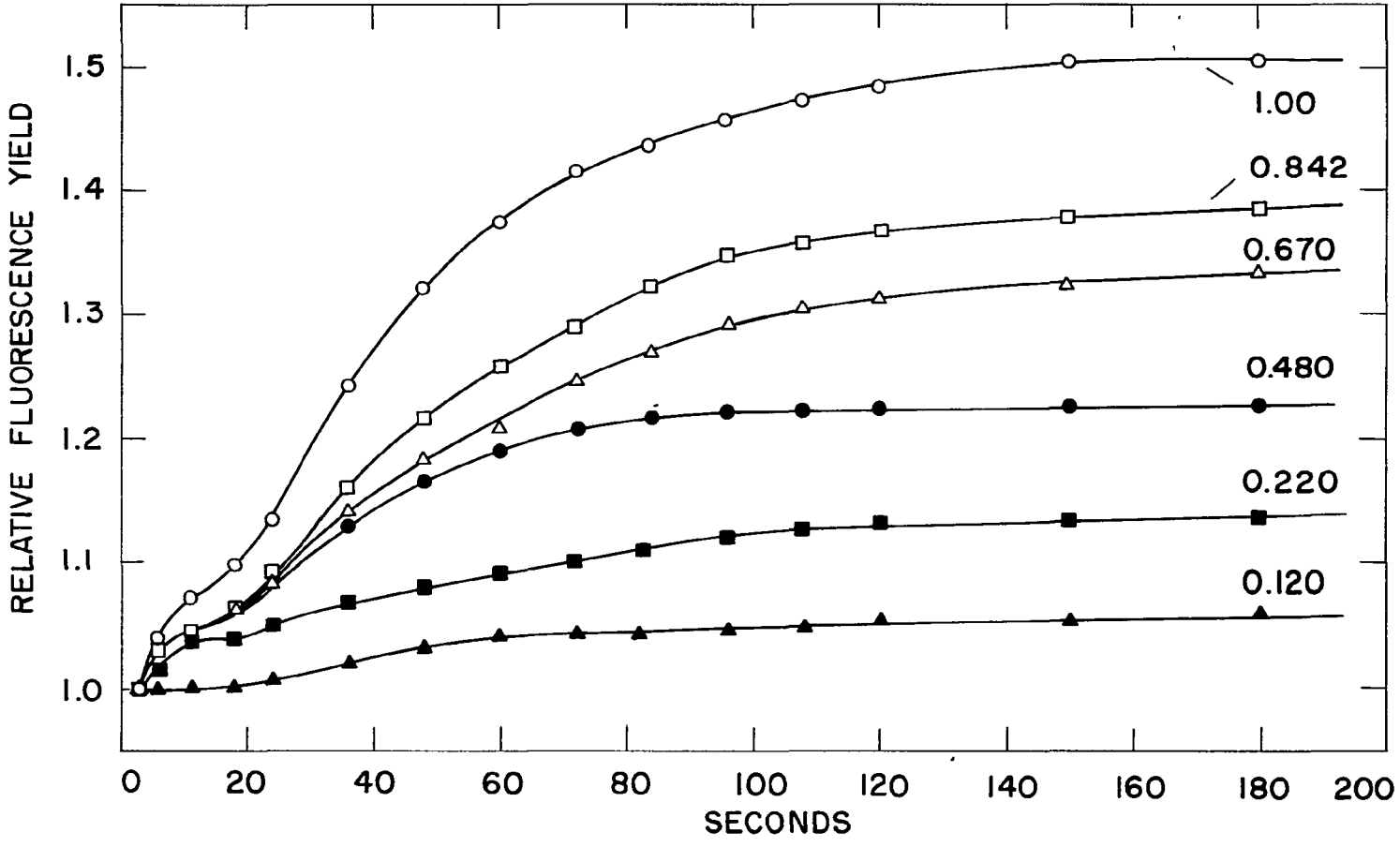

Fig. 32. Time course of the relative fluorescence yield ($f = F_t:F_3''$) in normal Anacystis at different exciting intensities, details as in fig. 31.

the rise rate increase. The maximal change increases almost linearly with the excitation at low intensities and then it saturates (fig. 33, Curve B). A fluorescence light curve (curve A) in which the stationary state (M) emission intensities are plotted against the incident intensity is given for comparison. No relationship is apparent between the maximal change (f_M-f_3'') and the fluorescence intensity at M, and consequently with the rate of photosynthesis. For example, at light intensities which correspond to saturation of photosynthesis (second segment of the light curve (A) in fig. 33), the maximal change is still increasing.

The time course of the fluorescence intensity and of the relative yield (F_t:F_3'') at various exciting intensities for a poisoned sample are given in the figs. 34 and 35. The two-phase character of the fluorescence yield rise is evident only at low intensities. The maximal change (f_M) saturates rapidly while the fluorescence light curve has a constant slope throughout the excitation intensity interval used (fig. 36, curves B and A, respectively). The constancy of the fluorescence quantum yield (in curve A) is, of course, an indication of the inhibition of the non-cyclic electron flow.

The light intensity dependence of the fluorescence rise rate (fig. 32 and 35) suggests that the processes which lead to the increased quantum yields are photochemical in character. The establishment of the higher constant fluorescence yield may then reflect a competition between these processes and opposing dark ones. Since the maximal change will be determined by the rate constants of the competing

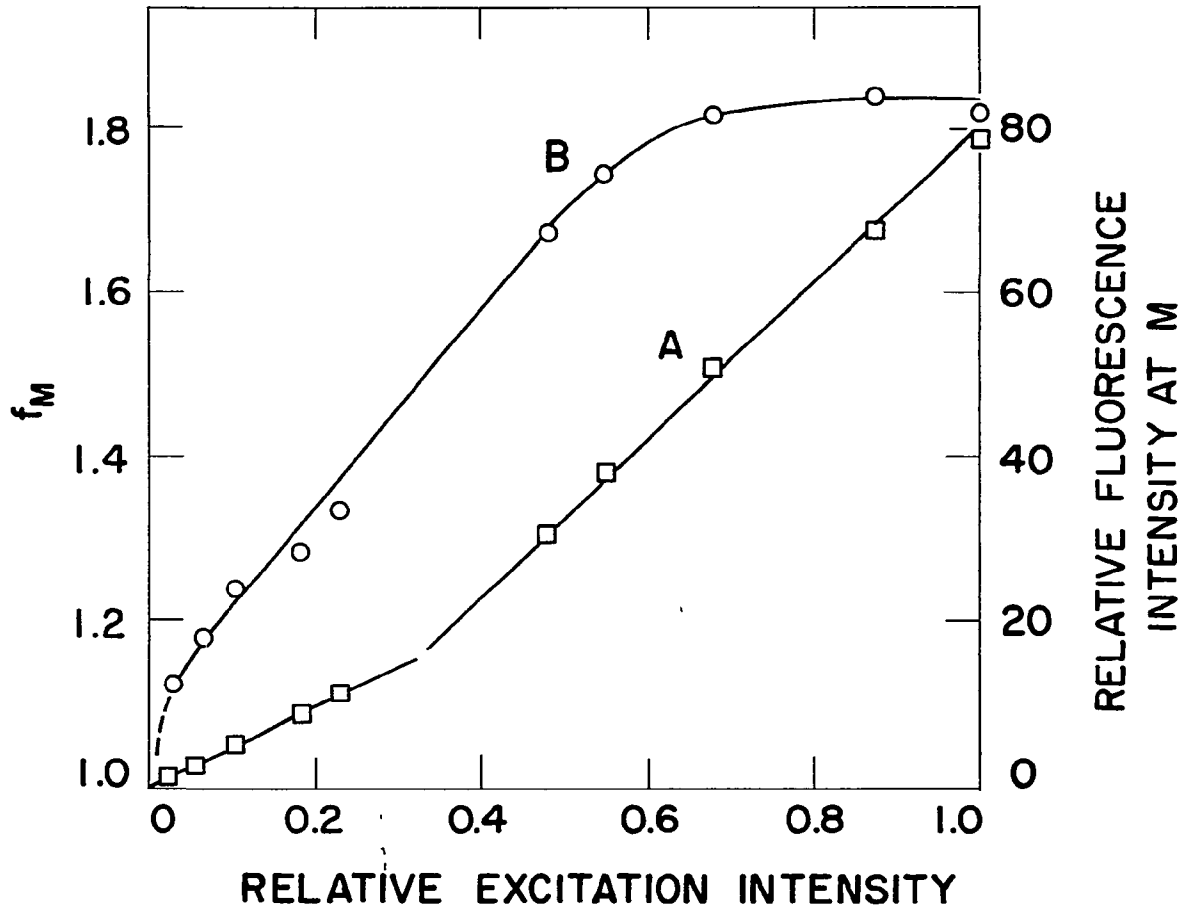

Fig. 33. The fluorescence intensity (A) and the relative fluorescence yield (B) at M in normal Anacystis, as a function of the incident light intensity. Intensity $1.0 \equiv 4 \times 10^3$ ergs. cm.$^{-2}$ sec.$^{-1}$ Excitation· λ = 620 nm, half-band width, 16.5 nm. Observation λ = 685 nm, half-band width, 6.6 nm· Corning filter, C.S. 2-64.

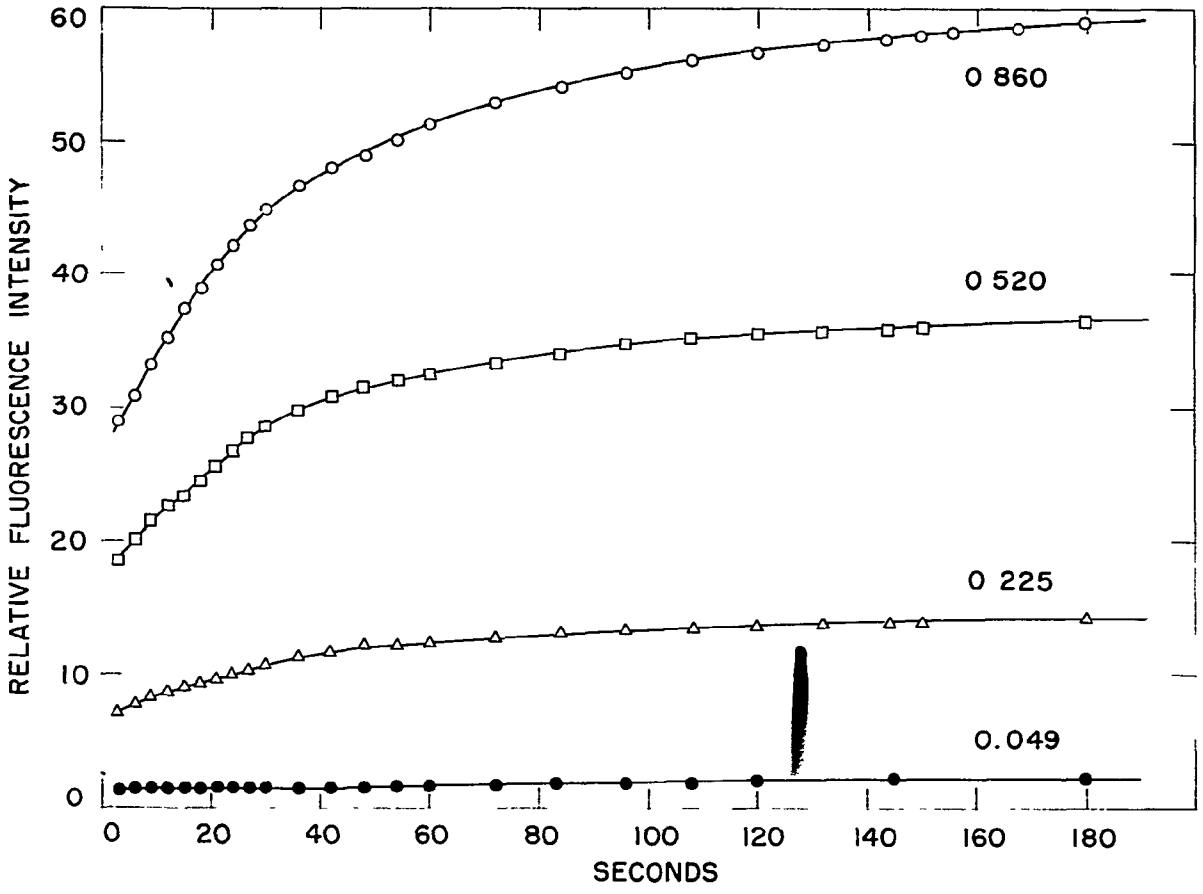

Fig. 34. Time course of the fluorescence intensity in DCMU (5×10^{-5} M) poisoned Anacystis at different exciting intensities. Intensity $1.00 \equiv 4.1 \times 10^{3}$ ergs. cm.$^{-2}$ sec.$^{-1}$ Excitation: $\lambda = 590$ nm; half-band width, 16.5 nm. Observation $\lambda = 685$ nm, half-band width, 6.6 nm, Corning filter, C.S. 2-58.

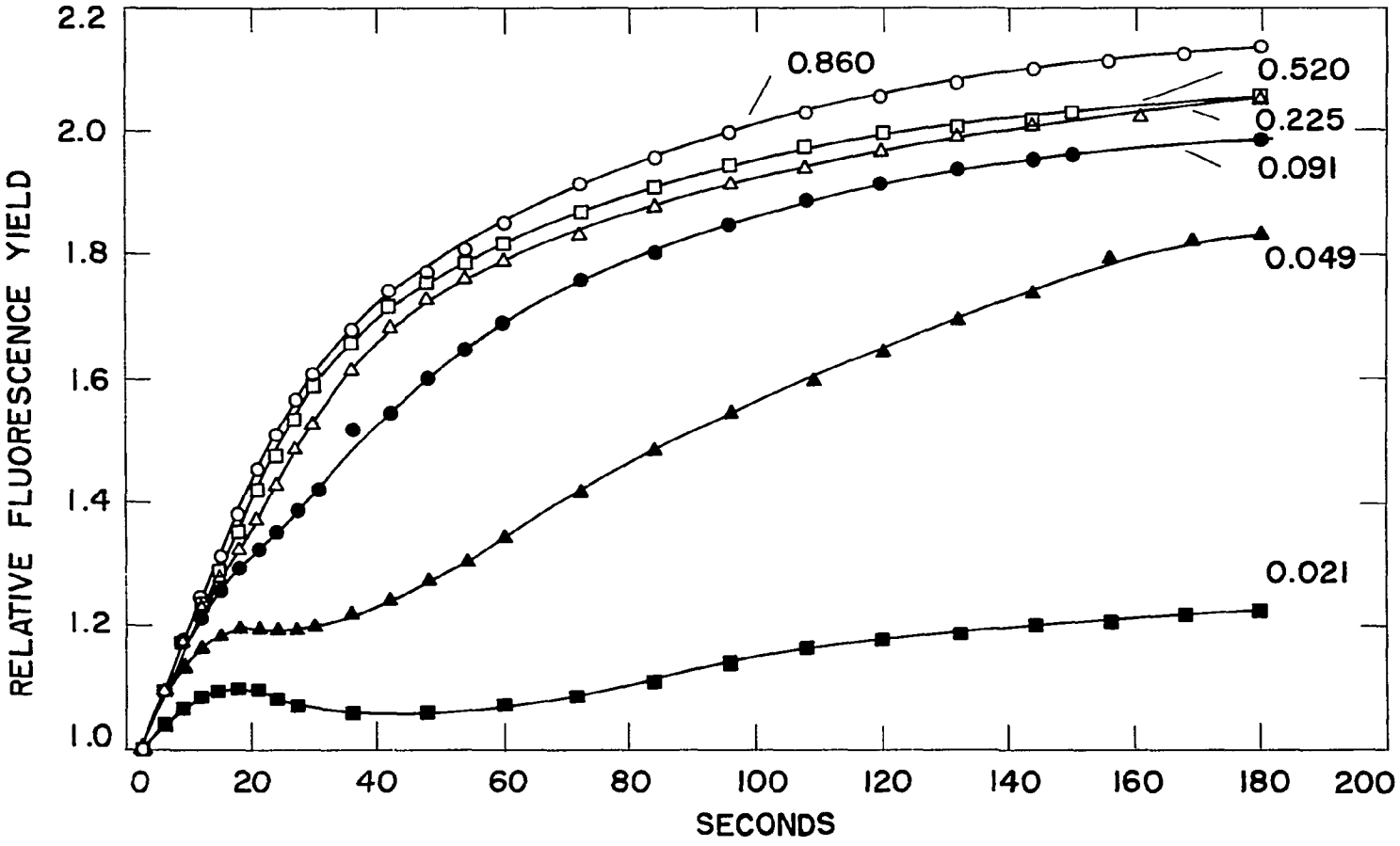

Fig. 35. Time course of the relative fluorescence yield ($f = F_t \cdot F_3''$) in DCMU (5×10^{-5} M) poisoned Anacystis at different exciting intensities, details as in fig. 34

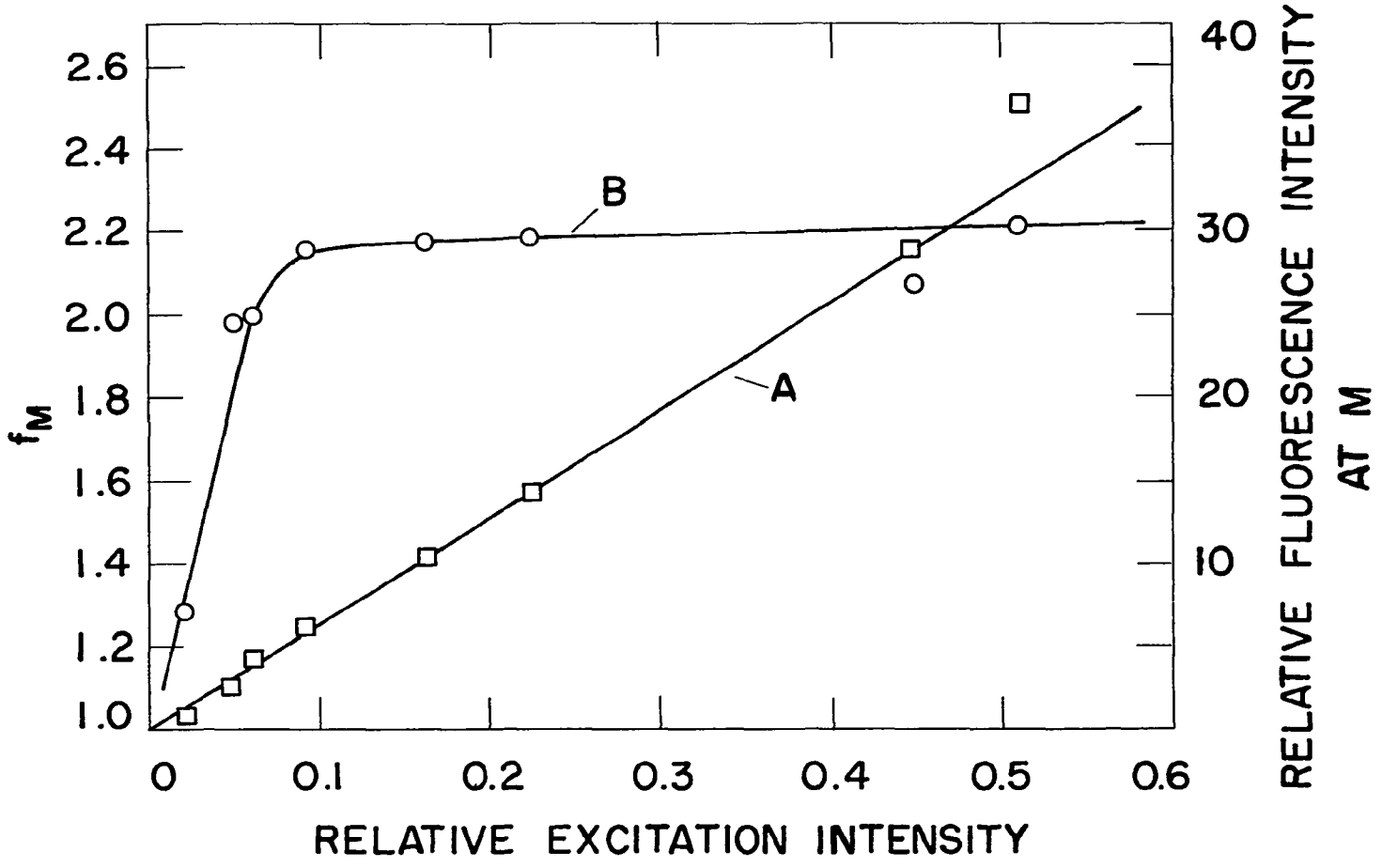

Fig. 36. The fluorescence intensity (A) and the relative fluorescence yield (B) at M in DCMU (5×10^{-5}M) poisoned Anacystis; details as in fig. 34.

processes, increased excitation intensity will lead to higher stationary fluorescence yields. The light saturation of the maximal change is suggestive of the enzymatic nature of the processes involved. At low excitation intensities, for example, the rate limiting factor is the photon flux while at high the supply of the enzyme.

The comparison of the fluorescence and maximal change light curves of normal Anacystis (fig. 33) suggests the absence of a simple and direct correlation between the rate of photosynthetic electron flow and the fluorescence. The existence of this electron flow, however, appears to be indispensible for the occurrence of the change in the normal sample, since system I excitation alone is ineffective (cf. sections A and C). Poisoned cells, on the other hand, are capable of large fluorescence changes in the absence of any appreciable photosynthesis. We therefore suggest that different electron transport pathways are operating in the normal and the DCMU poisoned samples and that the fluorescence change is caused by the different electron pathways. Support for this idea is provided by the earlier light saturation of the maximal change in the poisoned samples.

The effectiveness of blue light to promote fluorescence induction (increase) in DCMU poisoned Anacystis nidulans may suggest that the operation of system I only is sufficient to cause this change. Under inhibition, system I can drive only the cyclic electron flow whose sole effect is the production of high energy phosphate. The cyclic pathway is especially resistant to inhibition by substituted phenylureas[103]

(DCMU is a member of the class). The cyclic pathway seems to be the predominant source of ATP in the blue-green algae, since cell-free extracts of Anacystis nidulans[104] and Anabaena variabilis[105] are relatively inactive in ferricyanide and NADP Hill reaction, but vigorously phosphorylate in the presence of the cyclic pathway cofactor N-methyl-phenazonium methosulfate (PMS). These considerations may explain the presence of a fluorescence induction in the DCMU-inhibited Anacystis and its absence in Chlorella.

E. HYDROGEN ION CONCENTRATION

The rate of photophosphorylation and the formation of ionic gradients (X_E) in isolated higher plant chloroplasts are strongly dependent on the proton concentration of the suspension medium (Chapter III, section D). On the hypothesis that these phenomena are the basis for the fluorescence induction changes, we measured the time course of fluorescence as a function of the pH of the suspension. (We realize that we don't know the pH of the inside of the cells.) The algae were suspended in the tris-NaCl buffer and the pH was varied by the addition of NaOH or HCl. The pH of the samples was checked routinely, prior and after the optical measurements, it remained constant. This check was important, especially at pH values below 6.0 where the buffering capacity of the medium declines rapidly. The pH curves to be given were repeatable when the direction of the pH change was reversed.

The initially recorded fluorescence yields (S - level) of both the

normal and DCMU poisoned Anacystis were found to be pH insensitive. On continuous excitation, however, the fluorescence increase (S-M) shows a characteristic dependence on the proton concentration of the medium. These results are shown in fig. 37, where the pH curves of the maximal change for a normal (left) and for a DCMU poisoned sample (right) are given. Typical of these curves is the opposite trend in the acidic region. (The minimum and the maximum depicted in fig. 37 were not observed in some experiments and only a plateau was registered in the alkaline region.) The observed results coincide with the pH dependence of the light induced cation transport.[42,45]

Our results show that only under actinic illumination of the sample will the hydrogen ion concentration of the medium influence the fluorescence yield. We deal, therefore, with the pH effect on a photochemical process, which on the basis of the similarity of the pH curves may be related to the light induced cation transport and its associated "conformation" changes. Light driven acidification of membrane enclosures may cause changes in the membrane conformation, e.g., by the neutralization of bound negative sites and displacement of the osmotic equilibrium. Polyelectrolyte behavior of the Chl a carrying membranes has been demonstrated with isolated higher plant chloroplasts[106] and with algal chloroplasts in situ (Nitella).[107] The different trends in the pH curves of normal and DCMU poisoned Anacystis is an additional indication of the different fluorescence induction mechanisms operating in each case.

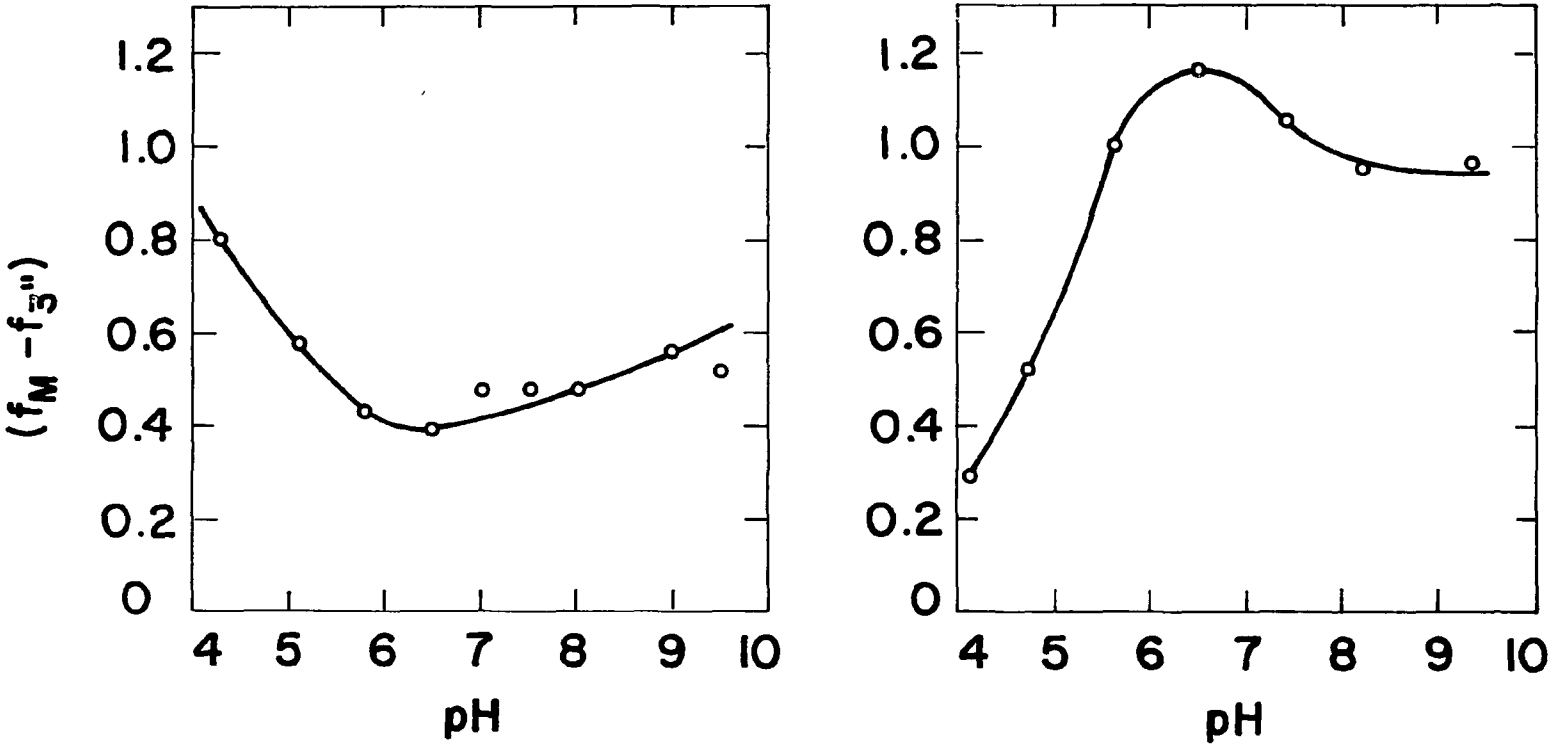

Fig. 37. The fluorescence change $f_M - f_3''$ as a function of the pH of the suspension medium. Left: Normal Anacystis. Right: DCMU (5×10^{-5}M) poisoned Anacystis. Excitation: λ = 590 nm; half-band width, 16.5 nm, incident intensity, 4.1×10^3 ergs. cm.$^{-2}$ sec.$^{-1}$ Observation: λ = 685 nm; half-band width, 6.6 nm, Corning filter, C.S. 2-58.

F. INHIBITION OF PHOTOSYNTHESIS AND UNCOUPLING OF PHOTOPHOSPHORYLATION

In the preceding sections, we demonstrated that the presence of DCMU in Anacystis nidulans enhances the light induced fluorescence increase. Since DCMU inhibits almost completely the oxygen evolution (cf. section G), the fluorescence changes cannot be related to the non-cyclic electron flow. Inhibition of photosynthesis with o-phenanthroline has the same effect as DCMU, namely an increased fluorescence induction in comparison to the control sample (fig. 38). Thus, the enhancement of the maximal change must be related to the cessation of the photosynthetic electron flow and not to specific effects of the individual inhibitor.

Addition of FCCP to a normal Anacystis sample suppresses the fluorescence induction change (fig. 39). The suppression may be caused by the inhibition of the light dependent fluorescence increase, by the acceleration of the competing dark decay, or by the combined effect on both processes. On the basis of the almost identical rise rates of the control and the FCCP samples in the first few seconds of illumination, we favor the second alternative, namely the acceleration of the dark decay. FCCP is known to accelerate the dissipation of the light induced ionic gradients in chloroplasts.[40] By analogy we may consider that the increased dark decay of the fluorescence yield with FCCP corresponds to an accelerated destruction of the accumulated ionic gradients.

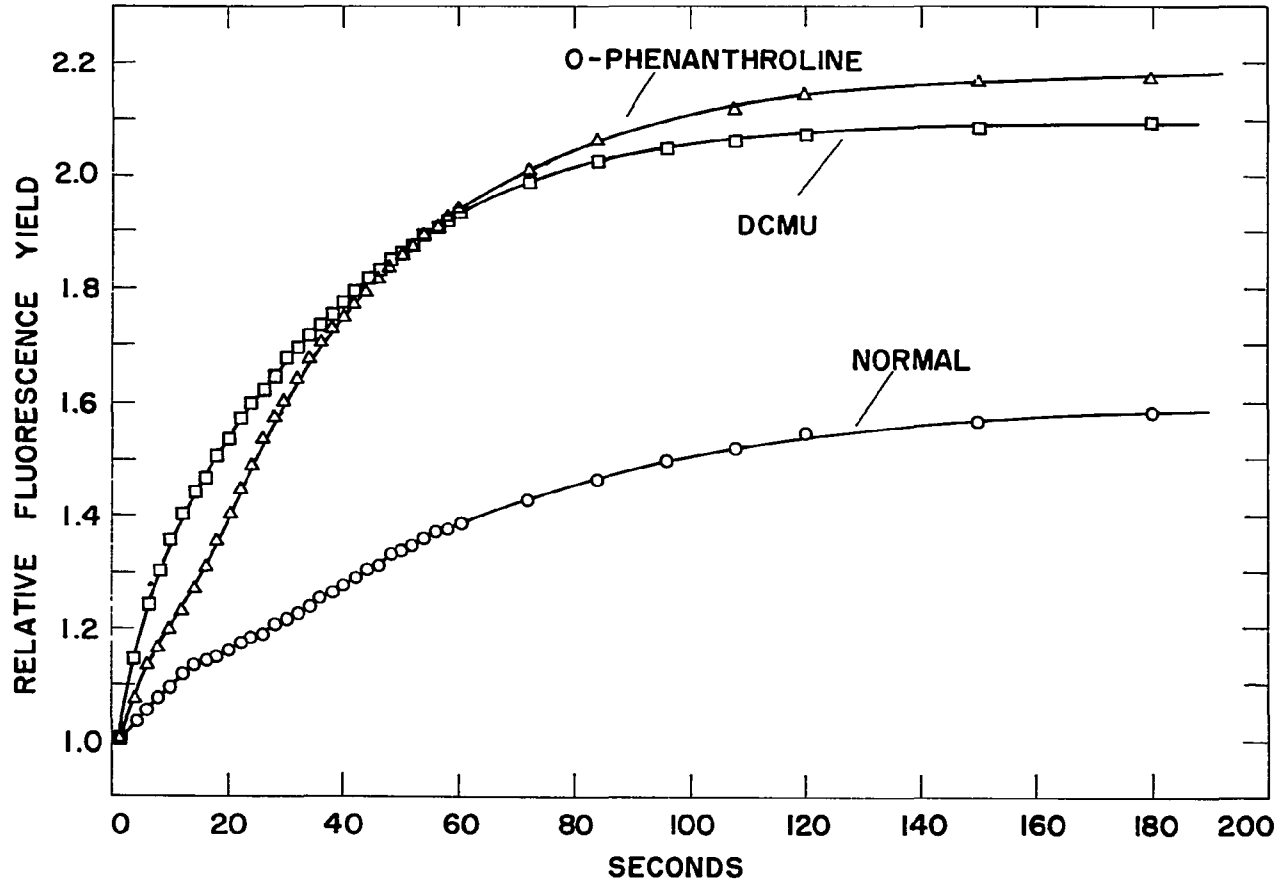

Fig. 38. The time course of the fluorescence yield ($f = F_t \cdot F_3''$) in normal, DCMU (5×10^{-5}M) poisoned and o-phenanthroline (5×10^{-4}M) poisoned Anacystis; details as in fig. 37.

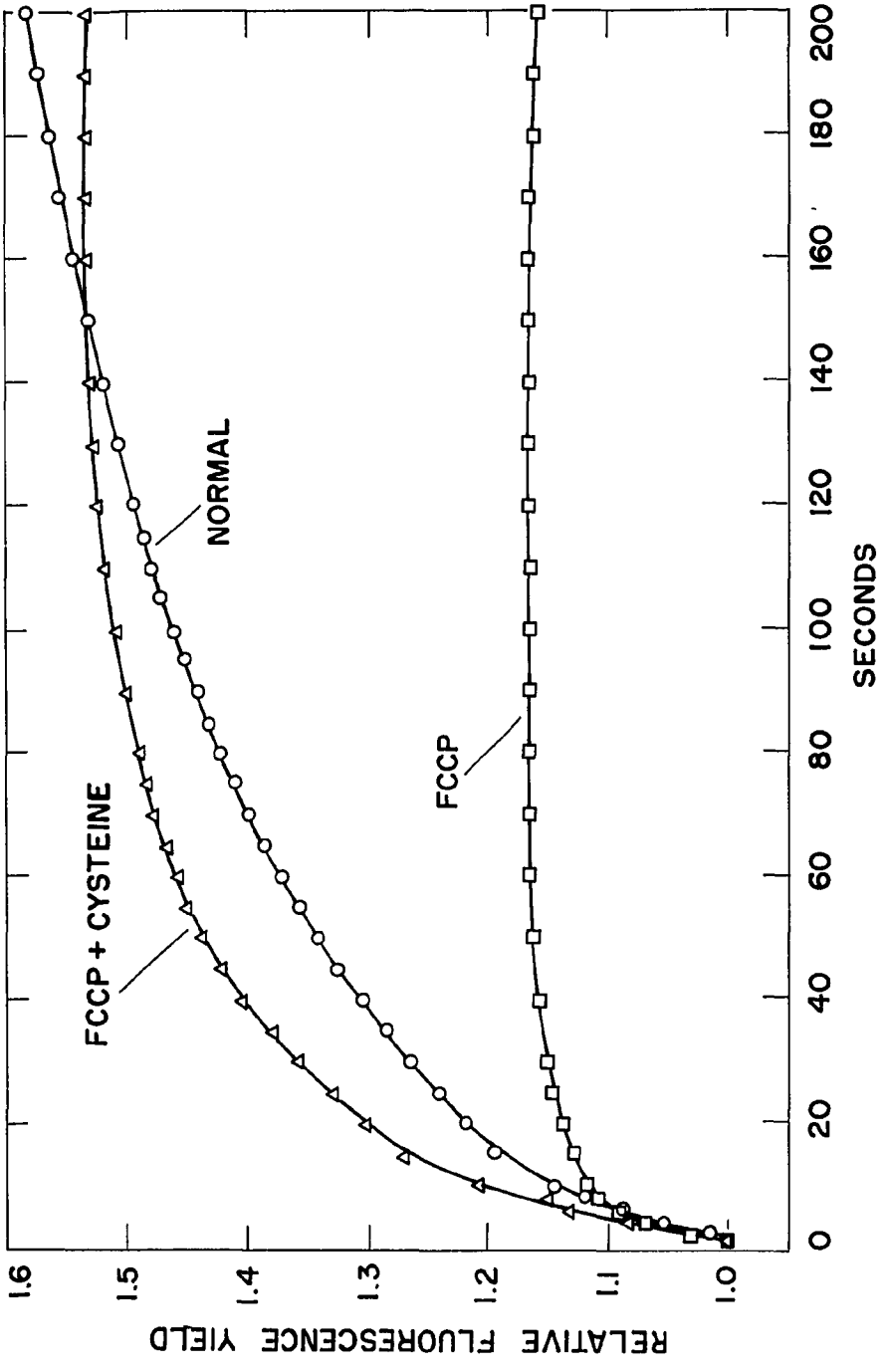

Fig. 39. Time course of the relative fluorescence yield ($f = F_t':F_3''$) in normal Anacystis. Control; with 3×10^{-5}M FCCP and 10^{-3}M cysteine; details as in fig. 37.

The FCCP inhibition is reversed by the addition of 10^{-3}M cysteine hydrochloride (fig. 39), which indicates that the uncoupler reacts with sulfhydryl groups. According to Heytler,[79] only 1,2- and 1,3-aminothiols can reverse the FCCP inhibition of the mitochondrial phosphorylation. (Addition of KCN or malonylnitrile to a normal Anacystis sample did not inhibit the fluorescence increase. Consequently, the activity of FCCP is not due exclusively to the presence of the nitrile groups.)

The effects of the uncouplers atabrin and phlorizin on the fluorescence time course of normal Anacystis are shown in fig. 40. Atabrin acts like FCCP, obliterating the fluorescence increase. Atabrin is known to inhibit the formation of X_E[56, 57] and the volume changes in isolated chloroplasts.[58] On the other hand, the phosphorylase inhibitor phlorizin had no influence on the fluorescence time course. Since this uncoupler inhibits only the terminal phosphorylation step,[87, 90] it should not prevent the accumulation of X_E and the changes of the plastid and lamellar conformation. In this respect therefore it is expected to have no influence on the fluorescence induction changes. The effect of various additions on the maximal fluorescence induction change in Anacystis nidulans is summarized in table IV.

Contrary to what we observed with normal Anacystis, the presence of FCCP and atabrin in the DCMU poisoned samples did not influence significantly the fluorescence maximal change. The fluorescence time courses, however, are modified; the rise phase is decelerated in the uncoupled samples (fig. 41). The different response of the

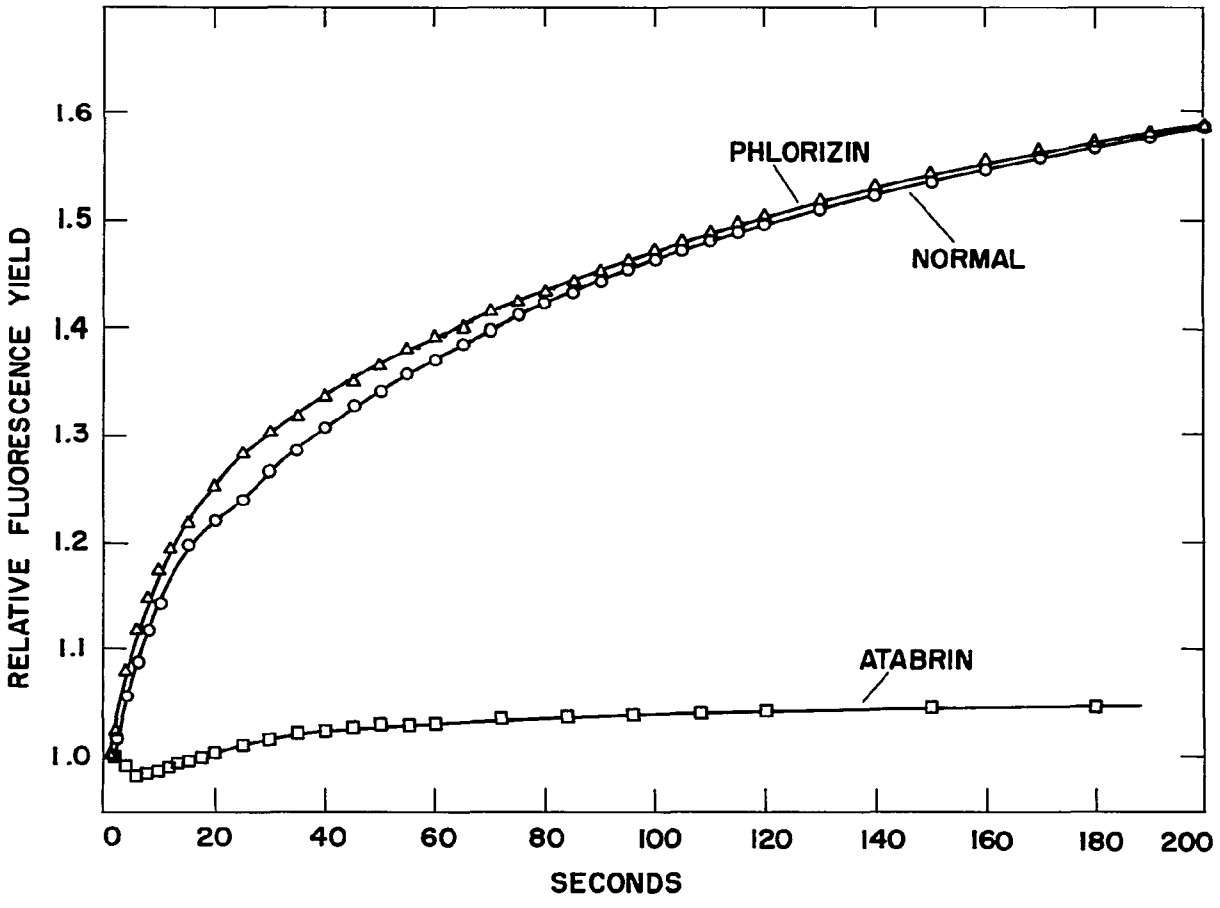

Fig. 40. Time course of the relative fluorescence yield ($f = F_f : F_3''$) in normal Anacystis. Control; with 3×10^{-5}M atabrin, with 2×10^{-3}M phlorizin, details as in fig. 37.

TABLE IV

MAXIMAL INCREASE OF THE FLUORESCENCE YIELD OF NORMAL *ANACYSTIS NIDULANS* SUSPENSIONS*

Sample	Added Chemicals and Concentration	Maximal Change f_M
1	None (control)	1.65
2	FCCP (3×10^{-5} M)	1.16
3	FCCP (3×10^{-5}M) + Cysteine (10^{-3}M)	1.61
4*	Malonylnitrile (3×10^{-4}M)	2.23
5*	KCN (3×10^{-3}M)	1.64
6*	NH_4Cl (10^{-2}M)	1.64
7*	$CH_3NH_2 \cdot NCl$ (10^{-2}M)	1.64
8	Atabrin (3×10^{-5}M)	1.04
9	Phlorizin (2×10^{-3}M)	1.61

*All samples were suspended in Tris-NaCl buffer, at pH = 8.0, and their optical density at the red Chl *a* maximum was adjusted to 0.50 units for 1 cm path. Figures given in the last column are the average of three separate samples, except those denoted with an asterisk with which only one experiment was carried out.

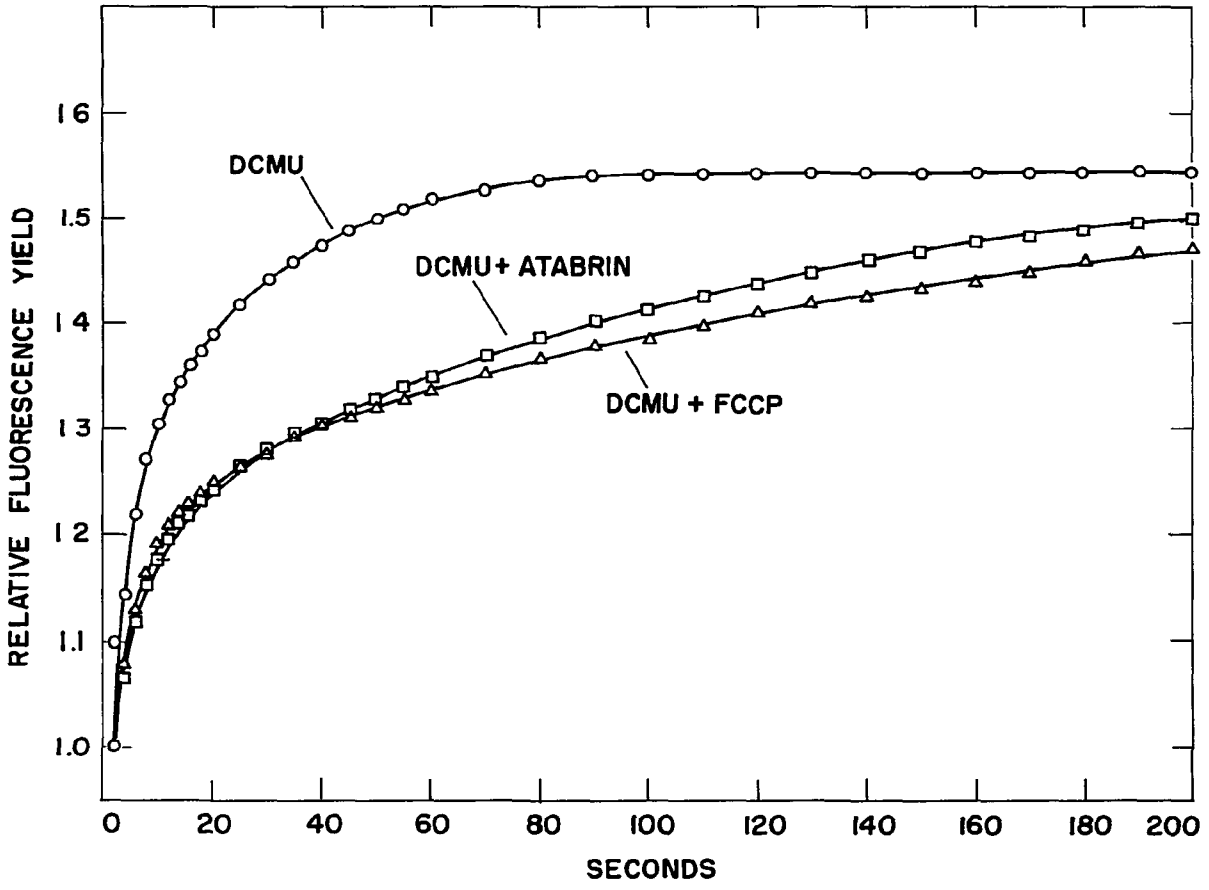

Fig. 41. Time course of the relative fluorescence yield ($f = F_t:F_3$) of DCMU (1.8×10^{-5}M) poisoned Anacystis, with 1.8×10^{-5} M DCMU and 3×10^{-5}M atabrin; with 1.8×10^{-5}M DCMU and 3×10^{-5}M FCCP; details as in fig. 37.

fluorescence induction changes of normal and DCMU poisoned Anacystis, elicited by these uncouplers, may again be indicative of the different mechanisms involved in each case. The possibility that these changes in the poisoned systems are linked to the cyclic electron pathway has been suggested previously (section D). The relative insensitivity of the cyclic photphosphorylation to FCCP is in favor of this correlation.[40] The effects of Atabrin and FCCP on the maximal change of poisoned Anacystis samples are summarized in table V.

Fig. 42 shows the emission spectra, adjusted at 660 nm, of Anacystis nidulans in the presence of some of the compounds discussed above. Atabrin and FCCP exert little effect on the shape of the spectrum, since in both the uncoupled samples and in the control, the phycocyanin and Chl a bands are approximately of the same height. Poisoning with DCMU enhances the Chl a yield, its band becoming the predominant one. The difference emission spectrum between the DCMU poisoned sample and the control is clearly a Chl a emission band peaked at 684 nm. Poisoning of photosynthesis therefore causes the Chl a fluorescence yield to increase more than the fluorescence yield of phycocyanin.

G. OXYGEN EVOLUTION AND FLUORESCENCE INDUCTION

The possibility that the fluorescence quantum yield changes correspond to changes in the rate of the photosynthetic electron flow was examined by measuring the rate of oxygen evolution and fluorescence time courses in two samples prepared from the same stock culture.

TABLE V

MAXIMAL INCREASE OF THE FLUORESCENCE YIELD OF DCMU POISONED ANACYSTIS NIDULANS SUSPENSIONS*

Sample	Added Chemicals and Concentrations	Maximal Change f_M
1	DCMU (1.8×10^{-5}M) control	1.58
2	DCMU (1.8×10^{-5}M) + FCCP (3×10^{-5}M)	1.60
3	DCMU (1.8×10^{-5}M) + Atabrin (3×10^{-5}M)	1.65

*See Table IV

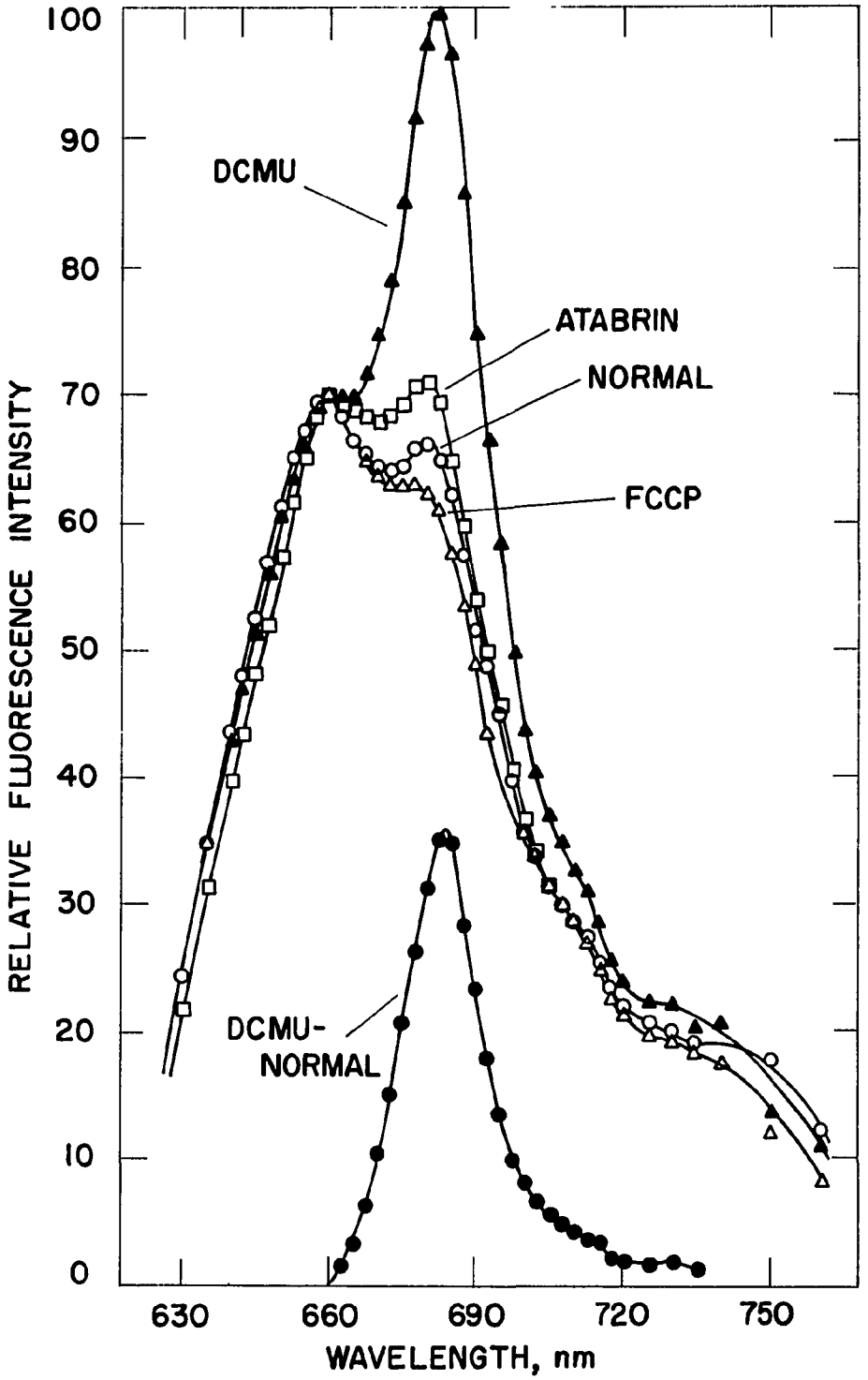

Fig. 42. Emission spectra of Anacystis. Control; with 1.8×10^{-5}M DCMU; with 3×10^{-5}M atabrin; with 3×10^{-5}M FCCP; the difference spectrum DCMU - normal. Excitation as in fig. 37. Observation: Half-band width, 4 nm; Corning filter, C.S. 2-63.

(Care was taken to subject both samples to identical light conditions). The lack of correlation appears dramatically in fig. 43. The rate of oxygen evolution experiences several oscillations before the attainment of the maximal steady value, while at the same time the fluorescence intensity increases without any oscillations whatsoever. Similar oxygen evolution oscillations, characteristic of the transition from a dark to a light period, were recently observed by Bannister[108] in Chlorella. Since the oscillations were enhanced by the presence of KCN or iodoacetamide, it was suggested that they are caused by an inhibition of the carbon fixation cycle. In Bannister's experiment, fluorescence intensity oscillations accompany those of oxygen evolution in Chlorella.[109]

On poisoning with DCMU (1.8×10^{-5} M) the oxygen evolution is suppressed although not completely abolished. As shown in fig. 44, poisoned samples are capable of a pronounced change in the fluorescence intensity, while at the same time the rate of the oxygen evolution remains low and virtually steady.

H. FLUORESCENCE INDUCTION IN ANACYSTIS NIDULANS: CONCLUSIONS

In the preceding sections, we investigated the fluorescence induction phenomena in normal and DCMU poisoned Anacystis nidulans. Several dissimilarities we re noted in the fluorescence response of the normal and of the poisoned samples. The inhibited samples have a more pronounced fluorescence yield increase (fig. 23 and 24) which is induced by either system II or system I excitation (fig. 27 and 29). In normal

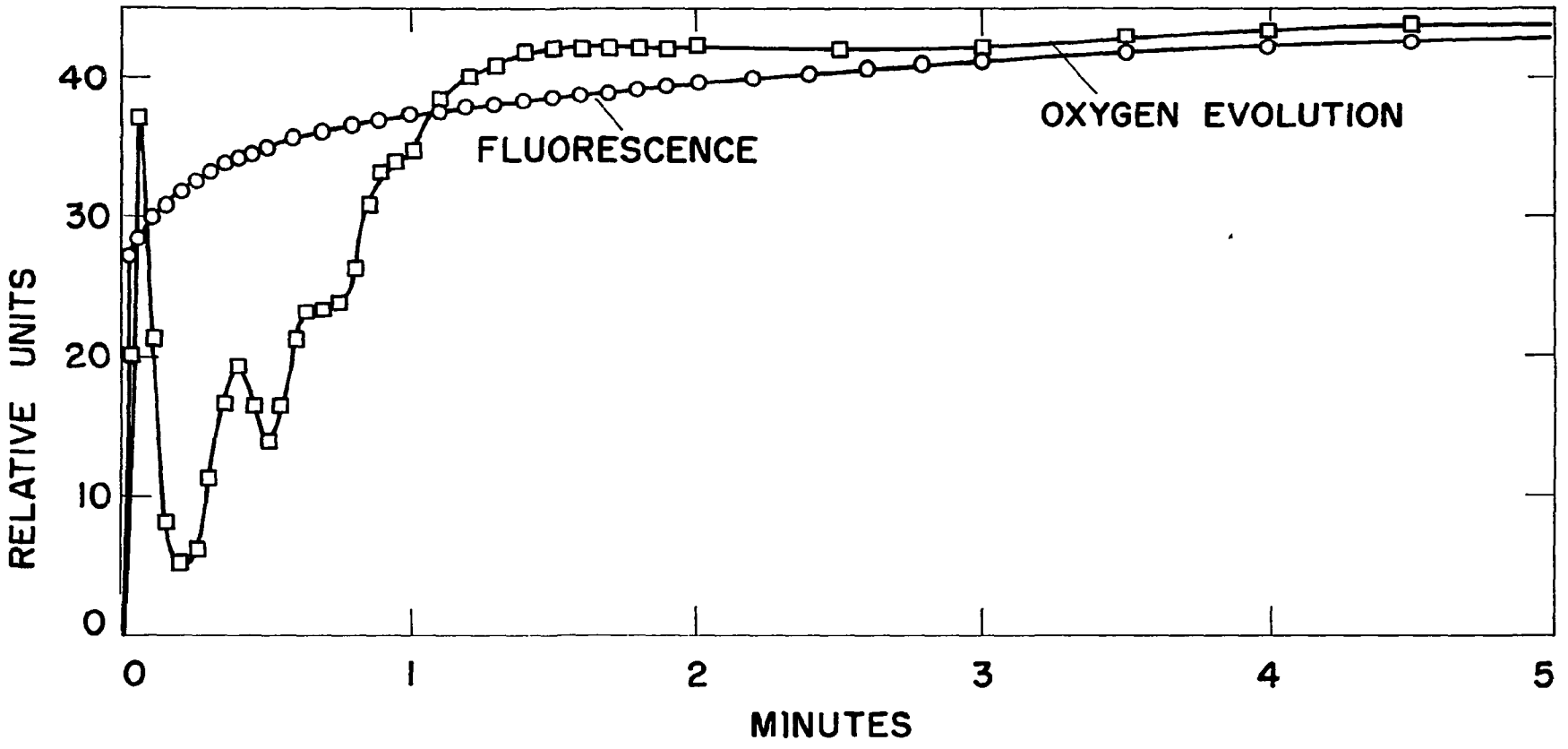

Fig. 43. Time course of the fluorescence intensity and of the rate of oxygen evolution in normal Anacystis. Excitation as in fig. 37. Observation: λ = 685 nm; half-band width, 8.3 nm; Corning filter, C.S. 2-60.

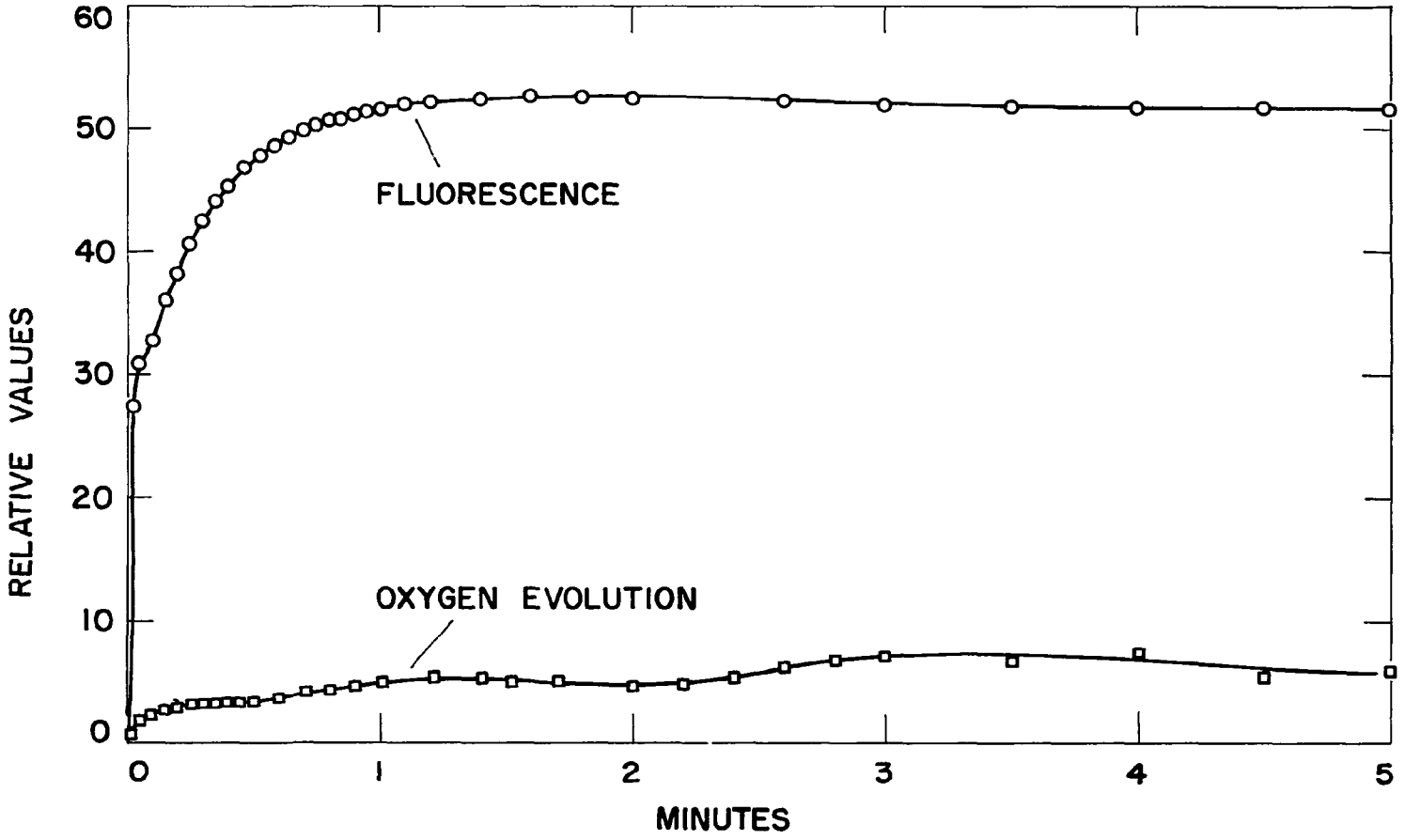

Fig. 44. Time course of the fluorescence intensity and of the rate of oxygen evolution in DCMU (5×10^{-5}M) poisoned Anacystis. Excitation as in fig. 37. Observation: $\lambda = 685$ nm; half-band width, 4 nm; Corning filter, C.S. 2-58.

Anacystis, however, only light absorbed in system II is effective. Differences have been also observed in the light intensity curves (fig. 33 and 36) and the pH curves (fig. 37) of the maximal change as well as in the effects of added photophosphorylation uncouplers (fig. 39, 40 and 41). On the basis of this information we propose that different electron pathways are involved in the normal and the inhibited Anacystis.

The comparison of the time course of fluorescence and of the rate of oxygen evolution shows no correlation between the two processes. This is most convincingly illustrated by the oscillatory character of the oxygen evolution curve, while under similar conditions the fluorescence time course is devoid of such peculiarities (fig. 43). However, the phenomenon is not completely independent of the non-cyclic electron flow. This is suggested by the requirement of system II excitation for the fluorescence increase in normal Anacystis. Light absorbed in system II is able to support the non-cyclic electron flow by transferring a fraction of its excitation to system I. The effects of exogenous uncouplers point also to the requirement of the non-cyclic electron flow for the appearance of the fluorescence induction phenomena in normal Anacystis.

The most powerful of the uncouplers we employed, FCCP, inhibits almost completely the induction in normal samples (fig. 39), presumably by combining with sulfhydryl groups. Since FCCP uncouples close to the non-cyclic electron pathway, the fluorescence changes must be affected by a later stage of the reaction sequence which leads to ATP

synthesis. However, inhibition of the terminal phosphate esterification by phlorizin had no effect on the fluorescence time course (fig. 40). These results indicate that the "origin" of the fluorescence changes must be "localized" between the non-cyclic electron pathway and the terminal phosphorylation step. Since FCCP, which accelerates the non-photochemical reversal of the fluorescence increase, is also known to accelerate the dissipation of the accumulated ionic gradient potential we postulate that the fluorescence increase is associated with the formation of these gradients. That these two phenomena are interrelated is also supported by the similarity of their pH curves (although we have some reservations as to the interpretation of these curves), by their sensitivity to added phosphorylation uncouplers and by the comparable illumination times required for their completion.

Contrary to our results with normal Anacystis, the most potent of the uncouplers we employed did not suppress the fluorescence yield increase when DCMU was present (fig. 41). Since the cyclic electron pathway, which is a major contributor to the ATP pool of the blue-green algae,[110] is rather insensitive to photophosphorylation uncoupling, we suggested the possibility of its indirect influence on the fluorescence induction changes. This correlation is supported by the capacity of poisoned Anacystis to undergo fluorescence changes with system I (440 nm) excitation and by the earlier light saturation of the maximal change in comparison to the normal cells.

The overall emission spectrum of Anacystis consists of the

phycocyanin and Chl a fluorescence contributions. The emission band of the latter is the envelope of three bands originating from different Chl a in vivo forms. We demonstrated that the changes, occurring in the first few minutes of excitation, are localized in the Chl a emission band, that of phycocyanin remaining nearly invariable (fig. 25 and 26). Technical difficulties, due to the monitoring of the spectrum at the S-level point by point did not allow for an analysis of the fine structure of the Chl a band. When, however, automatic recording of the spectrum was possible, as in the case of changes induced by prolonged illumination, we found two regions within the Chl a emission envelope where the fluorescence changes are maximal, one at 685-687 nm, the other at 692-699 nm (fig. 28 and 30). The second minor band cannot be observed by direct spectroscopy, being concealed by the strong Chl a emission at 685 nm. Our results confirm similar findings of other investigators in respect to the multiplicity of Chl a forms in vivo. The evidence for their existence and their participation in the mechanisms of photosynthesis have been discussed extensively elsewhere.[14, 94]

V. GENERAL DISCUSSION AND CONCLUSIONS

The fluorescence yield of dark adapted photosynthetic organisms undergoes characteristic variations during a light period, known as the fluorescence induction. A fast initial transient (first wave), which lasts for $\sim$2 sec, is directly related to the rate of the photosynthetic electron flow. This wave has been recently studied in detail by J. C. Munday[122] in our laboratory. The first wave is followed by a slower change in the fluorescence yield which is only indirectly affected by the primary photochemical reactions. The slow fluorescence induction of Chlorella pyrenoidosa and Anacystis nidulans and the parameters (such as light intensity, pH, inhibition of photosynthesis and uncoupling of the photophosphorylation) which influence it were investigated. We will now discuss only the slow changes in the fluorescence yield.

Several similarities in the long-term fluorescence induction of Chlorella pyrenoidosa and Anacystis nidulans may be noted, which indicate a common mechanism for both algae. The operation of the non-cyclic electron transport is essential since the excitation of system I only is ineffective and since inhibition of photosynthesis in Chlorella abolishes the fluorescence change. This dependence raises the possibility that changes in the fluorescence yield reflect inverse changes in the rate of photochemistry. Indeed, since the photochemical utilization of the Chl a excitation is by far the most efficient process, it must be in a virtually direct competition with Chl a fluorescence (Chapter III, section C). Such competition requires that the light induced changes in the rate of

photochemistry and the fluorescence yield must be of opposite sign. Our results, however, indicate the absence of correlation between the time courses of the rate of oxygen evolution and fluorescence (fig. 22 and 43). Consequently, the fluorescence induction must be only indirectly related to the photosynthetic electron flow.

Photophosphorylation (the conservation of a fraction of the absorbed light energy as ATP) indirectly influences the long term fluorescence induction. Since variations of the fluorescence yield are observed not only on illumination but also in the ensuing dark interval (measured by short flashes; fig. 9, 23 and 24), the processes which cause these changes are not necessarily simultaneous with the light reactions of photosynthesis. A similar temporal separation exists for the formation of ATP; the light induced electron transport creates an ATP forming potential X_E in the form of a trans-membrane ion gradient, which can be converted to ATP in the absence of light.[46] The accumulation of X_E is associated with drastic changes in the shape of the Chl a carrying lamellae and consequently in the spatial distribution of the pigment molecules. A tentative diagram indicating the correlation between the light induced ionic shifts and the fluorescence induction changes is as follows. (The electron pathway shown by the vertical arrow is the simplified version of the two light reactions scheme; for details see fig. 1).

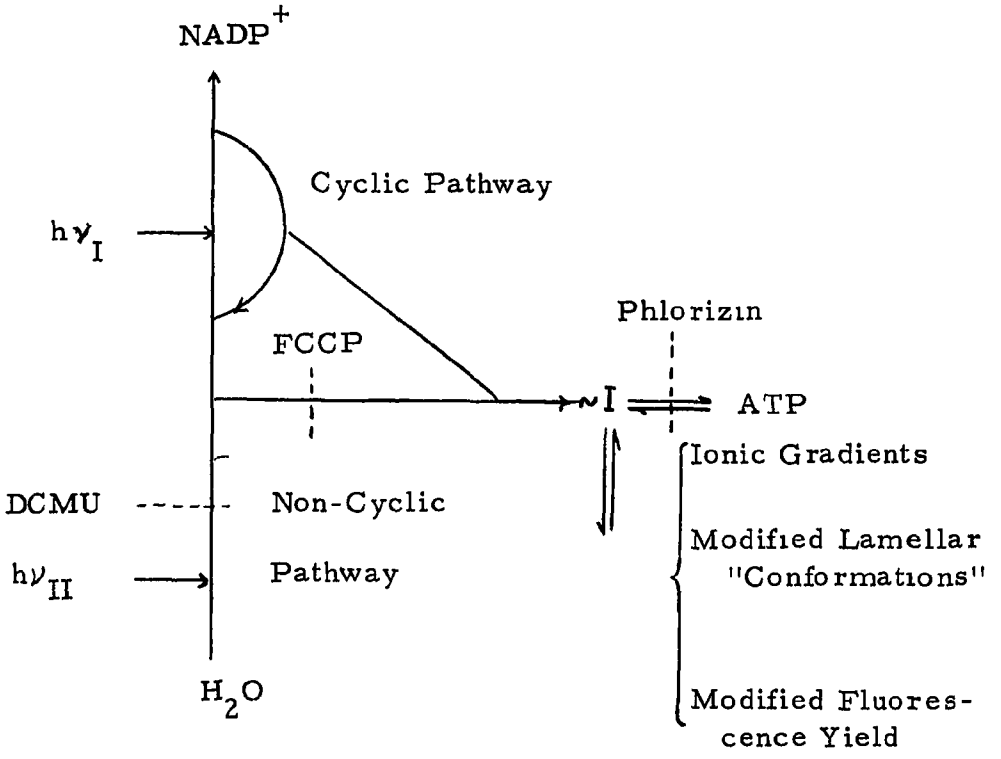

A modification of the arrangement of the Chl a molecules, imposed by the variable "conformation" of the supporting lamella, may in principle alter the fluorescence yield. For example, shrinkage or distention of the quantasome may form or dissociate non-fluorescing Chl a aggregates which drain the electronic excitation from the photosynthetic unit. Changes may also occur in the excitation energy migration which will affect the probability of thermal quenching via the non-fluorescent species.[9]

In this thesis we show that an indirect relation exists between the fluorescence induction phenomena and the rate of photophosphorylation which, as pointed out above, is likely to be due to the induced changes in the lamellar "conformation". The presence of photophosphorylation uncouplers exerts a profound effect on the time courses of

fluorescence both in Chlorella and in Anacystis. Since these compounds do not fluoresce (where we measure fluorescence) and do not establish alternate electron pathways their effects on the Chl a fluorescence yield must be related to the inhibition of the photophosphorylation itself. The low concentration (10^{-5}M) at which they act and the reversal of the light induced fluorescence change (in the presence of uncouplers) in a subsequent dark interval (measured with short flashes) preclude the possibility that they cause non-specific and irreversible changes in the photosynthetic apparatus.

When the accumulation of X_E is assumed to be prevented by the addition of FCCP to Chlorella, we found that the decay of the second wave of fluorescence (M⟶T) is greatly retarded (fig. 18). A similar treatment of Anacystis results in the obliteration of the fluorescence increase (S→M; fig. 39). Since FCCP is known to accelerate the dissipation of ionic gradients we must assume that the stationary fluorescence yield in Chlorella and Anacystis (levels T and M, respectively) correspond to a high level of X_E. The different responses of these algae to FCCP must be related to their widely different cellular organization (cf. Chapter II) and to the higher rate of cyclic phosphorylation in Anacystis. The uncoupler atabrin is totally inhibitory for the fluorescence induction in both algae. Since its effect on the Chlorella fluorescence time course differs from that of FCCP (fig. 18 and 21), the two compounds must act on different sites of the energy conservation sequence.

When the phosphorylation is inhibited at the terminal esterification reaction with phlorizin (phosphorylase inhibitor) the fluorescence

time courses are not affected (fig. 21 and 40). This is in accordance with the expectations since phlorizin does not affect the formation and the storage of X_E. Thus, on the basis of these results we suggest that the fluorescence induction (S→M→T) is affected by events that precede the terminal phosphorylation step and in particular is related to the light induced changes in the lamellar conformation. This correlation is also supported by the coincidence of the pH optima (pH = 6-7) of the light induced cation transport and the total fluorescence induction change.

The above discussion ascribes the fluorescence induction to processes associated with the non-cyclic photophosphorylation. This correlation, however, cannot apply to the extensive fluorescence change of Anacystis poisoned with DCMU or o-phenanthroline. In this case, the operation of the cyclic pathway is suggested as the possible cause on the basis of the following observations: (i) Poisoned Anacystis is capable of fluorescence induction with light absorbed primarily by system I (fig. 29). Such light is adequate for the operation of the cyclic pathway, (ii) the cyclic pathway is a major contributor to the ATP pool of the blue-green algae[104, 105, 110], (iii) the time course of fluorescence of poisoned Anacystis is insensitive to photophosphorylation uncouplers such as FCCP, and atabrin (fig. 41) in the same manner as the cyclic photophosphorylation.[40]

The light induced changes in the fluorescence yield are restricted mainly to the Chl a emission. Since more than one Chl a forms contribute to the fluorescence spectrum it is possible that the fluorescence yield

does not change uniformly throughout the emission envelope. In Chlorella it appears that the induction effects are relatively greater at 685 nm (system II emission) than at 715 nm where system I contributes considerably. Changes in the Chl a fluorescence spectrum of Anacystis, caused by prolonged illumination, appear as difference bands, peaked at 685 nm (major) and 693-699 nm (minor). In all likelihood these bands originate from system II Chl a forms (fig. 28 and 30).

The localization of the fluorescence induction in Chl a leads to gross changes in the composite emission spectrum of Anacystis, which consists of Chl a and phycocyanin bands (fig. 25 and 26). Since the phycocyanin emission is invariable, the light induced "conformational" changes (changes in shape of the chloroplast lamellae followed by changes in orientation of Chl molecules) must not affect the efficiency of energy transfer from phycocyanin to Chl a.

In conclusion, we may say that the evidence we presented suggests an indirect correlation between the fluorescence induction phenomena and the photophosphorylation process in the green alga Chlorella pyrenoidosa and the blue green alga Anacystis nidulans. Specifically, it was shown that the Chl a fluorescence yield is influenced by the rate of photophosphorylation which, we believe, affects changes in the lamellar "conformation." The similar origin of the fluorescence induction changes in such disparate systems as the two algae studied in this investigation is indicative of the generality of these phenomena.

APPENDIX I

ABSORPTION SPECTROSCOPY OF TURBID SYSTEMS

The measurement of the true absorption spectrum of a turbid system is complicated by two phenomena, the scattering of the measuring beam and the sieve effect (p. 1865).[9] Light scattering depends on the refractive indices of the medium and the suspended particles and affects both the location and the shape of the absorption band. The sieve effect refers to the lower optical density of a suspension as compared to that of true solution having the same pigment concentration. It affects the shape of the absorption band but not the location of the maxima.

1. Light Scattering: Although treatments of the light scattering properties of particles larger than $\lambda/2$ exist for special cases (spheres of uniform size,[111] oriented cylinders[112]), they cannot be applied to cell suspensions because of the polyphasic nature of the suspended particle. Due to interference, such systems scatter mostly in the forward direction so that a detector which subtends a large solid angle will observe almost all the scattered and the transmitted light.

A second type of light scattering, which appears whenever the scattering particle absorbs the incident radiation, is the selective scattering.[113] This phenomenon originates from the fact that the refractive index of the absorbing substance passes through a maximum located on the long wavelength side of the absorption peak at ca. a half-band width distance from it. Thus the 90° scattering in Chlorella shows

three peaks at 460, 515 and 690 nm. These are related to the absorption bands at 436 nm (Chl a), 480 nm (Chl b), and 675 nm (Chl a). In the blue-green alga Synechocystis the scattering peaks and their associated absorption bands are at 465 nm (Chl a 436 nm), 520 nm (carotenoids 490 nm), 635 nm (phycocyanin 620 nm) and 700 nm (Chl a 675 nm).[113] The effects of the selective scattering on the absorption spectrum can also be compensated with a large solid angle of collection.[114]

The errors which the light scattering introduces to the true absorption spectrum of a suspension, especially when the latter is measured with a small solid angle of collection, are as follows:

(i) Since scattered light is observed by the detector as absorbed light, the spectrum appears less sharp because non-absorbing regions (valleys) are "filled up".

(ii) The light path in the sample is increased. As a consequence the spectrum is intensified.[115] Butler and Norris[116] observed an intensification in the absorption spectrum of dilute cytochrome on the addition of enough $CaCO_3$ to make a thick paste.

(iii) The absorption bands are shifted along the wavelength axis. Non-selective scattering tends to displace the band toward shorter wavelengths because of its dependence on λ^{-4} (Rayleigh scattering). Selective scattering has the opposite effect since the maximum of the refractive index is on the long wavelength side of the absorption band.

(iv) The unspecified light path in the sample does not allow the correlation of the measured optical densities with the molar extinction coefficients of absorbing material.

The methods employed to compensate for the scattering errors rely invariably on an increased solid angle of collection. An extreme case, in which a 4π collection angle is achieved, is that of the Ulbricht integrating sphere. The sphere is coated on the inside with a diffusely reflecting substance having a high reflectance and the sample and reference are positioned near its center. Openings on the sphere wall provide for the entrance of the measuring beams and for the positioning of the detection device. The latter must not be in the direct path of the measuring beam and it is usually protected by a baffle. Theoretically, each area element of the inside surface is illuminated with the same intensity.[117] This is the method that was used in the present thesis for the measurement of the absorption spectra of Chlorella and Anacystis suspensions.

The integrating sphere corrects all the errors introduced by the light scattering except those due to the increased light path. In fact, since multiple passages through the samples are involved, the total path length for the less absorbed wavelengths will increase leading to a spectrum of lesser detail and depressed peaks.[114] A second error appears when the absorbing substance is capable of fluorescence. In this instance the emitted light is detected as transmitted and in consequence a depression of the absorption band appears. Thus, for example, the

absorption spectra of indentical samples of normal and DCMU-inhibited Chlorella should differ by virtue of the higher fluorescence yield of the latter. Still another error originates from the reflectance losses. Thus, the reflectance of a fresh MgO coating is ca. 0.97 so that 3% of the light is lost in each reflection.[117] With aged coatings the losses are greater.

Errors due to the multiple passage of the measuring light through the sample can be eliminated if the large solid angle of collection is achieved by juxtaposition of the sample and the photomultiplier entrance window. Since for large particles the back scattering is minimal, almost all the transmitted light will be detected.[115]

2. The Sieve Effect: The sieve effect is described in terms of the flattening coefficient Q_A, defined as the ratio of the optical density of the suspension A_{susp} to that of the true solution A_{sol}, under the restriction that both have the same pigment concentration. Duysens[11] and Rabinowitch[9] (p. 1865) derived the following expression for a system of oriented cubical particles:

$$Q_A = \frac{A_{susp}}{A_{sol}} = \frac{1 - T(a_p)}{a_p}$$

where a_p is the optical density of the particle along a particular dimension (along the edge of the cube in this case) and $T(a_p)$ the transmittance of the particle. Duysens,[117] in a more generalized approach, obtained a similar equation applicable to particles of any shape:

$$Q_A = \frac{A_{susp}}{A_{sol}} = \frac{C_2}{C_1} \frac{1 - \bar{T}(a_p)}{a_p}$$

Here C_2 and C_1 can be obtained from the projected area of the particle a_p (assumed to equal the optical density of the particle) and its volume V_p from the relationships $a_p = C_2 L^2$ and $V_p = C_1 L^3$, L being a certain dimension of the particle The coefficient $C_2:C_1$ is referred to as the form factor.

These equations allow the calculation of the true absorption spectrum from that of the suspension provided that a_p and the explicit form of $T(a_p)$ are known. Alternatively, if the flattening coefficient can be measured, e.g., by dispersing the pigment as to obtain a true solution, the particle optical density can be estimated. The second application also requires a knowledge of the explicit form of $T(a_p)$.

In a first approximation, a cell can be represented by a sphere. In this case $C_2:C_1 = 3:2$ while $T(a_p)$ is given as follows:[118]

$$\bar{T}(a_p) = \frac{1 - (1 + a_p)e^{-a_p}}{a_p^2}$$

with a_p being defined along the diameter. A better model for Chlorella or Anacystis cells is that of a spherical shell (see Chapter IIA). If R and r are the outer and the inner radius of the shell, then a_p is defined as $2(R - r)a$, a being the optical density for unit path length, and the form factor is equal to $3(R^2 + Rr + r^2)/2R^2$. We derived an expression for the average transmittance of such a model in terms of a_p and a form

parameter τ, defined as $\tau = R-r/R+r$.

$$T(a_p) = \frac{1}{2a_p^2(\tau+1)^2}\left[16 + a_p^4 \sum_{n=1}^{\infty}(-1)^n \frac{a_p^n}{n\cdot n!}(\tau^{n/2}-1) + \right.$$

$$\left. 2\left\{a_p\sqrt{\tau}\,(a_p\sqrt{\tau}-1)-6(a_p\sqrt{\tau}+1)\right\}e^{-a_p\sqrt{\tau}} - 2\left\{2(a_p+1)+a_p^2\tau^2(a_p-1)\right\}e^{-a_p}\right]$$

For $r \to 0$ ($\tau \to 1$) the spherical shell becomes a solid sphere. In this limit, the above equation becomes identical with the equation for the transmittance of a solid absorbing sphere. The validity of the above expression has been verified also by L. Szalay by numerical integration.[119]

In fig. 45, Q_A and $T(a_p)$ for R:r = 2 are plotted against a_p. From the flattening coefficients of Chlorella Q_A (674 nm) = 0.70 and Q_A (434 nm) = 0.55 given by M. Das *et al.*[120] the average transmittances obtained from this monogram are $\bar{T}$(674 nm) = 0.51 and $\bar{T}$(434 nm) = 0.31. Duysens[11] obtained $\bar{T}$(680 nm) = 0.36 by a method based on the reabsorption of fluorescence. The discrepancy is partly due to the radial ratio R:r = 2 used and to the representation of the Chlorella cell by a non-refracting model. Refraction, for example, will increase the average path of the light in the cell leading to lower values of the flattening coefficient. Consequently the transmittance values calculated from fig. 45 will be lower and will approach the value given by Duysens.

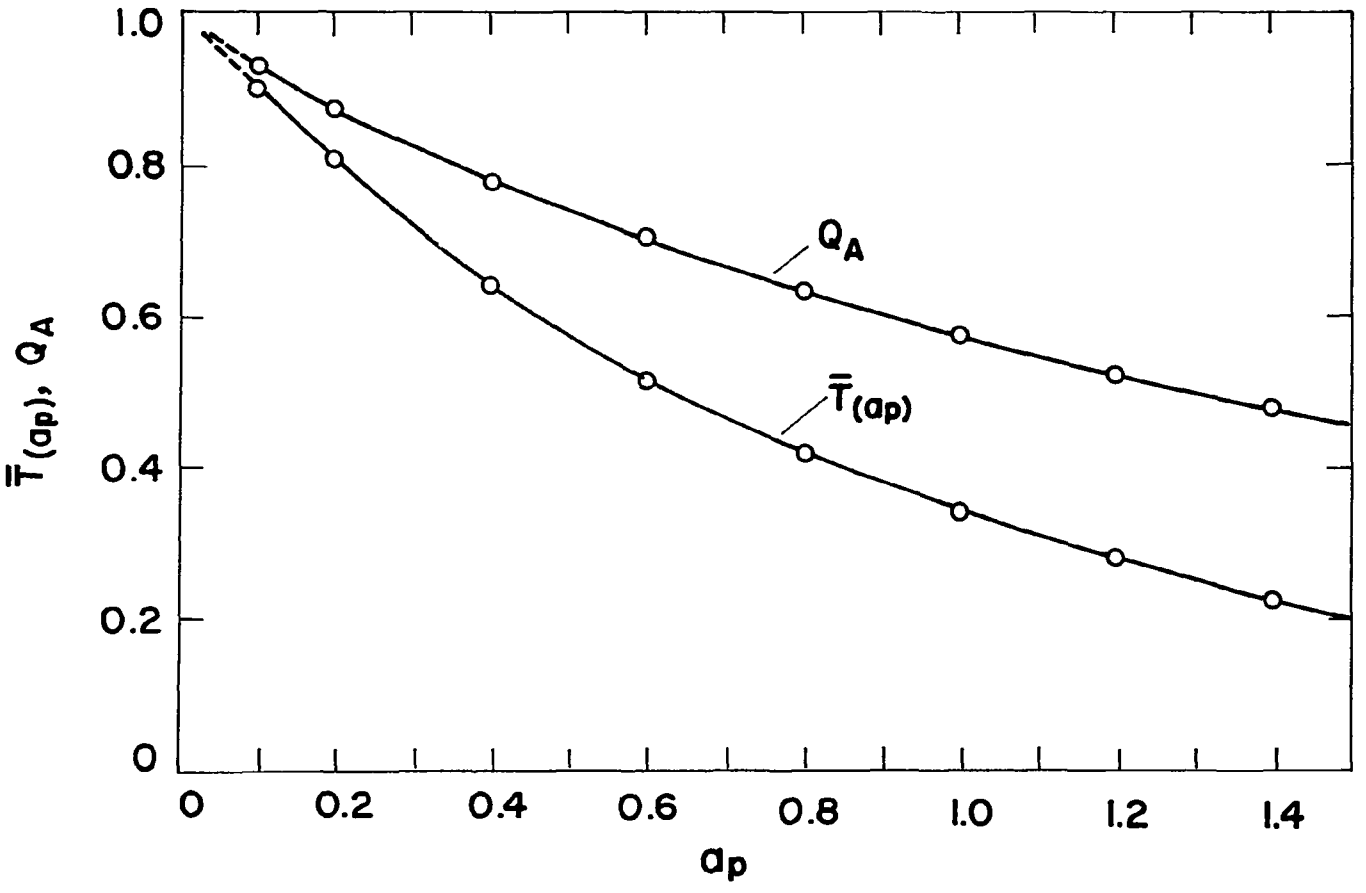

Fig. 45. The flattening coefficient Q_A and the average transmittance $T(a_p)$ of a spherical shell as a function of the optical density along its diameter, radial ratio, R:r = 2.

APPENDIX II

REABSORPTION OF FLUORESCENCE

When the absorption and emission spectra overlap, as for example in the case of Anacystis and Chlorella, the fluorescence will be partly reabsorbed. Of the two possible types of reabsorption, the inner which refers to events occurring within the cell and the outer referring to the suspension as a whole, we will consider only the latter. Following the procedure outlined by Förster[121] we obtained an equation relating the apparent $F(\lambda, \lambda')$ and the true $f(\lambda, \lambda')$ fluorescence intensity per spectral interval. The derivation was based on the optics of our instrument, namely that the light path of the excitation is inclined by $\theta = 30^{\circ}$ to the normal on the air-sample boundary and that only the normal to this boundary portion of fluorescence is collected (cf. fig. 7).

$$\frac{F(\lambda, \lambda')}{f(\lambda, \lambda')} = CI_o a \quad \frac{1-\exp -(a_\lambda + a_{\lambda'} \cos\theta) L/2.3 \cos\theta}{a_\lambda + a_{\lambda'} \cos\theta}$$

Here, unprimed quantities refer to excitation, primed to fluorescence, a, L, I_o and C are respectively the optical density for unit path, the sample thickness, the excitation intensity and a geometric factor accounting for the fraction of the total emission observed.

In our experiments we had L = 0.1 cm. Since the maximum error will be at the absorption peak we can set $a_{\lambda'} = 0.5$ (Chapter II). Assuming also $a_\lambda \simeq a_{\lambda'}$ we calculate for the exponent the value of 0.047. We may then expand the exponential and retain only the first power of the

expansion, the error being of the order of 0.1%. The above equation is simplified to

$$\frac{F(\lambda, \lambda')}{f(\lambda, \lambda')} = CI_o \frac{a_\lambda L}{2.3 \cos \theta}$$

Since the right hand is independent of the wavelength of observation, the true and the apparent spectra differ only by a constant. Consequently, there is no shape distortion in the emission spectra we presented.

REFERENCES

1. R. Emerson, R. V. Chalmers and C. Cederstrand: Proc. Natl. Acad. Sci. U.S., 43, 133, 1957.

2. R. Emerson and E. Rabinowitch: Plant Physiol., 35, 477, 1960.

3. L. N. M. Duysens, J. Amesz and B. M. Kamp: Nature, 190, 510, 1961.

4. R. Emerson and W. J. Arnold: J. Gen. Physiol., 16, 191, 1932.

5. G. W. Robinson: Brookhaven Symp. in Biology, 19, 16, 1966.

6. P. Latimer, T. T. Bannister and E. Rabinowitch: Science, 124, 585, 1956.

7. W. L. Butler and K. H. Norris: Biochim. Biophys. Acta, 66, 72, 1963.

8. G. Weber and F. J. W. Teale· Trans. Faraday Soc. 53, 646, 1957.

9. E. I. Rabinowitch: Photosynthesis and Related Processes, Vol. I, II, part 1 and part 2, Interscience, New York (1945, 1951, 1956).

10. W. F. Watson and R. Livingston: J. Chem. Phys., 18, 802, 1950.

11. L. N. M. Duysens: Ph.D. Thesis, Utrecht, The Netherlands, 1952.

12. L. N. M. Duysens: Progress in Biophysics, 14, 1, 1964.

13. H. C. Longuet-Higgins, G. W. Rector and J. R. Platt: J. Chem. Phys. 18, 1174, 1950.

14. Govindjee, G. Papageorgiou and E. Rabinowitch: In Fluorescence: Theory, Instrumentation and Practice (G. G. Guilbault, edt), Marcel Dekkar, Inc., New York, N.Y., p. 511, 1967.

15. H. Kautsky· Naturwiss., 19, 964, 1931.

16. E. C. Wassink: Advances in Enzymology, 11, 91, 1951.

17. H. Kautsky and R. Hormuth: Biochem. Z., 221, 285, 1937.

18. J. Franck, C. S. French and T. T. Puck· J. Phys. Chem., 45, 1268, 1941.

19. J. Franck, P. Pringsheim and D. T. Lad: Arch. Biochem., 7, 103, 1945.

20. Y. G. Shiau and J. Franck: Arch. Biochem., 14, 253, 1947.

21. L. S. Ornstein, E. C. Wassink, G. H. Reman and D. Vermeulen· Enzymologia, 5, 110, 1938.

22. H. Kautsky, W. Appel and H. Amann: Biochem. Z., 332, 277, 1960.

23. Govindjee, S. Ichimura, C. N. Cederstrand and E. Rabinowitch: Arch. Biochem. Biophys., 39, 322, 1960.

24. W. L. Butler: Plant Physiol. Suppl., 36, IV, 1961.

25. W. L. Butler: Biochim. Biophys. Acta, 69, 309, 1962.

26. W. L. Butler: Biochim. Biophys. Acta, 66, 275, 1963.

27. L. N. M. Duysens and H. E Sweers: In Studies on Microalgae and Photosynthetic Bacteria(edited by Japanese Society of Plant Physiologists, p. 353), U. of Tokyo Press, 1963.

28. P. Joliot: Biochim. Biophys. Acta, 102, 135, 1965.

29. P. Joliot: Brookhaven Symp. in Biology, 19, 418, 1966.

30. H. Kautsky and U. Franck· Biochem. Z., 315, 156, 1943.

31. E. C. Wassink and E. Katz: Enzymologia 6, 145, 1939.

32. A. V. Trebst, M. Losada and D. I. Arnon: J. Biol. Chem., 235, 840, 1960.

33. E. C. Wassink, E. Katz and R Dorrestein: Enzymologia 10, 285, 1942.

34. H. Kautsky and R. Eberlein: Biochem. Z., 302, 137, 1939.

35. E. D. McAlister and J. Myers: Smithsonian Inst. Pubs. Misc. Collections, 99, 1, 1940.

36. L. R. Blinks and R. K. Skow: Proc. Natl. Acad. Sci., U.S., 24, 413, 1938.

37. O. Kandler: Z. Naturforsch., 5b, 423, 1950.

38. O. Kandler: Z. Naturforsch., 12b, 271, 1957.

39. B. L. Strehler: Arch. Biochem. Biophys., 43, 67, 1953.

40. N. E. Good, S. Izawa and G. Hind: In Current Topics in Bioenergetics (D. R. Sanadi, edt.) Vol. 1, p. 75, Academic Press, New York, 1966.

41. A. L. Lehninger: Physiol. Rev., 42, 467, 1962.

42. J. Newmann and A. T. Jagendorf: Arch. Biochem. Biophys., 107, 109, 1964.

43. R. A. Dilley: Biochem. Biophys. Res. Commun., 3, 817, 1964.

44. R. A. Dilley and L. P. Vernon: Arch. Biochem. Biophys., 111, 365, 1965.

45. L. Packer, D. W. Deamer and A R. Crofts: Brookhaven Symp. in Biology, 19, 280, 1966.

46. P. Mitchell: Nature, 191, 144 (1961).

47. G. Hind and A. T. Jagendorf: J. Biol. Chem., 240, 3195, 1965.

48. A. T. Jagendorf and E Uribe: Brookhaven Symp. in Biology, 19, 215, 1966.

49. L. Packer: Biochem. Biophys. Res. Commun., 9, 355, 1962.

50. M. Itoh, S. Izawa and K. Shibata: Biochim. Biophys. Acta, 66, 319, 1963.

51. S. Izawa and N. E. Good: Plant Physiol., 41, 544, 1966.

52. R. A Dilley, R. B. Park and D. Branton: Photochem. Photobiol., 6, 407, 1967.

53. H. Hilgenheger and W. Z. Menke: Z. Naturforsch., 20b, 699, 1965.

54. R. A. Dilley and L. P. Vernon: Biochemistry, 3, 318, 1966.

55. A. T. Jagendorf and G. Hind: Natl. Acad. Sci. - Natl. Res. Council Publ. 1145, 599, 1963.

56. G. Hind and A. T. Jagendorf: J. Biol. Chem., 240, 3202, 1965.

57. A. T. Jagendorf and J. Newmann: J. Biol. Chem., 240, 3210, 1965.

58. S. Izawa: Biochim. Biophys. Acta, 102, 373, 1965.

59. R. A. Olson and E. K. Engel· Brookhaven Symp. in Biology, 11, 303, 1958.

60. R. Emerson and C. M. Lewis: Am. J. Botany, 30, 1965, 1943.

61. F. W. J. Teale: Report to U. S. Army Research and Development in Europe (DA-91-508-EUC-281), 1951.

62. Govindjee: Personal communication.

63. F. F. Litvin and V. A. Sineschchekov: Biofisika, 7, 433, 1967.

64. G. R. Seely and R. G. Jensen: Spectrochim. Acta, 21, 1835, 1965.

65. S. B. Broyde and S. S. Brody: J. Chem. Phys., 46, 3334, 1967.

66. J. Brown: Photochem. Photobiol., 2, 159, 1963.

67. C. N. Cederstrand, E. Rabinowitch and Govindjee: Biochim. Biophys. Acta, 126, 1, 1966.

68. A. K. Ghosh and Govindjee: Biophys. J., 6, 611, 1966.

69. A. Hattori and Y. Fujita· J. Biochem. (Tokyo), 46, 633, 1959.

70. Govindjee and E. Rabinowitch: Biophys. J., 1, 74, 1960.

71. G. McKinney· J. Biol. Chem., 140, 315, 1941.

72. Govindjee: In Currents in Photosynthesis (J. B. Thomas and J. H. C. Goedheer, edts.), p. 93, Ad Donker, Rotterdam, 1966.

73. T. T. Bannister and M. J. Vrooman: Plant Physiol., 32, 622, 1964.

74. J. A. Bergeron: Natl. Acad. Sci. - Natl. Res. Council Publ. 1145, 527, 1963.

75. J. Lavorel: Coll. Intern. C.N.R.S., 119, 159, 1963.

76. J. L. Rosenberg, T. Bigat and S. Dejaegere: Biochim. Biophys. Acts, 79, 9, 1964.

77. Govindjee, J. Munday and G. Papageorgiou: Brookhaven Symp. in Biology, 19, 434, 1966.

78. L. N. M. Duysens· Proc. Roy. Soc. (London) 157B, 301, 1963.

79. P. G. Heytler: Biochemistry, 2, 357, 1963.

80. M. Avron and N. Shavit· Biochim. Biophys. Acta, 109, 317, 1965.

81. D. Y. De Kiewiet, D. O. Hall and E. L. Jenner: Biocheim. Biophys. Acta, 109, 284, 1965.

82. L. Packer· Biochim. Biophys. Acta, 75, 12, 1963.

83. P. H. Homann: Plant Physiol., 42, 997, 1967.

84. H. Baltscheffsky: Acta Chem. Scand., 14, 264, 1960.

85. F. E. Hunter: Methods in Enzymology, 2, 610, 1955.

86. R. A. Dilley and L. P. Vernon: Cited by Good et al., ref. 40.

87. S. Izawa, G. D. Winget and N. E. Good: Biochem. Biophys. Res. Commun., 22, 223, 1966.

88. G. F. Cori, G. T. Cori and A. A. Green· J. Biol. Chem., 151, 39, 1943.

89. D. M Keller and W. D. Lotspeich: J. Biol. Chem., 234, 987, 1959.

90. S. Izawa, T. N. Connolly, G. D. Winget and N. E. Good: Brookhaven Symp. in Biology, 19, 169, 1966.

91. J. S. C. Wessels and R. Van der Veen: Biochim. Biophys. Acta, 19, 587, 1956.

92. P. Nobel and L. Packer· Biochim. Biophys. Acta, 88, 453, 1964.

93. C. S. French and V. K. Young· J. Gen. Physiol., 35, 873, 1952.

94. G. Papageorgiou and Govindjee: Biophys. J., 7, 375, 1967.

95. A Krey and Govindjee: Proc. Natl. Acad. Sci., U. S., 52, 1568, 1964.

96. Govindjee and L. Yang: J. Gen. Physiol. 49, 763, 1966.

97. S. S. Brody and M. Brody: Natl. Acad. Sci. - Natl. Res. Council Publ. 1145, 455, 1963.

98. G. Weber: Nature, 190, 27, 1961.

99. W. P. Williams, N. R. Murty and E Rabinowitch: Submitted to Photochemistry and Photobiology.

100. C. N. Cederstrand, E. Rabinowitch and Govindjee. Biochim. Biophys. Acta, 120, 247, 1966.

101. F. Cho, J. Spencer and Govindjee: Biochim. Biophys. Acta, 126, 174, 1966.

102. F. Cho: Manuscript in preparation.

103. A. T. Jagendorf and M. Avron: Arch. Biochem. Biophys., 80, 246, 1959.

104. C. C. Black, C. A. Fewson and M. Gibbs: Nature, 198, 88, 1963.

105. J. L. Lightbody and D. W. Krogmann: Biochim. Biophys. Acta, 120, 57, 1966.

106. R. A Dilley. Brookhaven Symp. in Biology, 19, 258, 1966.

107. F. V. Mercer, A. J. Hodge, A. B. Hope and J. D. McLean. Australian J. Bot. Sci., 8, 1, 1955.

108. T. T. Bannister: Biochim. Biophys. Acta, 109, 97, 1965.

109. T. T. Bannister. Brookhaven Symp. in Biology, 19, 432, 1966.

110. D. Teichler-Zallen and G. Hoch: Arch. Biochem. Biophys., 120, 228, 1967.

111. G. Mie. Ann. Physik., 25, 377, 1908.

112. H.C. Van de Hulst: Light Scattering by Small Particles, John Wiley and Sons, New York, 1957.

113. P. Latimer: Ph. D. Thesis, University of Illinois, 1956.

114. P. Latimer: Science, 127, 29, 1958.

115. W. L. Butler: Ann. Rev. Plant Physiol., 15, 451, 1964.

116. W L. Butler and K. H. Norris: Arch. Biochem. Biophys., 87, 31, 1960.

117. W. Wm. Wendlandt and H. G. Hecht: Reflectance Spectroscopy, Interscience Publishers, New York, N. Y., 1966.

118. L. N. M. Duysens: Biochim. Biophys. Acta, 19, 1, 1956.

119. L. Szalay: Personal Communication.

120. M. Das, E. Rabinowitch, L. Szalay and G. Papageorgiou: J. Phys. Chem., 71, 3543, 1967.

121. T. Förster: Fluoreszenz Organischer Verbindungen, Vandenhoeck & Ruprecht, Göttingen, 1951.

122. J. C. Munday, Jr., Ph. D. Thesis, University of Illinois, 1968.

VITA

George Papageorgiou was born on May 9, 1933, in Thessalonike, Greece. He graduated from Anatolia College High School in Thessalonike in 1952 and obtained his diploma in Chemistry from the Aristotelian University of Thessalonike in 1958. From 1958 to 1960 he served in the Greek Army and from 1960 to 1963 he taught General Organic and Analytical Chemistry in the "Pythagoras" preparatory school in Thessalonike. He was admitted to the department of Physiology and Biophysics of the University of Illinois in 1963.

He is a member of the Northern Greece Association of Chemists and of Sigma Xi.

He is co-author of the following publications:

1. "Oxygen Evolution from Lyophilized Anacystis with Carbon Dioxide as Oxidant", Biochim. Biophys. Acta, 131, 173-178 (1967).

2. "Fluorescence Studies with Algae; Changes with Time and Pre-illumination", Brookhaven Symposia in Biology, 19, 434-445 (1966).

3. "Changes in Intensity and Spectral Distribution of Fluorescence, Effect of Light Treatment on Normal and DCMU-poisoned Anacystis nidulans," Biophys. J., 7, 375-389 (1967).

4. "Chlorophyll Fluorescence and Photosynthesis", in Fluorescence, Theory Instrumentation and Practice, edited by G. G. Guilbault, Marcel Dekker, Inc., New York, pp. 511-564 (1967).

5. "The Sieve Effect in Chlorella Suspensions", J. Phys. Chem., 71, 3543-3549 (1967).